THE SIMULATION OF TEMPERATURES IN GRAIN BINS

by

Rosemary Anne Bell

Thesis submitted for the
Degree of Master of Science
in the Australian National University

January 1978

STATEMENT OF AUTHORSHIP

Except where otherwise indicated, the contents of this thesis are entirely my own work.

Rosemary A. Bell.

Rosemary A. Bell

ACKNOWLEDGEMENTS

I should like to thank a great number of people in generously helping me to produce this thesis.

My supervisors, Dr I.R. Cowan, Dr A.R.G. Lang and Dr J.M. Hardman have offered invaluable advice during the course of this work. Dr M.J. Dallwitz and Mr J.P. Higgins have helped with many of my computing problems. Dr H.J. Banks, Mr P.C. Annis and Mr G.P. Smith have answered many queries and been of great assistance in the pressure testing of the silos. Mr J.J. Finningan has used much time and energy in helping with the measurement of the air-wall heat transfer coefficient, Miss J.G. Henry has aided in the making of thermocouple cables and Mr C. Waterford helped to position them in the silos. Many of the staff at the Stored Grain Research Laboratory, particularly Mr J.B. McCabe, have assisted in filling the silos.

I also wish to thank Dr J.M. Desmarchelier for determining the malathion content, Dr E.R. Rumbo for his help in calibrating the thermometer, Mr E.A. Christie for his measurements of the radiative properties of the silos, Mr L.F. O'Brien for measuring the conductivity of the wheat, Mr J.P. Green and Mr P.J. Hay for their photography, Mrs G.C. Palmer for her diagrams of the silo shading, and Mr K.G. Pullen for taking temperature measurements in my absence.

Finally I should like to thank Mrs P.E. Dawson and Mrs R. Drury for their excellent typing of this thesis.

ABSTRACT

A digital computer model is developed to predict temperatures in cylindrical grain bins.

The temperatures at the walls, base and grain surface are determined on an hourly basis. Heat transfer into the grain is ignored in these calculations because it is small compared to the external fluxes. The meteorological parameters used are the maximum and minimum daily temperature, wind speed and hours of bright sunshine. Solar radiation on the walls is estimated for the particular locality and time of year. Other modes of heat transfer to the walls and grain surface are thermal radiation and free convection. Heat is also transferred to the walls by forced convection. The forced convection coefficient was determined experimentally using a model bin in a wind tunnel, where a very high value was obtained. However this value appeared to be appropriate to the large experimental bin, which had large corrugations, but half of the value is used for the computation of temperature in the small bins.

An implicit finite difference method is used to describe heat transfer in three dimensions within the grain bulk. The temperature changes are dependent on the initial temperature and thermal properties of the grain and the changing boundary temperatures.

The model is compared with three experimental metal farm silos and is shown to be concordant with observed temperature patterns.

TABLE OF CONTENTS

TABLE OF CONTENTS

TABLE OF CONTENTS

LIST OF FIGURES

LIST OF FIGURES

LIST OF TABLES

CHAPTER 1

INTRODUCTION

INTRODUCTION

1.1 The Beginnings of Grain Storage

Archaeologists have found that storage of grain began in the Neolithic period of the Stone Age (about 8000 BC). It has been used ever since that time as a means of providing a reserve food supply.

The ease of storing grain in dry conditions was an important reason for civilization being born in a relatively dry part of the world. Ancient Egyptian drawings clearly show methods of grain storage (Waterhouse 1973). However they obviously had insect problems like we have today as specimens of grain weevils and flour beetles have been found in grain residues from the tombs of the various Pharoahs, dating back to 3000 BC (Solomon 1965).

1.2 Grain Storage Today

In less developed communities, grain is stored in anything from earthenware jars to sacks, or left in heaps on the ground. In industrialized countries it is stored in large bulk stores, allowing for rapid handling with little spillage, minimal manual labour and low running costs. The nature of the store depends on the availability and suitability of materials and the overall cost of construction.

On Australian farms grain is stored mainly in small steel silos. It is transported by road or rail to the country terminals and ports where it is stored in large horizontal steel sheds or concrete or steel silos. (Steel silos are now being built in preference to concrete ones as they can be purchased complete and therefore erected more easily and cheaply and are also easier to seal for application of control measures.) Most of these stores have a concrete base.

1.3 Problems of Grain Storage

Cereal grains are seeds, alive but in a dormant resting stage. They

produce heat, water and carbon dioxide, but at a very slow rate and under normal conditions can be stored indefinitely with very little loss of quality.

There are, however, two main features which can upset this dormant state and these are described below.

1.3.1 High water content

When the water content of the grains is too high, above about 14%*, respiration increases considerably. Furthermore, fungi are able to grow. Both these processes cause additional water and heat, and thus degrade the grain bulk.

1.3.2 Insects

There are hundreds of known species of insects which attack stored grain. They generally increase fastest in grain that is moist and warm, but not excessively so. Fig. 1.1 from Hardman (1975) shows the effect of temperature on rate of development (represented here by the reciprocal of the number of days to reach maturity).

Insects often consume large quantities of grain before they are driven to the surface by their own heat. Since grain is a poor conductor, this heat does not dissipate quickly and a 'hotspot' develops, with the internal parts of the bulk reaching a temperature of about 42°C (or that temperature lethal to the insect). Convection currents cause water to condense on the cooler parts of the grain, particularly the surface. This results in damp grain heating, steaming and sprouting, as mentioned in Section 1.3.1.

Although few accurate figures on the overall losses of grain in storage are available, they may vary from 1% in some countries to 50% in others. The high losses in the poorer countries are often caused by rodents, which are not found in well constructed stores.

---

* All moisture contents are expressed as a percentage of the wet weight.

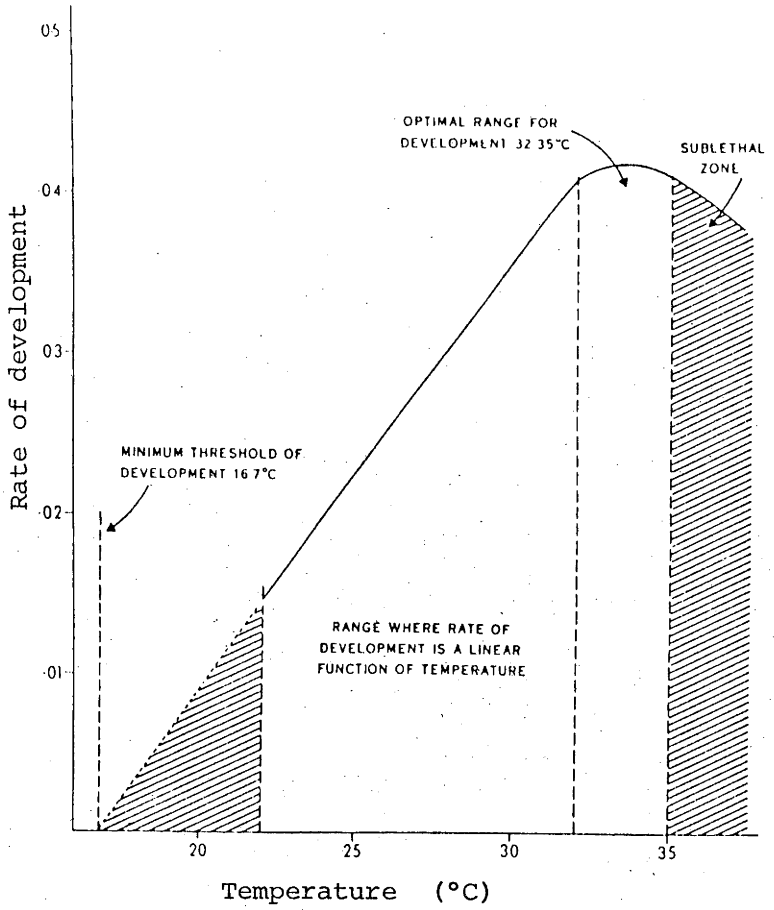

Figure 1.1 - The influence of temperature on the rate of development of *Tribolium castaneum* (a typical stored product insect). Shaded zones allow survival but are too cool or too warm to allow rapid population growth.

Figure 1.2 - The breakdown of malathion on stored wheat

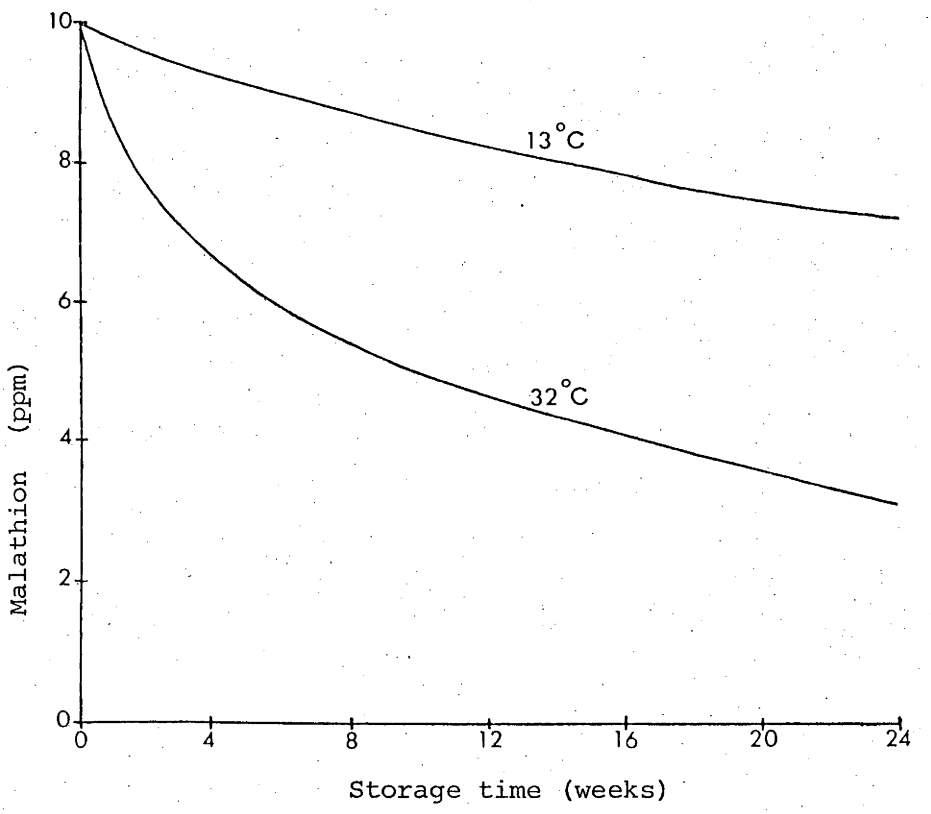

1.4 Control Measures and the Significance of Temperature upon Them

In many countries, including Australia, it is illegal to export grain with any live insects. Measures used to protect grain from damage in the industrialized countries, and possible future methods, will be discussed below, with particular reference to the importance of a knowledge of grain temperatures in each case.

1.4.1 Drying

In Australia the legal upper limit of moisture content of wheat for receival at country stores is 12%. Driers are installed at many stores. It is important that grain temperature rise during drying is kept to a minimum to prevent damage (Sutherland 1976).

1.4.2 Insecticides

On receival at country stores, grain is sprayed with an insecticide. Malathion was an extremely effective, safe and cheap protectant in the 1960's. Now, with increasing resistance of pests to malathion, other insecticides have been developed, notably, bioresmethrin. (However, this costs about 70¢ per tonne to apply, compared to 2.5¢ for malathion.)

Fig. 1.2 from Belcher and Minett (1966) shows the important effect of temperature on the rate of breakdown of malathion applied at 10 ppm. 8 ppm is considered an effective level for control (or was until resistance became significant) and this level is reached after about one week at 32°C and 15 weeks at 13°C.

The importance of low temperatures on rate of breakdown applies to all protectants.

1.4.3 Turning

If stored for more than a few weeks, it is advisable to 'turn' grain - that is, move it from silo to another. This cools the grain and breaks up

infestations. Gay (1941) found an average temperature drop of 8.9°C resulted from turning a bulk of wheat in a commercial store during winter.

1.4.4 Fumigation

If an infestation develops, the grain can be treated with a fumigant, such as methyl bromide or phosphine. Recirculatory equipment is being installed for methyl bromide application in some storages in Australia (Druce 1976).

Typical temperature gradients found in grain stores can readily affect the flow rate of fumigants (Berck 1975) and temperature variations inside a bin cause gas to flow between the inside and outside through leaks. Temperature thus plays a very important role in effective fumigation.

1.4.5 Inert Atmospheres

An atmosphere of <1% oxygen in nitrogen or >60% carbon dioxide in air is proving to be suitable for controlling insects in stored grain. Field studies (Banks *et al.* 1974) have shown that these atmospheres can be maintained in commercial stores, when appropriately sealed.

Temperature gradients within the silo and across its walls must be kept small (as for fumigation) for a high and even concentration of nitrogen or carbon dioxide to be maintained.

1.4.6 Aeration and Refrigeration

The lowering of the grain temperature is being used increasingly to reduce the reproductive capacity of insects. In general a temperature of 10° to 15°C over prolonged periods is required to eliminate most insects (Howe 1965; Childs *et al.* 1970). However a complete kill will not be obtained, so subsidiary control measures must be applied.

Natural aeration is practised in cool climates and many new storages have forced aeration equipment. In warm climates, experiments are being

conducted to investigate the possibility of refrigerating storages (Sutherland et al. 1970).

1.5 The Benefits of a Three-Dimensional Model

It would be extremely useful to have information of the spatial temperature distribution at any time. The reasons are outlined below:

(a) Insect population increase is extremely temperature dependent (Fig. 1.1) and it is important to know the likely places in which they will occur if control measures are not applied or fail.

(b) A more successful application of control measures can be achieved if a predicted temperature distribution can be obtained, e.g. where to place aeration ducts to achieve maximum cooling and whether to apply fumigants and inert gases at the top or base of a bin.

(c) The effect of painting silos white can be demonstrated in regard to its reduction of the maximum temperature and gradients. (The effect was shown by Yacuick et al. only for the centre of a bin.)

1.6 Assumptions used in Temperature Prediction

In all attempts to predict grain temperatures, several assumptions have to be made to simplify the problem. Not all these assumptions apply to the various methods of prediction, but the most important ones are discussed below.

(A) Thermal properties of the grain are constant in time and space

The important aspects to consider are the variation of conductivity and specific heat of wheat with both temperature and moisture content.

From Table 5.3 it can be seen that O'Brien calculates the thermal conductivity of his sample to vary from 0.116 to 0.126 $Wm^{-1} {}^{\circ}C^{-1}$ over the

temperature range 9.7 - 29.4 °C, i.e. approx. 8% over 20°C. Muir et al. (1972) find that the specific heat of wheat is also a function of temperature, varying from 1.5 to 1.6 $kJ\,kg^{-1}\,°C^{-1}$ over the range 0-20°C, i.e. approx. 6% over 20 °C. The important thermal property which determines the rate of change of temperature in grain is the thermal diffusivity. It can be seen from Eq. B.6 that this is proportional to the ratio of the conductivity and specific heat. Since both of these properties increase with temperature at approximately the same rate, there is little variation in diffusivity with temperature.

In the absence of insects, moisture content changes in time and space are small (Griffiths 1964). It seems reasonable, therefore, to consider the thermal properties to be constant.

(B) Thermal convection within the grain bulk can be ignored

Oxley (1948) and Babbit (1945) showed experimentally that this is true for small bulks. Oxley was unable to detect any reduction in apparent conductivity when paper baffles were put between concentric spheres of wheat and Babbit noted very little difference in the rate of heat transfer vertically upwards and downwards from a heated wire inserted along a horizontal cylinder of grain. However it may not be justifiable in a large silo.

(C) There is insignificant internal heat generated by the grain or organisms within it

This is reasonable if no insects are present. Griffiths (1964) states that "The respiration of the grain and the microorganisms (moulds) normally present is of no practicable importance" for moisture contents below 14%.

(D) Effects caused by precipitation can be ignored

This would be true in general, but perhaps not in situations such as India in the monsoon season or Canadian winters, where the silo walls would be cooled by both sensible and latent heat transfer.

(E) Cooling caused by dew evaporation can be ignored

Disney (1969) has shown experimentally that at normal storage moisture contents, no dew will form on the surfaces in contact with wheat except in the instance of extremely rapid temperature changes. However, it is clear that dew forming on the outer surfaces and inner head space surfaces would have the effect of stabilizing these surface temperatures at the dew points of the surroundings.

(F) Temperature changes due to transfer of water need not be treated explicitly

This assumption is discussed in Appendix A.

(G) Diurnal ambient temperature changes do not affect bulk temperatures

Ward and Calverley (1972) state that "Daily variations of the order of 10°C will be reduced to 1°C at a depth of 10 cm". A similar damping of the external wave is calculated by Babbit (1945).

(H) There is a negligible temperature drop across the silo walls

This assumption is valid for steel silos as the walls are thin and steel has a high thermal diffusivity.(This is referred to in Appendix B.) It is not valid for concrete silos since the walls are thicker and concrete has a much lower thermal diffusivity, or for wooden ones as wood has an extremely low thermal diffusivity.

(I) No vertical heat flow occurs

This is only a reasonable assumption when estimating temperatures far from the surface or base of a silo which is tall in comparison to its diameter. This assumption was made in all previous prediction models.

(J) Solar radiation effects can be ignored

This is only a reasonable assumption for silos which are adjacent to other buildings or perhaps if painted white.

Sinha and Muir (1973) comment on the results obtained by Muir (1970) "... The numerical method satisfactorily predicted temperatures during the winter cooling period, but in the spring, measured grain temperatures increased more rapidly than predicted temperatures. This difference appeared to be due to solar radiation, which had not been taken into consideration.".

(K) The annual temperature variation is a harmonic function of time

This assumption is not valid for many locations where the temperature fluctuate throughout the year.

(L) The initial temperature of the grain is uniform

This assumption need only be made in analytical models. In computer simulations, actual initial temperatures can be used.

1.7 Analytical Solution of Grain Temperatures

An analytical solution to the problem of predicting temperatures in cylindrical silos was sought by Converse et al (1973).

They employed all of the assumptions discussed above. Since their test silo was 33 m tall and 5 m in diameter, it is reasonable to assume

no vertical heat flow. As the walls were of concrete, there would be a temperature drop across them and this could be the main reason why their experimental results lag behind calculated ones. Neglecting solar radiation is reasonable in this case as the silo was almost surrounded by other bins. The requirement of a uniform initial temperature meant that the grain had to be turned several times before the start of the experiment.

It appears, therefore that the theoretical and experimental results agreed well for this analytical solution only because a carefully designed experiment was used to test the theory and it would not be a suitable method in general.

1.8 Computer Simulations

Muir (1970) constructed a digital computer program to predict temperatures in a cylindrical grain silo. He divided a silo into annular increments and estimated the temperature of each segment by a finite difference technique. He used all of the assumptions of Section 1.6 except (K) and (L). There was a difference of up to 7°C between predicted and experimental temperatures at the centre of the bin. This can probably be explained by his ignoring solar radiation as a variable.

Lo et al. (1975) used the same assumptions as Muir, with the additional rather dubious one that "the effect of (solar) radiation can be neglected because its effect is compensated for by representing ambient temperature by the daily maximum air temperature". They did not test their results against experiment.

A model by Yacuick, Muir and Sinha (1975) used the same assumptions as Muir's earlier model apart from (H) and (J). In this model the effect of different bin wall materials was considered, by including heat balance

equations for the walls. The effect of solar radiation was only considered insofar as the radiation on the south wall was estimated for 50% cloud cover and temperatures were only measured from the south walls to the centre of the bin. The results for the centre of the bin were little better than those of Muir in 1970.

CHAPTER 2

MODES OF HEAT TRANSFER

MODES OF HEAT TRANSFER

The main processes of heat exchange within the ecosystem of a silo and its surroundings are shown in Fig. 2.1.

The most important modes of heat transfer to and from the outer surface of the walls are forced and free convection, thermal radiation and solar radiation. Transfer within the grain bulk and through the base is considered to be by conduction. Within the head space, thermal radiation exchange between the roof and grain surface and free convection from all surfaces to the head space air are the predominant heat transfer mechanisms.

2.1 Conduction in the Grain

The heat flux by conduction, q_k, for a one-dimensional system is given by the Fourier equation:

$$q_k = - kA \frac{dt}{dx} \qquad (2.1)$$

where k = thermal conductivity*

A = heat transfer area

$\frac{dt}{dx}$ = temperature gradient in direction of heat flow.

The three dimensional finite difference form of Eq. (2.1) is developed in Chapter 3. In practice, both heat and moisture diffuse through grain under a temperature gradient. In Appendix A it is shown that the latent heat transferred in the combined process can be included by assuming a larger thermal conductivity than that for heat transfer alone.

2.2 Conduction through the Ground

The consideration of three-dimensional heat flow through the ground is an extremely complex problem. It was therefore assumed that the temperature of the ground near the silo, as calculated in Chapter 3, is equal to the temperature of the silo base.

---

* All units are S.I., unless otherwise stated.

Figure 2.1 - Heat transfer processes for a silo

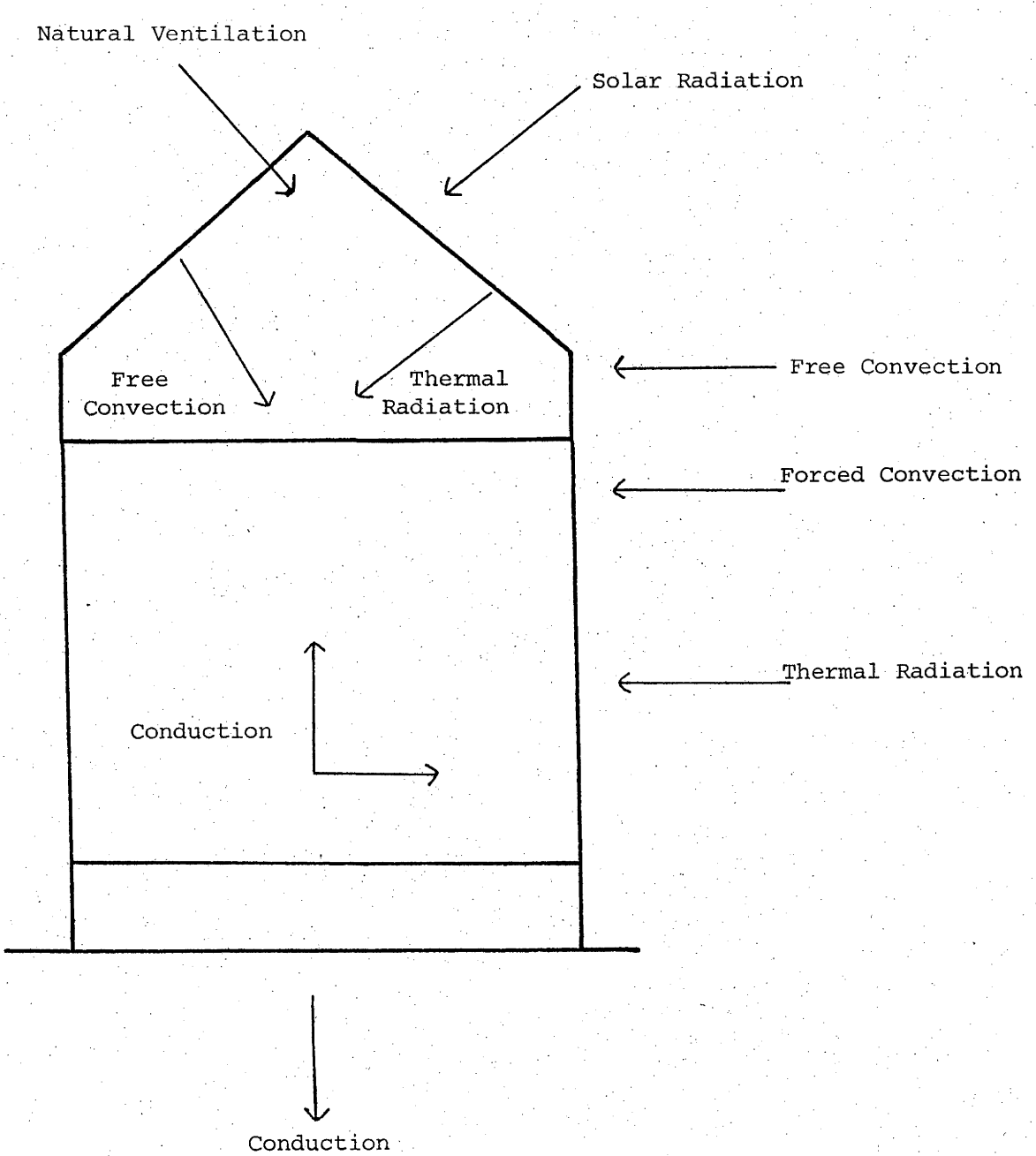

2.3 Forced Convection from the Walls and Roof

The heat flow, q_{wa}, by forced convection from the walls to the ambient air is given by:

$$q_{wa} = h_{wa} A_w (t_w - t_a) \tag{2.2}$$

where h_{wa} = coefficient of heat transfer by forced convection

A_w = heat transfer area of wall

t_w = wall temperature

t_a = ambient temperature.

An expression for h_{wa} is found in Chapter 5. Eq. (2.2) is also applicable to the roof, where 'w' is replaced by 'r'.

2.4 Free Convection in the Head Space

There are no simple expressions for convection in a cone. In his simulation of greenhouse temperatures, Kimball (1973) estimates convective heat flow by ignoring transfer from the walls and treating the roof as a flat horizontal surface. He assumes no heat is transferred when the roof is hotter than the vegetation, but since in the actual situation of a greenhouse (or a silo) there will be continual movement of the air due to one side of the roof being of a different temperature to the other, it is felt more appropriate to always have a finite heat flow.

The heat flux, q_{Fth}, by free convection between the grain surface and head space air can be expressed as:

$$q_{Fth} = h_{th} A_t (t_t - t_h) \tag{2.3}$$

h_{rh} and h_{th}, the transfer coefficients between the roof and head space and the bulk surface and head space respectively, can be described by expressions from Bosworth (1952), for horizontal surfaces:

$$h_{rh} = C_c \left| t_r - t_h \right|^{1/3} \tag{2.4}$$

$$h_{th} = C_c \left| t_t - t_h \right|^{1/3} \tag{2.5}$$

where C_c = 2.05 for a cool surface facing up or warm facing down

C_c = 0.97 for a warm surface facing up or cool facing down.

In these equations:

t_h = head space temperature

t_r = roof temperature

t_t = bulk surface temperature

These relationships are shown in Fig. 2.2, where Δt is the temperature difference in question. They are of the same order as typical values for a greenhouse given by Businger (1963).

2.5 Free Convection from the Walls and Roof

Approximating the roof by a flat horizontal surface, as was done in the previous section, the heat flux by free convection from the roof, q_{Fra}, is given by

$$q_{Fra} = h_{Fra} A_t (t_r - t_a) \tag{2.6}$$

where

$$h_{Fra} = C_c \left| t_r - t_a \right|^{1/3} \tag{2.7}$$

with C_c being defined as for free convection in the head space.

The free convective flux for the walls is calculated in the same manner, with 'w' replacing 'r' in the above equations and C_c being 1.53 (Bosworth, 1952).

2.6 Thermal Radiation Exchange between the Walls or Roof and Outside

Assuming that all the thermal radiation leaving the walls is absorbed by the sky and ground, the net radiant heat flow is given by:

$$q_{wg} + q_{ws} = \sigma A_w \varepsilon_w [F_{wg}(T_w^4 - T_g^4) + F_{ws}(T_w^4 - T_s^4)] \tag{2.8}$$

where q_{wg}, q_{ws} = radiant heat flow from wall to the ground and sky respectively

σ = Stefan-Boltzmann constant

Figure 2.2 - Free convection coefficient from a horizontal surface

(a) Bosworth - hot surfaces facing up

(b) Bosworth - cool surfaces facing up

(c) Businger - maximum value for a greenhouse

(d) Businger - minimum value for a greenhouse

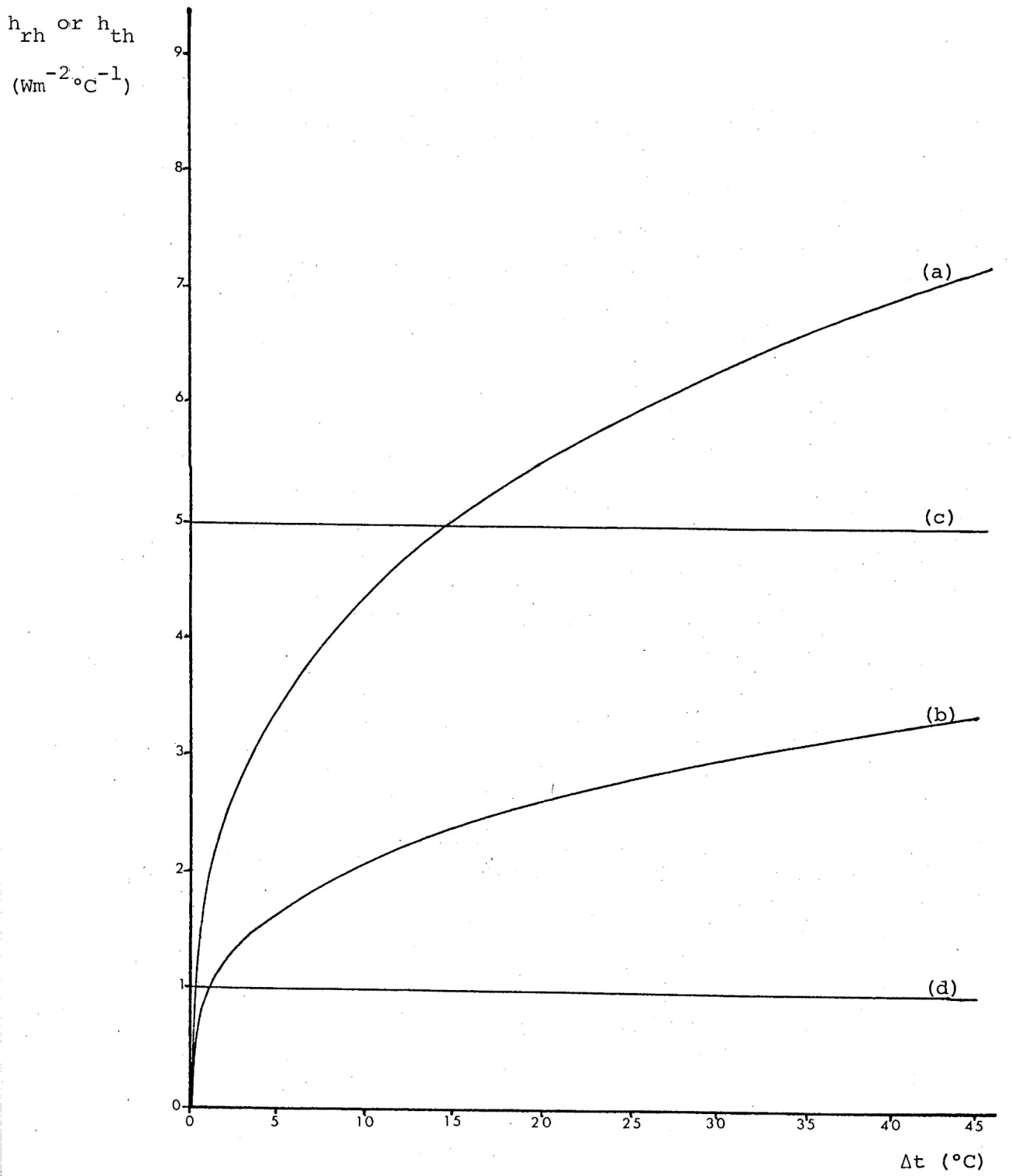

ε_w = thermal emittance of wall

A_w = surface area of wall

F_{wg}, F_{ws} = view factors

T_g = absolute temperature of ground

T_s = effective absolute temperature of sky

T_w = absolute temperature of wall

Holden (1961) proves that:

$$F_{wg} = \frac{1 - \cos \theta_w}{2} \tag{2.9}$$

where θ_w = angle between wall and ground.

When all the radiation from a wall is absorbed by other surfaces (ground and sky), the sum of the radiant interchange configuration factors must be one. This gives:

$$F_{ws} = \frac{1 + \cos \theta_w}{2} \tag{2.10}$$

Obviously, since $\theta_w = 90°$:

$$F_{wg} = F_{ws} = 1/2 \tag{2.11}$$

The effective radiating temperature of the sky is usually below ambient. Idso and Jackson (1969) found the following empirical relationship between clear sky and ambient temperatures:

$$T_s^4 = T_a^4 C_s \tag{2.12}$$

where C_s is given by Idso and Jackson as:

$$C_s = 1 - 0.261e^{-0.000777t_a^2} \tag{2.13}$$

Assuming that $T_s = T_a$ for a completely overcast sky, for a partly cloudy sky, the constant C_s is replaced by C_s' defined by:

$$C_s' = C_s {}^{n}/_{N} + (1 - {}^{n}/_{N}) \tag{2.14}$$

where ${}^{n}/_{N}$ = relative number of hours of bright sunshine.

To obtain a radiant heat flow in terms of a temperature difference,

as is the case for conduction and convection, the following approximation can be applied:

$$T_w^4 - T_g^4 = 4T_a^3(t_w - t_g) \tag{2.15}$$

$$T_w^4 - T_s^4 = 4T_a^3(t_w - C_s' t_a) \tag{2.16}$$

This linearization is valid since T_w, T_g and T_a are of similar magnitude.

Eq. (2.8) can now be expressed as:

$$q_{wg} + q_{ws} = h_{wg} A_w (t_w - t_a) + h_{ws} A_w (t_w - C_s' t_a) \tag{2.17}$$

where h_{wg}, h_{ws} = coefficients of radiant heat transfer, given by:

$$h_{wg} = 4\sigma\varepsilon_w \left(\frac{1 - \cos\theta_w}{2}\right) T_a^3 \tag{2.18}$$

$$h_{ws} = 4\sigma\varepsilon_w \left(\frac{1 + \cos\theta_w}{2}\right) T_a^3 \tag{2.19}$$

Expressions (2.9), (2.10) and (2.15) to (2.19) also hold for the roof, with 'r' replacing 'w'.

2.7 Radiation Exchange between the Roof and Grain Surface

Radiant heat flow, q_{rt}, between the roof of absolute temperature T_r and grain surface of absolute temperature T_t can be expressed by:

$$q_{rt} = \sigma A_t f_{rt} (T_t^4 - T_r^4) \tag{2.20}$$

where A_t = heat transfer area of grain surface

f_{rt} = modulus accounting for emittances and relative geometries of the roof and grain surface.

Since multiple reflections of thermal radiation occur inside the head space, the emittances and configuration factors cannot be separated (as was done in Section 2.6). Gebhart (1961) gives the following expression for f_{rt}:

$$f_{rt} = \frac{1}{\frac{1}{\varepsilon_t} + \frac{A_t}{A_r}\left(\frac{1}{\varepsilon_{ri}} - 1\right)} \tag{2.21}$$

where ε_{ri} = thermal emittance of inner surface of roof

ε_t = thermal emittance of grain surface

Using the approximation:

$$(T_t^4 - T_r^4) = 4T_r^3(t_t - t_r) \tag{2.22}$$

equation (2.20) becomes

$$q_{rt} = h_{rt}A_t(t_t - t_r) \tag{2.23}$$

where h_{rt} = coefficient of radiant transfer between roof and grain surface, given by:

$$h_{rt} = \frac{4\sigma T_t^3}{\frac{1}{\varepsilon_t} + \frac{A_t}{A_r}\left(\frac{1}{\varepsilon_{ri}} - 1\right)} \tag{2.24}$$

2.8 Solar Radiation on the Walls and Roof

Solar radiation records are available at very few places and data that is kept is usually only for a horizontal surface. However that absorbed by any part of a silo can be estimated from the following parameters:

(a) latitude, ϕ

(b) date and time

(c) air pressure, p

(d) relative number of hours of sunshine, $^n/_N$

(e) tilt angle of surface, θ

(f) azimuthal direction of surface, ψ

(g) albedo (reflectivity) of surroundings, η

(h) absorptivity of surface for solar radiation, α

Robinson (1966) develops a formula for solar irradiance, G_θ, including direct and diffuse components, falling on any surface at any location and time. It is:

$$G_\theta = I_\gamma [\cos\beta\ {}^{n}/_{N} + \sin\gamma \cos^3 {}^{\theta}/_{2}\ f({}^{n}/_{N}) +$$

$$\sin\gamma\ \eta\ (1 - \cos^2 {}^{\theta}/_{2})({}^{n}/_{N} + f({}^{n}/_{N}))] +$$

$$D_\gamma\ [0.25 \cos\beta/\sin\gamma\ {}^{n}/_{N} + 0.75 \cos^2 {}^{\theta}/_{2}\ {}^{n}/_{N} +$$

$$\cos^3 {}^{\theta}/_{2}\ f({}^{n}/_{N}) + \eta\ (1 - \cos^2 {}^{\theta}/_{2})({}^{n}/_{N} + f({}^{n}/_{N}))] \qquad (2.25)$$

where γ = angular height of the sun

I_γ = direct clear sky solar irradiance on a plane perpendicular to the beam at the earth's surface

D_γ = diffuse clear sky solar irradiance on a horizontal surface on the earth

β = angle between the position vector of the sun and the normal to the surface

$f({}^{n}/_{N})$ = sunshine function.

The parameters in Eq. (2.25) will be considered in turn.[1]

2.8.1 γ

The angular height of the sun, γ, is calculated using a heliocentric analysis (Smart, 1960). The equations will not be presented here, since use was made of a computer subroutine by Goodspeed (1970, 1975) which gives γ for any latitude at any time of day and time of year.

2.8.2 I_γ

Angström (1929) described I_γ by the following equation:

$$I_\gamma = \left(\frac{R_o}{R}\right)^2 \int_0^\infty I_\lambda 10^{-(m_p a_A + m_r a_d + a_w)}\, d\lambda \qquad (2.26)$$

where $\frac{R_o}{R}$ = mean sun-earth distance correction factor (from Goodspeed's program)

I_λ = direct, clear sky solar irradiance per unit wavelength, on a plane perpendicular to the beam, outside the atmosphere. It can be found from Table 2.1 from Robinson.

m_r = relative air mass (ratio of sun's path length to that if it were at the zenith). Robinson calculates it from:

$$m_r = \left(\left(\frac{R_e}{H_a} \sin\gamma\right)^2 + 2\,\frac{R_e}{H_a} + 1\right)^{1/2} - \frac{R_e}{H_a} \sin\gamma \qquad (2.27)$$

where R_e = radius of the earth

H_a = height of the atmosphere

m_p = relative air mass for a pressure of p, given by:

$$m_p = \frac{p\, m_r}{10^5} \qquad (2.28)$$

λ = wavelength in microns

a_A = Rayleigh extinction coefficient describing scattering by a pure atmosphere, given by Strutt (1881) as

$$a_A = 0.00386\ \lambda^{-4.05} \qquad (2.29)$$

a_d = coefficient representing extinction by dust, given by Robinson as:

$$a_d = B(2\lambda)^{-1.5} \qquad (2.30)$$

where the turbidity coefficient, B, can be obtained from Table 2.2.

a_w = coefficient representing absorption by water vapour, carbon dioxide and other gases. No simple formula, but Table 2.4 (from Robinson) gives a_w in terms of $m_r w$ for an average ozone concentration. w can be obtained from Table 2.3.

2.8.3 D_γ

Albrecht (1951) proposed the following formula for D_γ, which has been experimentally tested by Deirmendjian and Sekera (1956).

TABLE 2.1

The solar radiation spectrum outside the atmosphere

(Values of I_λ (Wm^{-2}) as a function of $\lambda(\mu)$)

λ	I_λ
0.2	30
0.4	1540
0.6	1810
0.8	1127
1.0	725
1.2	501
1.4	328
1.6	220
1.8	152
2.0	108
2.2	79
2.4	59
2.6	44
2.8	34
3.0	27

TABLE 2.2

Standard values of the turbidity coefficient, B, as a function of air pressure and latitude

Air pressure p (x 10^5 Pa)	Latitude ϕ 0°	30°	45°	60°	70°
1.0	0.13	0.10	0.08	0.06	0.05
0.9	0.08	0.06	0.05	0.04	0.03
0.8	0.05	0.04	0.03	0.02	0.02
0.7	0.03	0.02	0.02	0.01	0.01

TABLE 2.3

Total water content of the atmosphere, w (cm precipitable water), as a function of air pressure and latitude

Air pressure p (x 10^5 Pa)	Latitude ϕ 0°	30°	45°	60°	70°
Warm or wet season					
1.0	5.0	4.0	2.5	2.0	1.8
0.9	3.0	1.9	1.6	1.25	1.1
0.8	2.0	1.5	1.0	0.8	0.7
0.7	1.0	0.8	0.5	0.4	0.35
Cold or dry season					
1.0	3.0	1.5	0.8	0.5	0.3
0.9	2.0	1.0	0.5	0.35	0.2
0.8	1.0	0.6	0.3	0.2	0.1
0.7	0.6	0.3	0.15	0.1	0.05

TABLE 2.4

Values of a_w for absorption by water, carbon dioxide and other gases

$m_r w$ (cm)	Wavelength (μ) .76	1.125	1.75	2.5
1.0	0.011	0.058	0.160	0.435
4.0	0.040	0.129	0.223	0.683
10.0	0.081	0.210	0.266	0.863
20.0	0.138	0.272	0.295	1.000

TABLE 2.5

Values of $I_{m_r w}$ (Wm^{-2}) as a function of $m_r w$ (cm) and Δ_{m_r} (Wm^{-2}) as a function of m_r

$m_r w$	$I_{m_r w}$
1.0	1223
4.0	1145
10.0	1078
20.0	1027

m_r	Δ_{m_r}
1	22
2	42
4	70
10	134

$$D_\gamma = K_\gamma I_s \tag{2.31}$$

where I_s = loss in direct irradiance due to scattering.

K_γ is given by Robinson as:

$$K_\gamma = 0.5 \sin^{1/3}\gamma \tag{2.32}$$

I_s is expressed by Robinson as:

$$I_s = I_{m_r w} - \Delta_{m_r} - I_\gamma \tag{2.33}$$

where $I_{m_r w}$ = direct irradiance with absorption by water, dust and gases, excluding ozone, but with no scattering

Δ_{m_r} = direct solar irradiance absorbed by ozone.

$I_{m_r w}$ and Δ_{m_r} can be calculated from Table 2.5, which are Robinson's values converted to Wm^{-2} for an average ozone concentration.

2.8.4 $f(^n/_N)$

To understand the function $f(^n/_N)$, the clear sky global irradiance, G_γ, must be defined. It is given by:

$$G_\gamma = I_\gamma \sin\gamma + D_\gamma \tag{2.34}$$

$f(^n/_N)$ is defined by:

$$f(^n/_N) = \frac{D_c}{G_\gamma} \tag{2.35}$$

where D_c = diffuse irradiance passing through the clouds. Table 2.6 gives the average value of $f(^n/_N)$ for the four stations cited by Robinson.

2.8.5 β

β, the angle between the sun and the normal to the surface is given by:

$$\cos\beta = \sin\theta \cos\gamma \cos|\chi - \psi| + \cos\theta \sin\gamma \tag{2.36}$$

The azimuth of the sun, χ, can be obtained from Goodspeed's program.

TABLE 2.6

$f(^{n}/_{N})$ as a function of $^{n}/_{N}$

$^{n}/_{N}$	$f(^{n}/_{N})$
1	0
.9	.06
.8	.12
.7	.18
.6	.23
.5	.27
.4	.32
.3	.36
.2	.40
.1	.42
.0	.36

As was stated by Meiman et al. (1971), it is correct to use cos β in Eq. (2.36) and not sin β as was done by Robinson. If the term on the right hand size of Eq. (2.36) becomes negative, cos β is assigned the value zero.

The total radiation incident on a sloping surface in partly cloudy weather can now be calculated from Eq. (2.25). The heat absorbed by solar radiation, q_s, for a wall of area A_w and solar absorptivity α_w is given by:

$$q_s = \alpha_w A_w G_w \tag{2.37}$$

where G_w = solar irradiance falling on the wall. The same formula applies to the roof, with 'r' replacing 'w'.

2.9 Ventilation in the Head Space

Heat flow into the head space, q_{ha}, caused by ventilation, can be expressed by:

$$q_{ha} = h_{ha} A_r (t_h - t_a) \tag{2.38}$$

The formula developed by Businger (1963) for the ventilation coefficient, h_{ha}, of a greenhouse can be applied here. It is:

$$h_{ha} = \frac{v_h c_a \rho_a}{A_r} \tag{2.39}$$

where v_h = volume of air exchanged with the atmosphere each second

A_r = surface area of roof

c_a = specific heat of air

ρ_a = density of air.

v_h is discussed in Chapter 5 and A_r is given by:

$$A_r = \pi R_m (2H_e + R_m \sec \theta_r) \tag{2.40}$$

R_m, H_e and θ_r are shown in Fig. 3.1.

2.10 Magnitude of the Flux Densities

It is essential to have a quantitative estimate of the thermal flux densities involved for the various transfer mechanisms so that the relative

importance of each mode of transfer can be judged. It can then be decided which processes can be ignored and where an accurate estimate of a transfer coefficient is needed. The transfer processes in question are shown in Fig. 2.1.

In the following discussion, all parameters are taken from Table 3.1. and heat flux densities are in Wm^{-2}. Estimates of temperature (in °C) are obtained from weekly readings for positions in the grain bulk and from chart recorder records for positions where there is a diurnal variation.

2.10.1 Heat Balance for the Walls

(a) Conduction to the Grain

As was discussed in Section 1.6 (G), daily variations of temperature are only about 1°C for grain 10 cm from the wall.

Assuming a constant thermal gradient over the first 10 cm of grain from the wall, the flux density, Q_{wb}, is given by:

$$Q_{wb} = k_b (t_b - t_w)/.1 \qquad (2.41)$$

where t_b = temperature of grain 10 cm from wall.

The following table can be set up, using typical temperatures:

	Midday	Midnight
t_b	20	20
t_w	35	5
Q_{wb}	- 23	+ 23

As can be seen, for this case, the heat flux into the grain for the middle of the day equals that out in the middle of the night. Since, in general, the bulk temperatures will lie between the maximum and minimum wall temperatures, it will be assumed that the heat fluxes into and out of the grain do not affect the average wall temperature. (This greatly simplifies the heat balance equation for the walls (Eq. (3.23)) since t_w can now be found explicitly from external conditions.)

(b) Forced Convection to the Outside Air

The flux density, Q_{wa}, in this case is given by:

$$Q_{wa} = h_{wa} (t_a - t_w) \tag{2.42}$$

A table is again set up for estimation of Q_{wa}. (From Eq. (5.29), $h_{wa} \simeq 18.7$)

	Midday	Midnight
t_w	35	5
t_a	20	10
Q_{wa}	- 280	+ 94

(c) Thermal Radiation to the Sky and Ground

The flux density for radiation to the sky, Q_{ws}, and ground, Q_{wg}, is given by:

$$Q_{ws} + Q_{wg} = h_{ws} (t_s - t_w) + h_{wg} (t_g - t_w) \tag{2.43}$$

where

$$h_{ws} = h_{wg} = 2\sigma\varepsilon_w T_a^3 \tag{2.44}$$

Using typical temperatures:

	Midday	Midnight
t_w	35	5
t_s	10	0
t_g	25	5
$Q_{ws} + Q_{wg}$	- 79	+ 12

(d) Solar Radiation on the Walls

This is obviously very dependent on the time of year and direction in which the wall is facing. The solar radiation on a north and south facing wall on a clear day in Canberra on 21 March will be considered, using the tables of Spencer (1965).

The flux density, Q_s, is given by:

$$Q_s = \alpha_w G_w \qquad (2.45)$$

This gives:

	Midday	Midnight
North	596	0
South	313	0
Average of North & South	+ 455	0

Table 2.7 compares all the flux densities estimated in the foregoing sections.

TABLE 2.7 - Flux densities for the walls

	Midday	Midnight
Forced Convection	- 280	+ 94
Thermal Radiation	- 79	+ 12
Solar Radiation	+ 455	0

It can be seen from Table 2.7 that it is particularly important to have a good estimate of h_{wa} and α_w.

2.10.2 Heat Balance for the Grain Surface

(a) Free Convection to the Head Space Air

The flux density, Q_{th}, for this case is given by:

$$Q_{th} = 0.97\ (t_h - t_t)^{4/3} \qquad t_h > t_t \qquad (2.46)$$

$$= 2.05\ (t_t - t_h)^{4/3} \qquad t_t > t_h \qquad (2.47)$$

An estimate of Q_{th}, using typical values of t_h and t_t obtained from experimental measurements, is given in the following table.

	Midday	Midnight
$t_h - t_t$	+ 5	- 5
Q_{th}	+ 8	- 18

(b) Thermal Radiation to the Roof

The flux density, Q_{rt}, is given by:

$$Q_{rt} = h_{rt} (t_r - t_t) \tag{2.48}$$

where h_{rt} is defined in Eq. (2.24).

The following table can now be set up:

	Midday	Midnight
t_r	35	5
t_t	25	10
Q_{rt}	+ 50	- 22

(c) Conduction into the Grain

This will be ignored as was done in considering fluxes on the walls, since it will be assumed that the day and night fluxes are equal and opposite.

Table 2.8 compares the flux densities considered in the preceding sections.

TABLE 2.8 - Flux Densities at the grain surface

	Midday	Midnight
Free Convection	+ 8	- 18
Thermal Radiation	+ 50	- 22

Both thermal radiation and free convection are significant in the calculation of surface temperatures since their flux densities are of comparable magnitude, particularly at night.

2.10.3 Heat Balance for the Head Space Air

(a) Free Convection

The importance of free convection in the head space was discussed in the last section.

(b) Ventilation

The flux density due to ventilation, Q_{ha}, is given by:

$$Q_{ha} = h_{ha} (t_a - t_h) \tag{2.49}$$

where h_{ha} is given by Eq. (2.39).

Using the maximum values of v_h as obtained in Chapter 5, and a temperature difference of 10°C between the head space and ambient air:

	Q_{ha}
Large bin	0.1
Small painted bin	1.0
Small unpainted bin	1.7

These fluxes are obviously extremely low in comparison to the free convection flux discussed in 2.9.2.(a), so ventilation will be ignored in the model.

2.10.4 Heat Balance for the Roof

The mechanisms of heat transfer to air from the roof, i.e. forced convection, free convection, thermal and solar radiation, have all been considered in the previous sections. They were all found to be significant.

CHAPTER 3

THE COMPUTER MODEL

THE COMPUTER MODEL

3.1 Division of a Silo

The temperature distribution of a cylindrical silo is described by a three dimensional network of 'cells' as shown in Fig. 3.1. Each internal cell has an equal volume and the reference point (from which all distances relating to the cell are measured) is taken to be the geometrical centre of the cell. The outer cells are half the volume of those inside, since it is desirable to have their reference point at the edge of the silo, to simplify heat transfer calculations.

This method of cell division is similar to that adopted by Sharp (1974) in his two dimensional model of food cans and is felt to be preferable to that of Yacuick et al. (1975) who, in their one dimensional model of a silo, used evenly spaced cells with reference points equidistant from each cell boundary.

3.2 The Prediction Equations

The prediction equations are developed by applying a heat balance equation to each cell, using an implicit finite difference method.

Consider the heat transfer between a cell i, where i is an arbitrary single index, used to define a cell, and its n neighbours, where n goes from 1 to the number of neighbours. By the conservation of energy, using the basic Fourier equation (Eq. (2.1)), the following equation can be set up, as was done by Chapman (1960):

$$C_i \frac{(t_i' - t_i)}{\tau} = \Sigma_n \frac{k_{in} A_{in}}{x_{in}} (t_n' - t_i') \qquad (3.1)$$

Heat stored in i = Net heat conducted to i

where C_i = thermal capacity of i

τ = time increment

x_{in} = distance between geometrical centres of i and a neighbour, n

Figure 3.1 - Division of a silo for the computer model

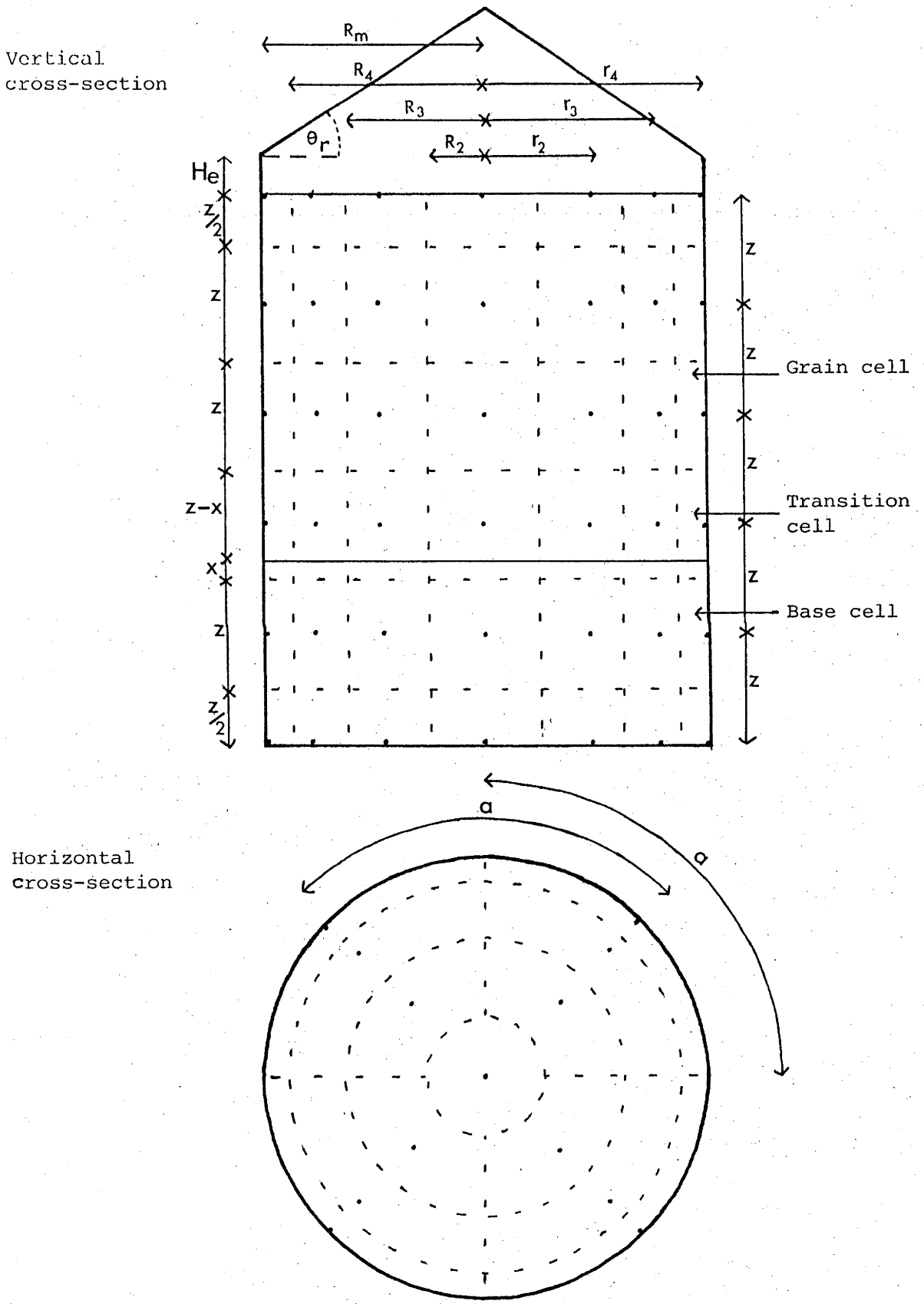

A_{in} = heat transfer area between i and n

k_{in} = thermal conductivity between i and n

t_i = present temperature of i

t_i', t_n' = future temperatures of i and n

C_i is defined by:

$$C_i = c_i V_i \rho_i \tag{3.2}$$

where c_i = specific heat of i

V_i = volume of i

ρ_i = density of i

Solving for t_i' in Eq. (3.1)

$$t_i' = \frac{t_i + \Sigma_n Fo_{in} t_n'}{1 + \Sigma_n Fo_{in}} \tag{3.3}$$

where the Fourier modulus, Fo_{in}, is given by:

$$Fo_{in} = \frac{k_{in} A_{in} \tau}{C_i x_{in}} \tag{3.4}$$

The choice of this implicit method is discussed in Appendix B.

3.3 Structure of The Computer Model

The basic structure of the model, designed to solve Eq. (3.3) is shown in Fig. 3.2. The segments of this diagram will be considered in the following sections.

3.3.1 Input

Table 3.1 gives a list of all parameters used by the model. Included in the table are values for the large experimental silo.

3.3.2 Fourier Moduli

These are considered in detail in Appendix C. The Fourier Moduli for each direction are given below. In the equations, j = 1 is at the centre and m = 1 at the base. R, r, z and a are shown in Fig. 3.1.

Figure 3.2 - Basic structure of the computer program

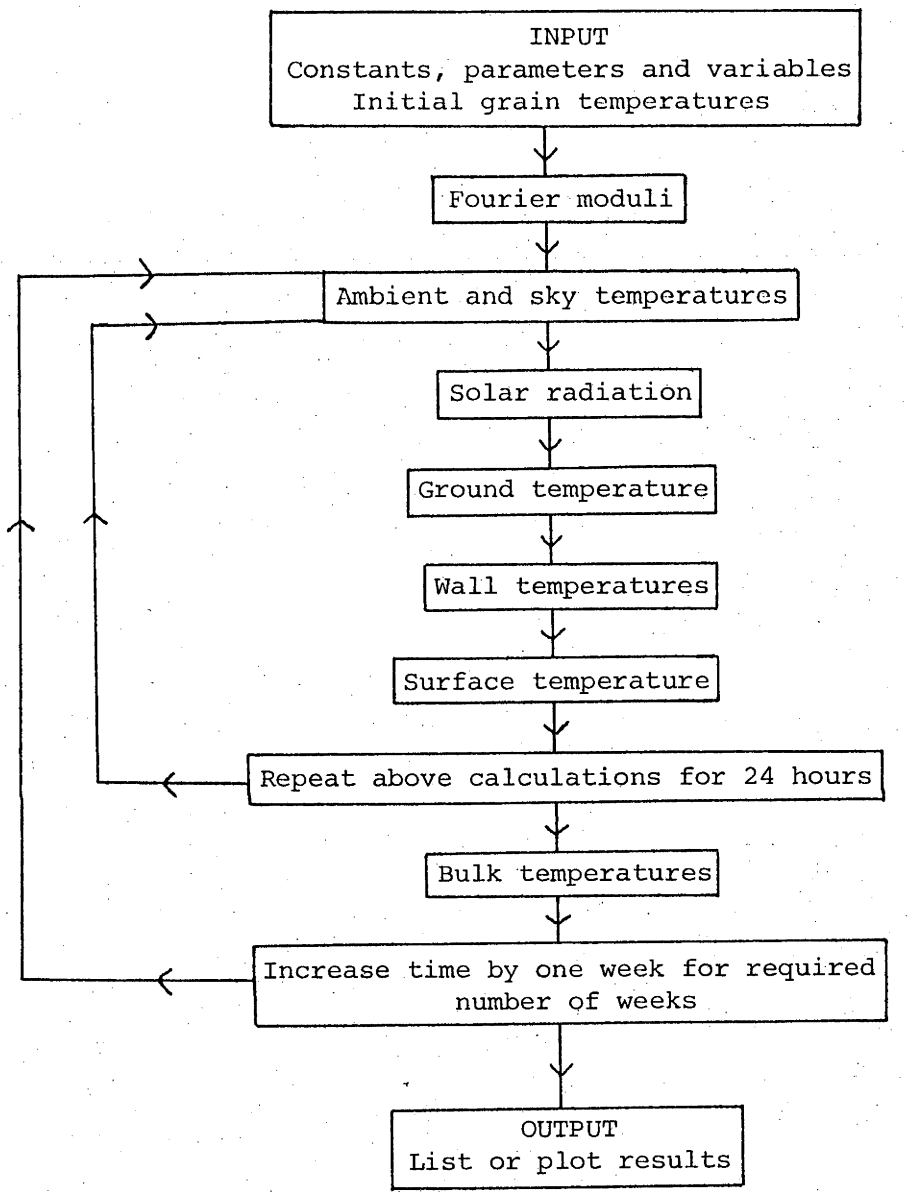

TABLE 3.1 - Parameters of the model

Key to References

C - Chosen

Ch.5 - See Chapter 5

L - Literature value

M - Measured

MB - Meteorolotical Bureau, Canberra

ME - Mechanical Engineering Data Sheet (1975)

R - Robinson (1966)

Parameter	Value for large silo	Reference
B	0.05	R
c_a	1012 $J kg^{-1} °C^{-1}$	ME
c_f	837 $J kg^{-1} °C^{-1}$	ME
H_b	2.2 m	M
H_e	0.4 m	M
H_f	0.5 m	M
j_m	3	C
k_a	0.026 $Wm^{-1} ° C^{-1}$	ME
k_b	0.15 $Wm^{-1} °C^{-1}$	ME
k_f	1.73 $Wm^{-1} °C^{-1}$	ME
l_m	4	C
m_m	5	C
$n/_N$	0.6	MB
p	0.95 x 10^5 Pa	MB
R_m	2.19 m	M

TABLE 3.1 (Cont'd).

t_{max}	27.5, 26.6, 24.3, 19.6, 14.9, 12.0, 11.1, 12.6, 15.8, 19.0, 22,0, 26.0 °C	MB
t_{min}	12.9, 12.6, 10.4, 6.5, 2.8, 0.8, -0.3, 0.8, 2.7, 5.8, 8.3, 11.1 °C	MB
u_r	1.5 m s^{-1}	MB
w	2 cm	MB
W_w	9.9%	M Ch.5
Z_o	0.01 m	L Ch.5
Z_l	2.0 m	MB
α_w	0.794	M Ch.5
ε_g	1.0	L Ch.5
ε_{ri}	0.83	M Ch.5
ε_t	0.95	Ch.5
ε_w	0.904	M Ch.5
η	0.26	R Ch.5
ρ_a	1.204 kg m^{-3}	ME
ρ_b	823 kg m^{-3}	M Ch.5
ρ_f	2400 kg m^{-3}	ME
ν	1.495 x 10^{-5} $m^2 s^{-1}$	ME
ϕ	-35°18'	

Radial (in) $$Fo_{i1} = \frac{k_{i1}A_{i1}\tau}{C_i(r_j - r_{j-1})} \qquad (j \neq 1) \qquad (3.5)$$

$$Fo_{i1} = 0 \qquad (j = 1) \qquad (3.6)$$

(Out) $$Fo_{i2} = \frac{k_{i2}A_{i2}\tau}{C_i(r_{j+1} - r_j)} \qquad (3.7)$$

Vertical (up) $$Fo_{i3} = \frac{k_{i3}A_{i3}\tau}{C_i z} \qquad (3.8)$$

(down) $$Fo_{i4} = \frac{k_{i4}A_{i4}\tau}{C_i z} \qquad (m \neq 1) \qquad (3.9)$$

$$Fo_{i4} = 0 \qquad (m = 1) \qquad (3.10)$$

Azimuthal $$Fo_{i5} = Fo_{i6} = \frac{k_{i5}A_{i5}\tau}{C_i r_j a} \qquad (3.11)$$

$$Fo_{i5} = Fo_{i6} = 0 \qquad (m = 1) \qquad (3.12)$$

3.3.3 Ambient and Sky Temperatures

The ambient temperature can be estimated from:

(a) The average monthly temperatures

(b) the time (date and time of day).

Meteorological data giving the average maximum, t_{max}, and average minimum, t_{min}, temperatures for each month is available for many locations. The average monthly temperature, t_M, is taken as the mean of these two values.

In the program, the start day is expressed in terms of one parameter (e.g. 210477 for 21 April 1977). For each week therafter, Goodspeed's subroutine is used to find the month number, M (M = 1-12) and the day of the month, K.

Letting the Mth month have N_M days, the average temperature of day K, t_{av}, can be expressed by a weighted averaging process:

For $K \leq N_M/2$, $M \neq 1$,

$$t_{av} = \frac{2(t_M(N_{M-1}/2 + K) + t_{M-1}(N_M/2 - K)}{N_M + N_{M-1}} \qquad (3.13)$$

For $K > N_M/2$, $M \neq 12$,

$$t_{av} = \frac{2(t_{M+1}(K - N_M/2) + t_M(N_M + N_{M+1}/2 - K))}{N_M + N_{M+1}} \qquad (3.14)$$

Obviously, for M = 1, M-1 is replaced by 12 in Eq. (3.13) and for M = 12, M+1 is replaced by 1 in Eq. (3.14).

The temperature range, t_{ar}, for a particular day can be found from equations analagous to Eqs. (3.13) and (3.14), with the temperature ranges for each month replacing the mean monthly temperatures.

The temperature, t_a, at a particular hour of the day, N_h, is calculated by assuming a sinousoidal variation with a minimum at 3 a.m. and maximum at 3 p.m. The appropriate equation is:

$$t_a = t_{av} + \frac{t_{ar}}{2} \cos(\pi(N_h + 9)/12) \qquad (3.15)$$

The sky temperature t_s can be found from t_a, using the theory in Section 2.6.

3.3.4 Solar Radiation

All terms for calculating I_γ from Eq. (2.26) are easily found (Section 2.8) except for a_w. The integral in Eq. (2.26) is to be calculated by obtaining its value at λ = 0.4, 0.6, 0.8 ..... 3.0 μ. As Table 2.4 does not give a_w at these precise points, the divided difference method (Williams 1973) is used.

The method is as follows:

First Table 3.2 is set up. y_o, y_1, y_2, y_3 are the points at which a function is given and f_0, f_1, f_2, f_3 the function values at these points. y must always lie between y_0 and y_3. From this table, coefficients a_o, a_1, a_2 and a_3 are calculated. These are used to define a polynomial P(y), for estimation of the function at any y. P(y) is given by:

TABLE 3.2 - Divided difference table

y_0 $\quad f_0 = a_o$

$$f_{01} = \frac{f_1 - f_0}{y_1 - y_0} = a_1$$

y_1 $\quad f_1$

$$f_{12} = \frac{f_2 - f_1}{y_2 - y_1}$$

$$f_{012} = \frac{f_{12} - f_{01}}{y_2 - y_0} = a_2$$

y_2 $\quad f_2$

$$f_{23} = \frac{f_3 - f_2}{y_3 - y_2}$$

$$f_{123} = \frac{f_{23} - f_{12}}{y_3 - y_1}$$

$$f_{0123} = \frac{f_{123} - f_{012}}{y_3 - y_0} = a_3$$

y_3 $\quad f_3$

$$P(y) = ((a_3(y-y_2) + a_2)(y-y_1) + a_1)(y-y_0) + a_0 \qquad (3.16)$$

When a_w has been calculated for the required values of λ and the values of $m_r w$ given in Table 2.4, the coefficients are obtained for finding a_w at any $m_r w$.

In Eq. (2.31), defining D_γ, there are two terms which are also given in tabular form. The above method is used to find these - i.e. $I_{m_r w}$ at any $m_r w$ and Δ_{m_r} at any m_r.

3.3.5 Ground Temperature

It is assumed that the temperature of the ground surface, t_g, is independent of temperatures under the ground. (This is analogous to the assumption made in the next section.)

A heat balance equation for the ground can now be set up:

$$(h_{ga} + h_{Fga})(t_a - t_g) + h_{gs}(t_s - t_g) + \alpha_g G_g = 0 \qquad (3.17)$$

where h_{ga} = coefficient of heat transfer by forced convection
h_{Fga} = coefficient of heat transfer by free convection
h_{gs} = coefficient of radiant heat transfer
G_g = solar irradiance on the ground
α_g = absorptivity of the ground for solar radiation (= 1-η).

h_{ga} can be expressed by the formula from Sellers (1965):

$$h_{ga} = u_r \left[\frac{0.4}{\ln (Z_r/Z_0)}\right]^2 c_a \rho_a \qquad (3.18)$$

where u_r = wind velocity at height Z_r
Z_0 = surface roughness.

For wind measured at a height of 2 m over short grass, $Z_0 \simeq 1$ cm, (Sellers, 1965)

$$h_{ga} = 6.94\, u_r \qquad (3.19)$$

h_{Fga} is analogous to h_{Fra} in Eq. (2.7) and h_{gs} is assumed to be given by:

$$h_{gs} = 4\sigma\varepsilon_g T_a^3 \qquad (3.20)$$

where ε_g = thermal emittance of the ground.

Rearranging Eq. (3.17) the ground temperature is given by:

$$t_g = \frac{(h_{ga} + h_{Fga})t_a + h_{gs}t_s + \alpha_g G_g}{h_{ga} + h_{Fga} + h_{gs}} \tag{3.21}$$

3.3.6 Wall Temperatures

The metal wall is considered to store no heat, since its thermal diffusivity is very high and it is very thin. This assumption was made by Muir (1970) in his simulation model of grain temperatures.

It is also assumed that the temperature of the wall is independent of the grain temperature (Section 2.10) and a function only of the external conditions.

A heat balance equation for the wall can be set up as follows:[2]

$$(h_{Fwa}+h_{wa})(t_a - t_w) + h_{wg}(t_g - t_w) + h_{ws}(t_s - t_w) + \alpha_w G_w = 0 \tag{3.22}$$

Solving for t_w:

$$t_w = \frac{(h_{wa} + h_{Fwa})t_a + h_{wg}t_g + h_{ws}t_s + \alpha_w G_w}{h_{wa} + h_{Fwa} + h_{wg} + h_{ws}} \tag{3.23}$$

h_{wg} and h_{ws} must be calculated from Eqs. (2.18) and (2.19) at each time step, since they are temperature-dependent.

3.3.7 Grain Surface Temperatures

Since the grain surface temperature is dependent on two unknown temperatures, that of the roof and the head space, it must be found from the solution of three simultaneous equations:[3]

$$t_r = \frac{h_{rh}t_h + h_{rt}t_r + (h_{ra} + h_{Fra})t_a + h_{rg}t_g + h_{rs}t_s + \alpha_r G_r}{h_{rh} + h_{rt} + h_{ra} + h_{Fra} + h_{rg} + h_{rs}} \tag{3.24}$$

$$t_h = \frac{h_{rh}t_r + h_{th}t_t + h_{ha}t_a}{h_{rh} + h_{th} + h_{ha}} \tag{3.25}$$

$$t_t = \frac{h_{th}t_h + h_{rh}t_r}{h_{th} + h_{rt}} . \tag{3.26}$$

These equations were obtained by setting up a heat balance, as was done for the wall temperatures.

An iteration method is adopted for the solution of these equations. An estimate of t_h, t_r and t_t is applied to Eqs. (2.4), (2.5) and (2.24) to obtain a value for h_{rh}, h_{th} and h_{rt}. (h_{rg} and h_{rs} are functions of T_a and are found explicitly by equations analogous to (2.18) and (2.19).) These heat transfer coefficients are used in the right-hand sice of Eqs. (3.24) to (3.26), along with the conjected temperatures, to give a new estimate of t_h, t_r and t_t. If the difference between the new and old estimates is greater than a given convergence criterion ($\simeq$ .1°C), the new temperatures are used to calculate a third set of temperatures. The process is repeated until the convergence criterion is satisfied.[4]

To speed up convergence, the new value of t_r from Eq. (3.24) and t_h from (3.25) are inserted into the other equations.

3.3.8 Bulk Temperatures

When the Fourier moduli and boundary conditions have been calculated, the new bulk temperatures are computed from Eq. (3.3). The iteration technique, described in the previous section is used.

3.3.9 Output

Since the number of cells in each dimension, j_m, m_m and l_m, can readily be altered and since certain aspects (like near-surface temperatures) were of interest experimentally, no attempt was made to make program and experimental temperature locations or 'points' coincide, except in the azimuthal direction where four positions seemed the most appropriate for experiment and theory.

However, predicted and experimental temperatures must be finally compared at the same locations, so a linear interpolation method was employed to estimate the program temperatures at the experimental points.

As an example of the method, the predicted temperature at experimental point C (with coordinates je, me, 1) in Fig. 3.3 will be determined. Fig. 3.4 is an enlargement of the area around C.

Figure 3.3 - Experimental and program temperature points

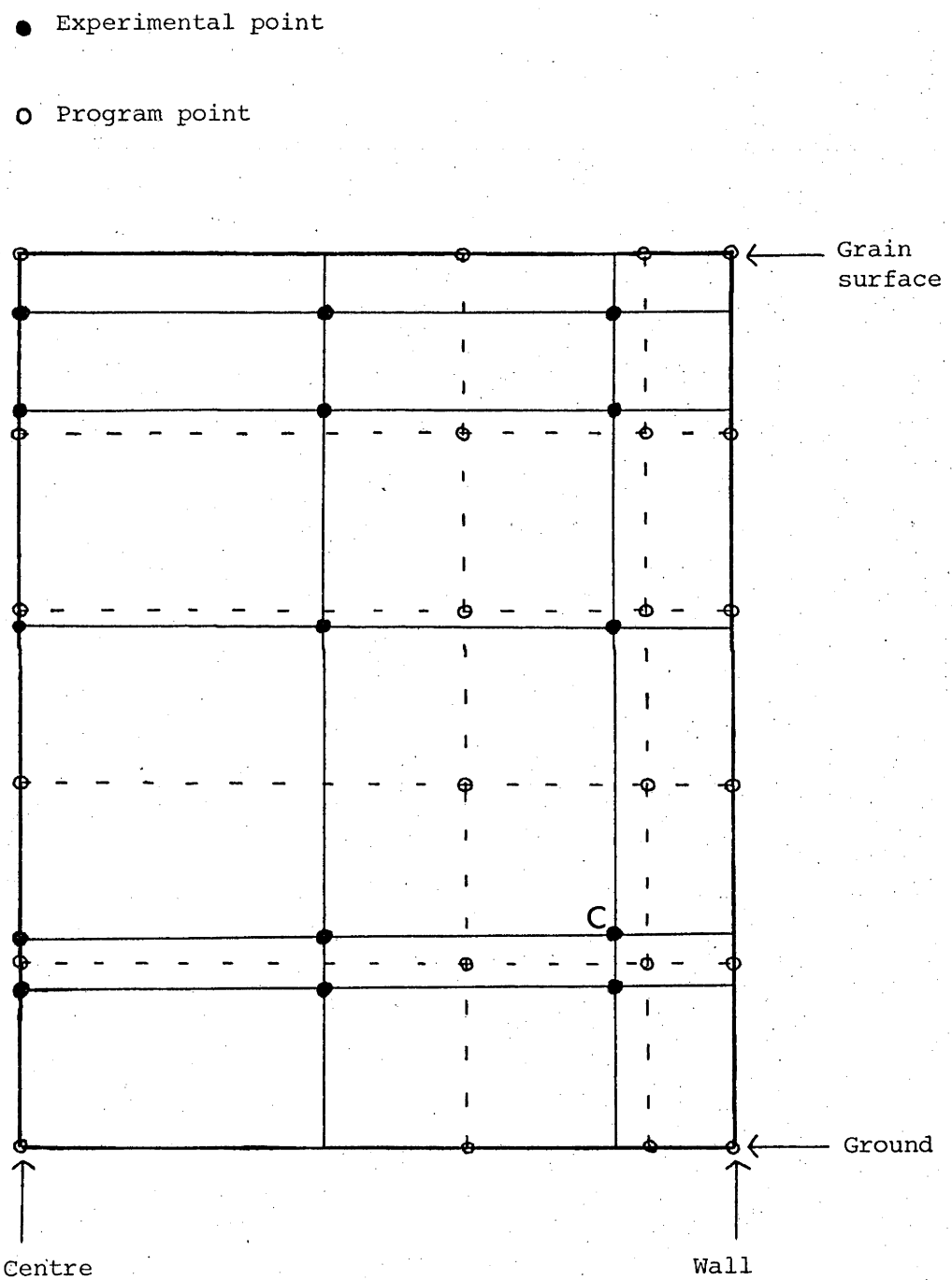

Figure 3.4 - Interpolation of predicted temperatures to find temperature at C

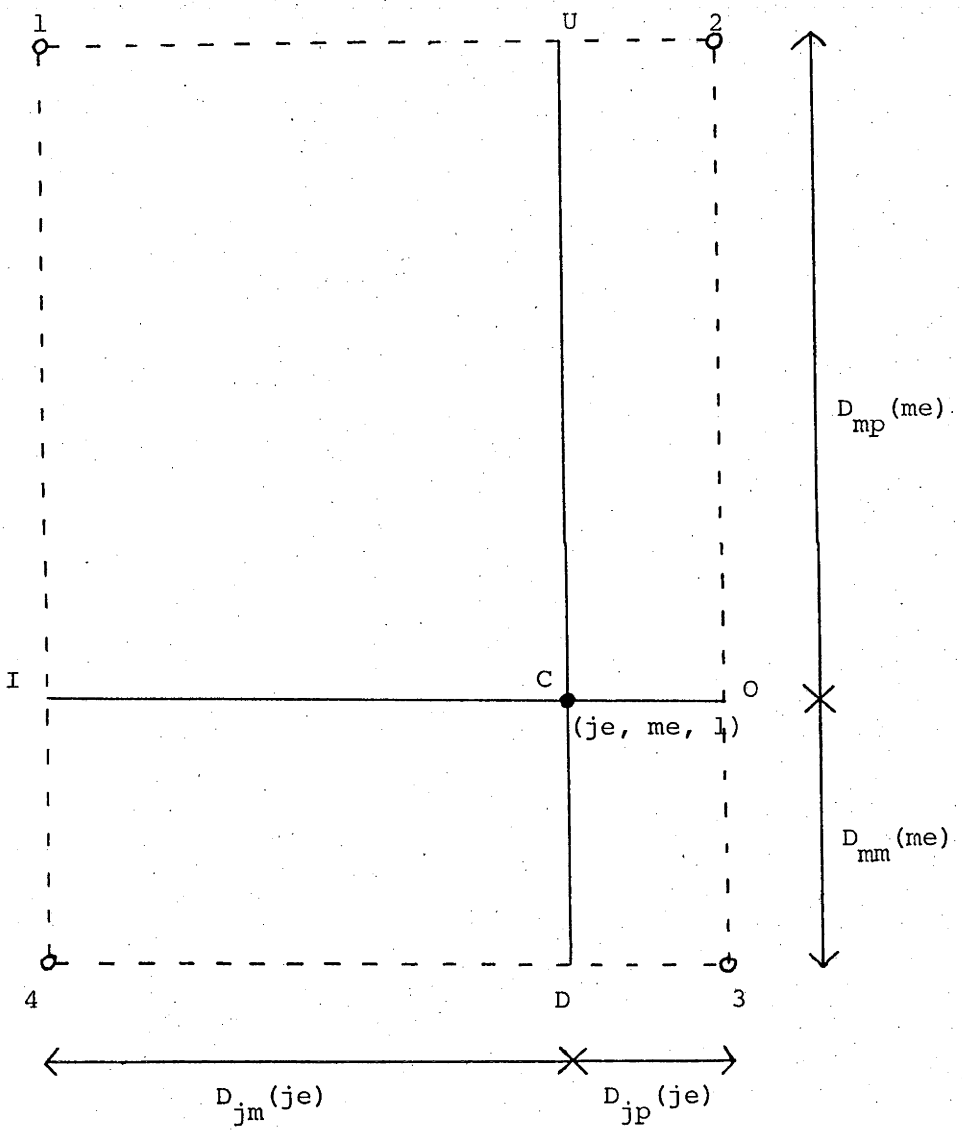

First the temperatures at O, I, D and U are found, assuming a constant temperature gradient between program points, e.g. the temperature at O, t_O, is given by:

$$t_O = \frac{t_2 D_{mm}(me) + t_3 D_{mp}(me)}{D_{mm}(me) + D_{mp}(me)} \qquad (3.27)$$

Then the temperature at C is found from the formula:

$$t_C = \frac{t_O D_{jm}(je) + t_I D_{jp}(je) + t_U D_{mm}(me) + t_D D_{mp}(me)}{D_{jm}(je) + D_{jp}(je) + D_{mm}(me) + D_{mp}(me)} \qquad (3.28)$$

The bulk temperatures predicted by the model can now be compared with those obtained by experiment. The results can be output in a tabular or graphical form. Some examples are shown in Chapter 6.

3.4 Cell Sizes and Time Steps

Computing time is saved by using large cell sizes and time steps, but the advantage of doing so must be weighed against any loss in accuracy, since errors using the finite difference technique depend on both these quantities.

3.4.1 Cell Sizes

By increasing the number of cells in the radial direction from three to six and those in the vertical direction from five to ten, the maximum difference in temperature was ·1°C. It therefore was decided that this four-fold increase in cell numbers was not warranted.

3.4.2 Time Steps for Prediction of Bulk Temperatures

As was discussed in Appendix B, there is no theoretical upper limit on the time step used for calculating bulk temperatures, using the implicit method. Since it was observed experimentally that bulk temperatures alter by approx. 1°C a week and since they cannot be measured to a much greater accuracy than this (Chapter 4), it was decided that a weekly time step would be suitable.

To check that this large time step produced effectively the same results as a much smaller one, the program was run on a daily basis and it was observed that the difference in temperatures was not greater than ·1°C.

3.4.3 Time Steps for Prediction of Boundary Temperatures

It was decided to estimate the temperatures of the walls and grain surfaces every hour ~~(on one day a week)~~. The reasons why this was thought necessary are:

(a) Solar radiation would have to be calculated at least every hour, anyway, to give an accurate daily value.

(b) Some heat transfer coefficients are temperature dependent, i.e.

  (i) Thermal radiation coefficients are proportional to the cube of the absolute temperature;

  (ii) Free convection coefficients are proportional to the temperature difference raised to the power 1/3 and their magnitude depends on the position of the hotter surface, which can reverse diurnally.

CHAPTER 4

THE EXPERIMENT

THE EXPERIMENT

4.1 Position and Structure of the Grain Bins

To test the validity of the computer model, three farm silos which had been erected on the CSIRO Black Mountain Site in Canberra were used. They are near to a small measurement shed and are shown in Fig. 4.1.

The largest silo is about fifteen years old and is made of corrugated galvanized iron sheets, 1.1 mm thick. The roof is made of eighteen flat sections of galvanized iron. The dimensions of the silo are shown in Fig. 4.4. The concrete base is square and just wide enough to accommodate the silo.

The two smaller silos are identical, except that one was later painted white. They are made of sheets of galvanized iron, 0.6 mm thick, the walls being very slightly corrugated and the roof being made of twelve flat sheets. The dimensions of the small silos are shown in Fig. 4.5. They both have a sand base.

Each silo contains twenty 'port-holes' so a check on the condition of the grain can easily be made.

The three silos were built closer together than would be desirable. This complicates the wind profile and therefore affects the convective transfer coefficient. It also influences the solar and thermal radiation.

The convective transfer coefficient is determined (in Chapter 5) as an average over the whole silo, independent of wind direction. It is calculated as a function of wind speed for turbulent conditions. The proximity of the silos to each other causes a change in wind direction and an increase in turbulence, but would not greatly alter the average value of the coefficient.

The effect of the closeness of the silos on solar radiation is shown in Fig. 4.6, where it can be seen that the cast (dark) shadows are only

Figure 4.1 - The three silos and measurement shed

Figure 4.2 - Inside a small silo

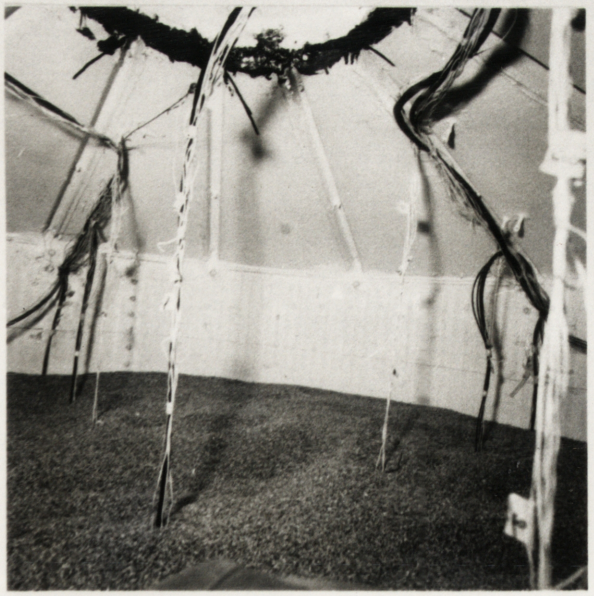

Figure 4.3 - Recording temperatures

Figure 4.4 - The large experimental silo (Distances in metres)

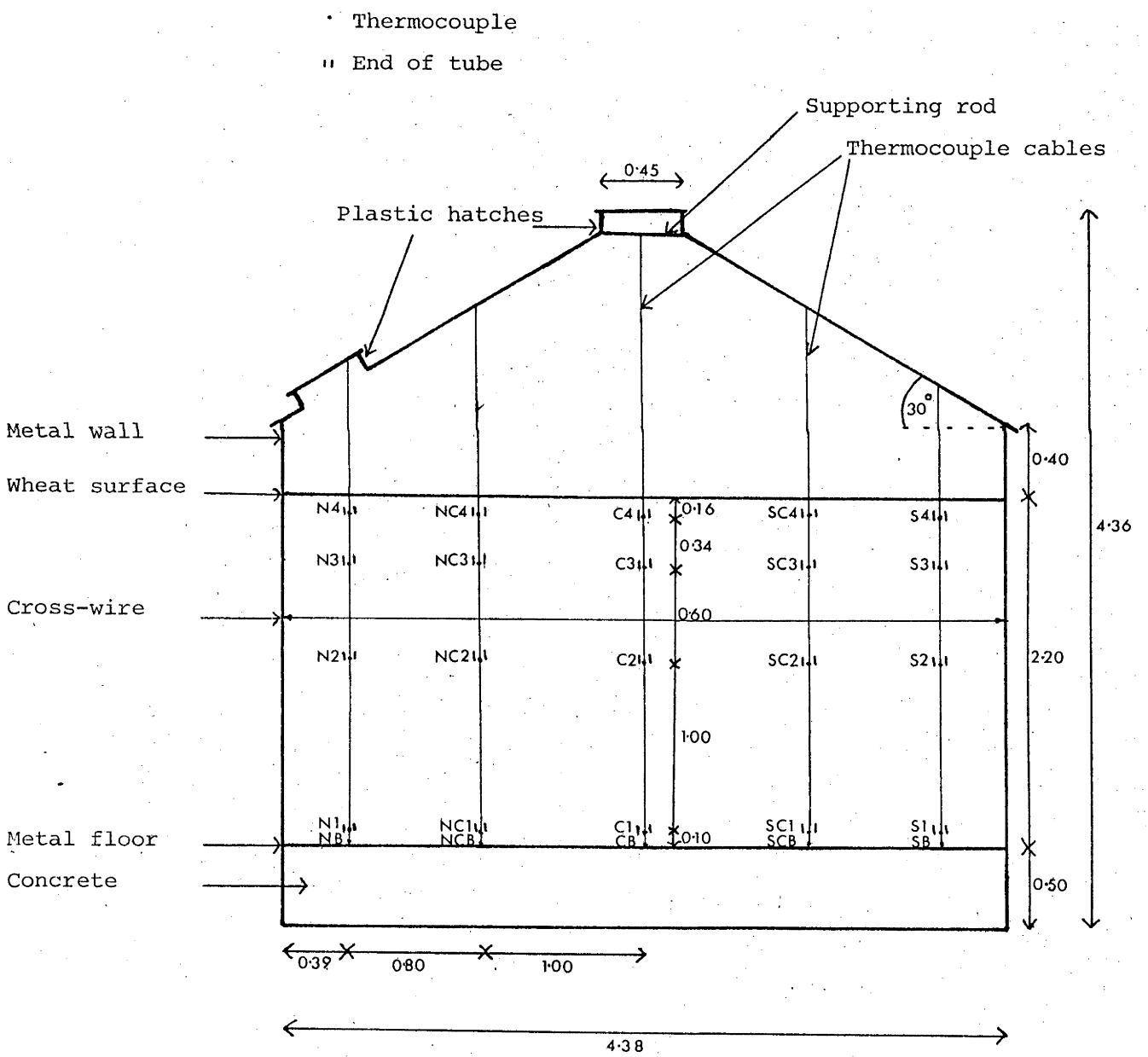

Figure 4.5 - The small experimental silos (Distances in metres)

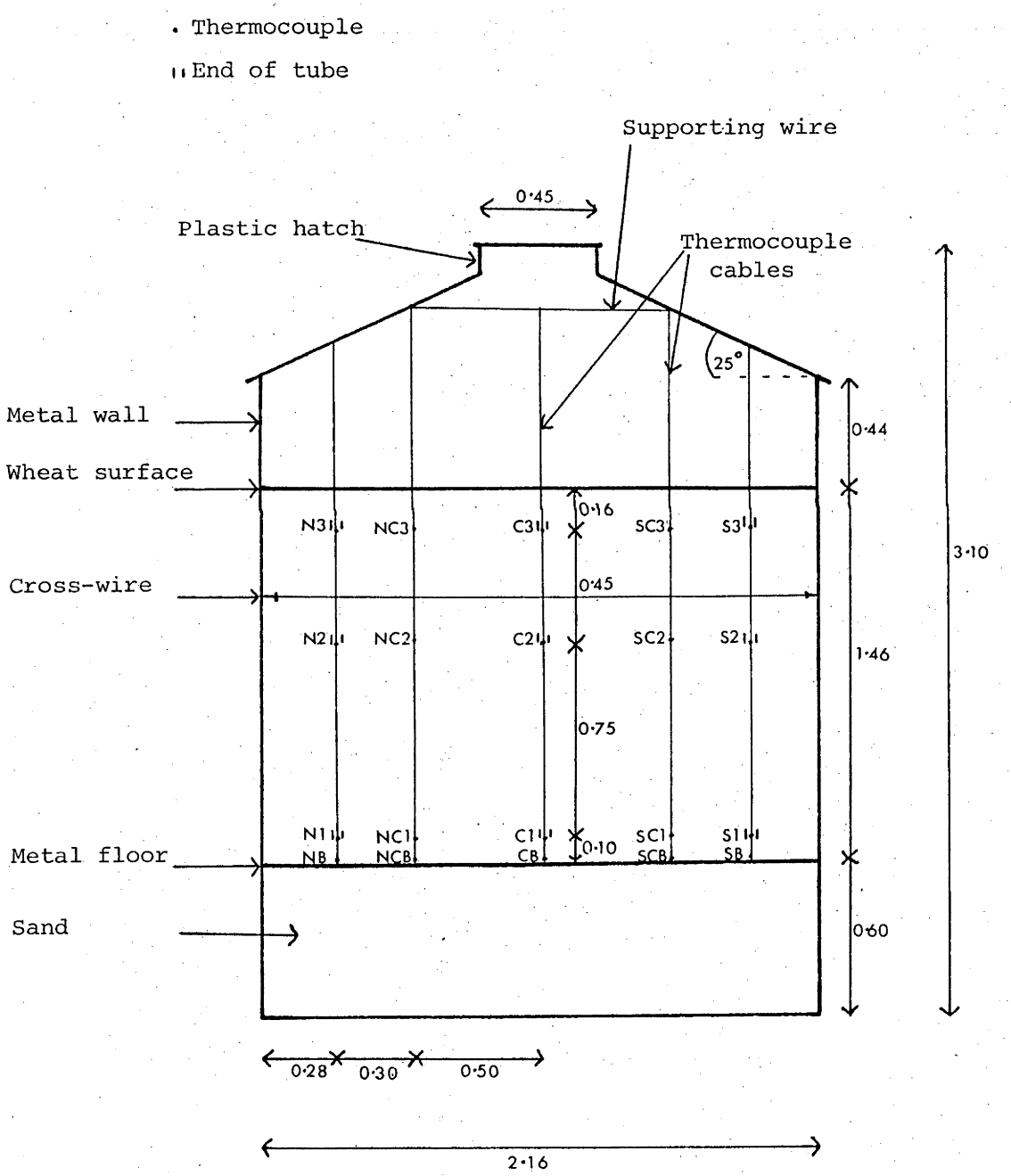

Figure 4.6 - Shading of the silos by one another.

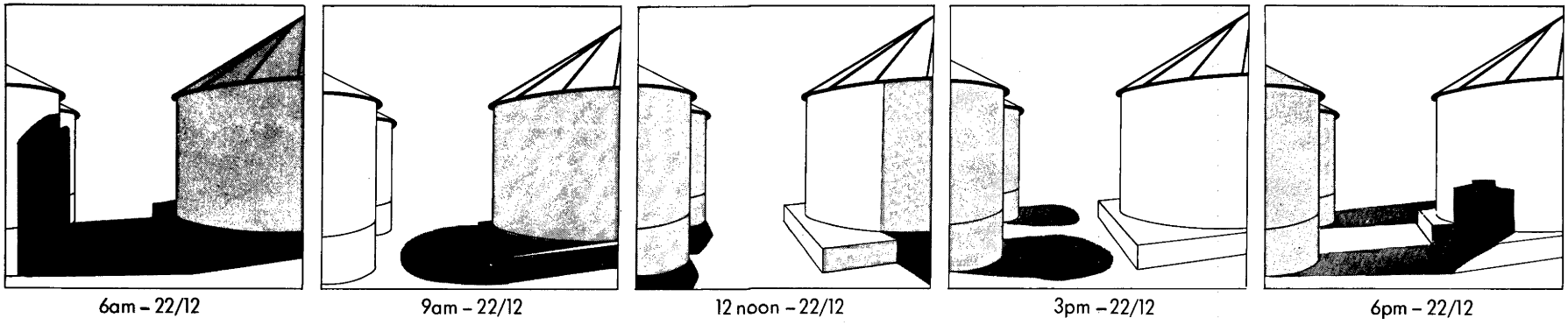

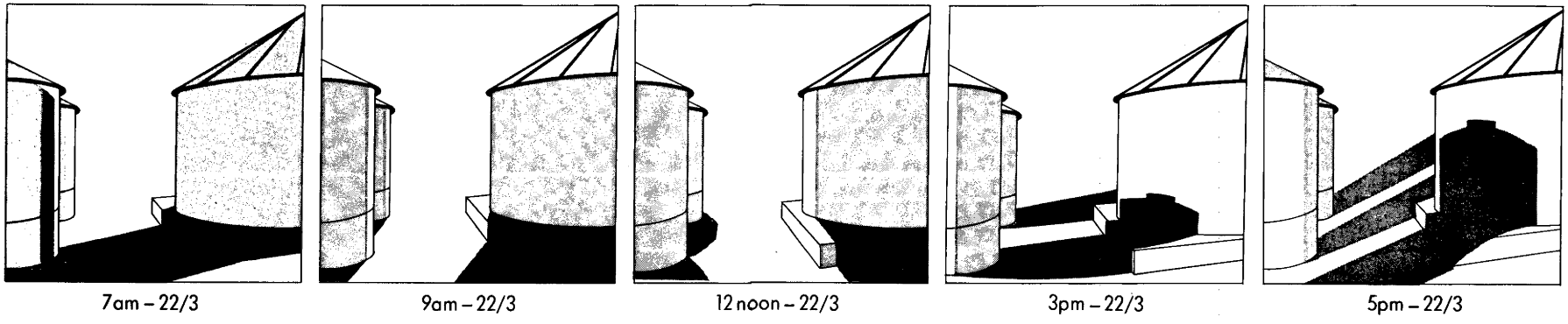

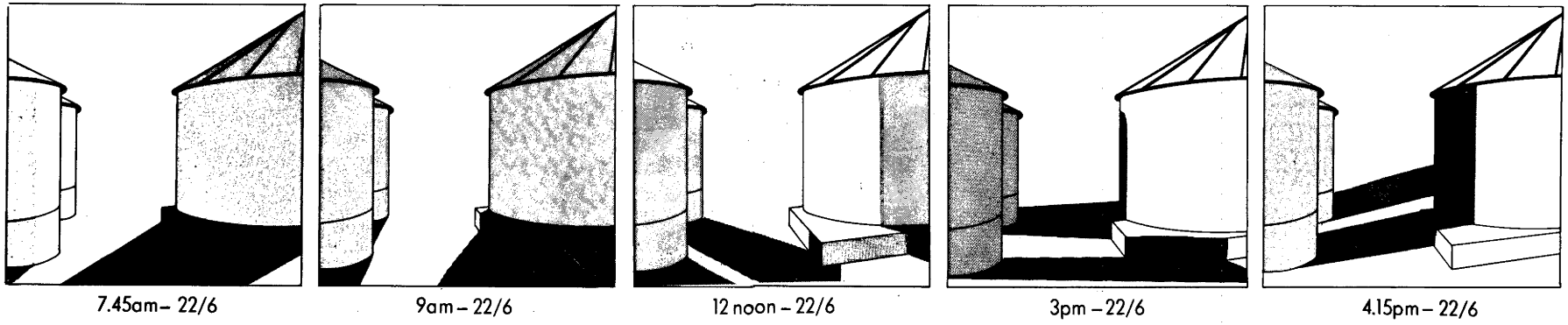

significant in the early morning and evening. This shading is discussed in Chapter 6.

Thermal radiation in general plays a smaller role in the overall transfer of heat from the silos than solar radiation and wind (Section 2.10). The consideration of complicated reflections of thermal radiation between silos is therefore not warranted.

The assumption that the proximity of the silos to each other has little effect on the internal temperatures is verified by an experiment, showing essentially the same temperature profiles in the two small silos before one was painted white (Chapter 6).

4.2 Preparation of Experiment

4.2.1 Cleaning and sealing

The silos were thoroughly swept, then cleaned with a wire brush and vacuum cleaner before any wheat filling.

In 1975 an attempt was made to seal the two smaller silos using 'Flintcote 5', a thick bitumen. Since the silos were constructed to be naturally ventilated, there were large gaps around the eves and these were sealed by covering fibreglass webbing with bitumen.

However, when the silos were emptied in January 1977, much wheat was damaged due to moisture ingress and wheat grains were extremely difficult to remove from the walls, since they stuck to the bitumen.

In 1977 all three silos were emptied and sealed with Envelon, a plastic substance which was sprayed on using special equipment. This job was done by Protecoat from Sydney. It was found to be much more satisfactory than 'Flintcote 5'.

The reasons for sealing the bins are given below:

(1) Many silos will be sealed in the future because of the increased use of storage under nitrogen and refrigeration as control measures.

(2) The grain keeps in better condition as the silo is watertight and

there is less likelihood of an infestation.

(3) Sealed silos are easier to model since the natural ventilation rate can be ignored (Section 2.10).

4.2.2 Eye-bolt attachments

Nine eye-bolts were fixed to the floor of all three silos. One was placed in the centre and the others at the radial positions desired for the cables (Figs. 4.4 and 4.5), two in each of the north, south, east and west sides. The direction was obtained using a compass, allowing for a magnetic variation of 12° to give the true bearings.

An eye-bolt was attached to the roof, above each one on the floor.

4.2.3 Thermocouple cables

Thermocouple cables were constructed as follows:

(1) The length needed to reach from the measurement shed to their position in the silo was determined for each thermocouple (about 10 m), then copper-constantin wire was cut to the correct length. It was labelled at one end by wrapping round a 2 inch piece of masking tape and marking with a felt pen. Figs. 4.4 and 4.5 show the notation for each thermocouple in the north and south positions. For east and west 'E' and 'W' replace 'N' and 'S'. Each silo is labelled with a different colour pen.

(2) Thermocouples were made at the opposite end of the wire from the label, by stripping 1/4" of the insulation and twisting the copper and constantin together three or four times. The end were clipped and the thermocouples soldered.

(3) Bowden cable, .045" in diameter, was cut long enough to reach from the floor to the roof of the silo and laid on a bench.

(4) Markings were placed alongside the Bowden cable corresponding to the positions for each thermocouple.

(5) The thermocouple to be at the base of the silo was attached first. This was done with filament tape, ensuring that the thermocouple was insulated from the cable by wrapping tape around the cable first.

(6) A second thermocouple was connected further up the cable, attaching the first wire to the cable at the same time. The whole cable was constructed in this manner.

(7) Nylon tubes were attached likewise, alongside certain thermocouples. (These tubes are to check the concentration of fumigants, should disinfestation be necessary, or to test for relative humidity.)

(8) The wires and tubes were taped together at intervals along their whole length.

The ends of the Bowden cable were attached to the eye-bolts in the silo by crimping on copper swages. The free end of the thermocouple cable was taken out of the silo through a suitable hole, which was then sealed with Silastic, a self-curing silicone rubber.

The thermocouples were connected to Comark selector units in the measurement shed. Each selector unit box can be connected in turn to a Comark thermometer. Fig. 4.3 shows temperature records being taken.

4.2.4 Cross-wires

The first time the small silos were filled (in 1975), the wheat flowing in through the top hatch pushed out all the cables, so that instead of being straight, they formed curves. In 1977 cross-wires were used. Eye-bolts were attached about half-way up the walls on the north, south, east and west sides of all three silos. Plastic-covered wire was tied through the eye at the north end. Measuring the required distance exactly, a knot was tied round the 'north (N) line', then 'north-centre' (NC), centre (C), 'south-centre' (SC) and 'south' (S). The other end was secured to the eye-bolt at the south side. The same was done for east-west, knotting this cross-

wire to the north-south one in the centre. This proved an extremely easy and satisfactory technique for keeping the thermocouples in position when the wheat was poured in.

4.2.5 Filling with wheat

In April 1975 Australian standard white (ASW) wheat was obtained from Cunningar, about seventy miles from Canberra. Each of the small silos, containing cables, were filled with about five tonnes of wheat, using an auger.

They were emptied in January 1977 and after sealing with Envelon and painting one white, all three silos were filled with new season's wheat on 6 and 7 April 1977. Again ASW wheat from Cunningar was delivered, this time using two loads of a truck and trailer having a capacity of twenty tonnes. About twenty-six tonnes was put in the large silo and five tonnes in each of the small ones. A pneumatic conveyor was used this time and it proved much quicker than the auger.

Although in the grain industry wheat is usually left in the pile it forms as it enters a silo, in the experiments a level surface was used. The reasons for this are:

(1) It is easier to walk on

(2) It is easier to put the grain surface back to its original position after walking on it

(3) It is easier to model.

It was critical to the experiment to have the same amount of wheat in each of the small silos. Bucket-loads of wheat were therefore carried between the silos until the same level was obtained! The wheat in these silos was then 16 cm above the top thermocouples. The height of the top thermocouples in the big silo were adjusted to this same depth. The completed inside of a small silo is shown in Fig. 4.2.

The hatches of the silos were then shut, to be opened as infrequently as possible to try to avoid rapid temperature changes or possibility of infestations.

4.3 Malathion determination

A representative sample of wheat was taken as the silos were filled and this was tested for Malathion content by Dr. Desmarchelier of the CSIRO Division of Entomology. The method is described in Desmarchelier et al. (1977).

The Malathion content was found to be 5.5%, which is not sufficient to control any insect pest. Therefore, throughout the experiment, a careful watch had to be made to ensure no infestations developed, by checking the surface and paying special attention to any high temperatures. Luckily there was no sign of infestations, probably because the silos were so well sealed.

4.4 Calibration of the Electronic Thermometer

The Comark thermometer was calibrated at the start of the experiment.

The circuit diagram for the calibration is shown in Fig. 4.7, alongside the expected values from Leeds and Northrup Temperature - Emf Tables (1975).

From Fig. 4.8. it can be seen that the ratio between experimental and theoretical values is constant. The thermometer is in error by $\simeq -.007°C$. Since other experimental errors are much greater than this (Section 4.5), this instrumental error can be ignored.

4.5 Errors in Temperature Measurement

The main sources of error in the measurement of temperatures in the grain bins are discussed below:-

Table 4.1

Calibration of the electronic thermometer:

Temperature difference on thermometer, °C	Digital Voltmeter Readings (V)		Expected Reading (V)
0-10	.391	.390	.391
0-20	.787	.784	.789
0-30	1.186	1.186	1.196
0-40	1.600	1.601	1.611
0-50	2.020	2.020	2.035

Figure 4.7 Circuit diagram for calibration of electronic thermometer

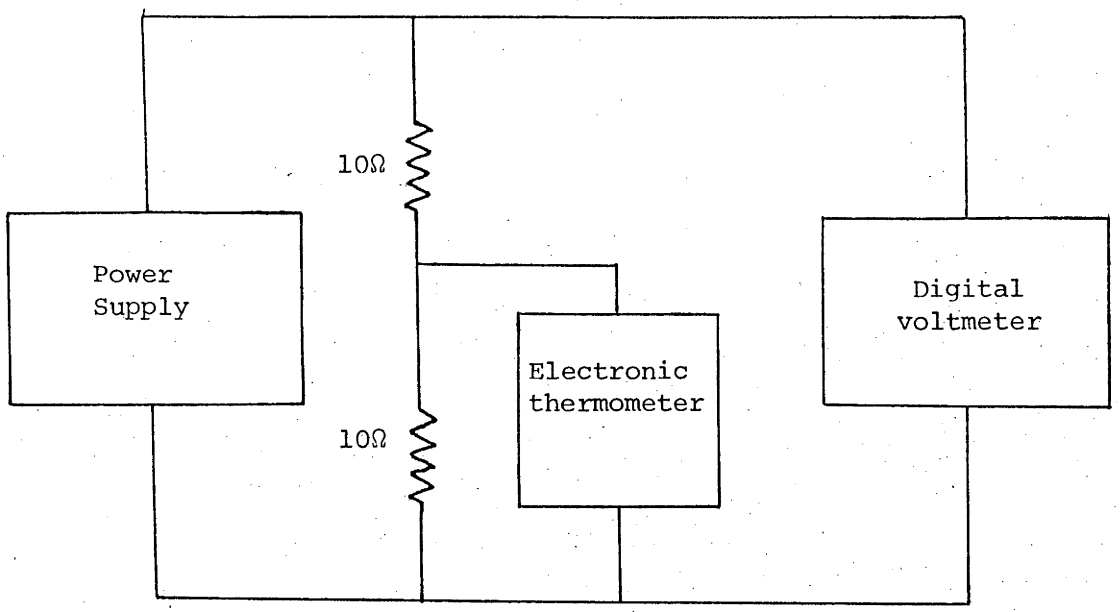

Figure 4.8 Calibration graph for electronic thermometer

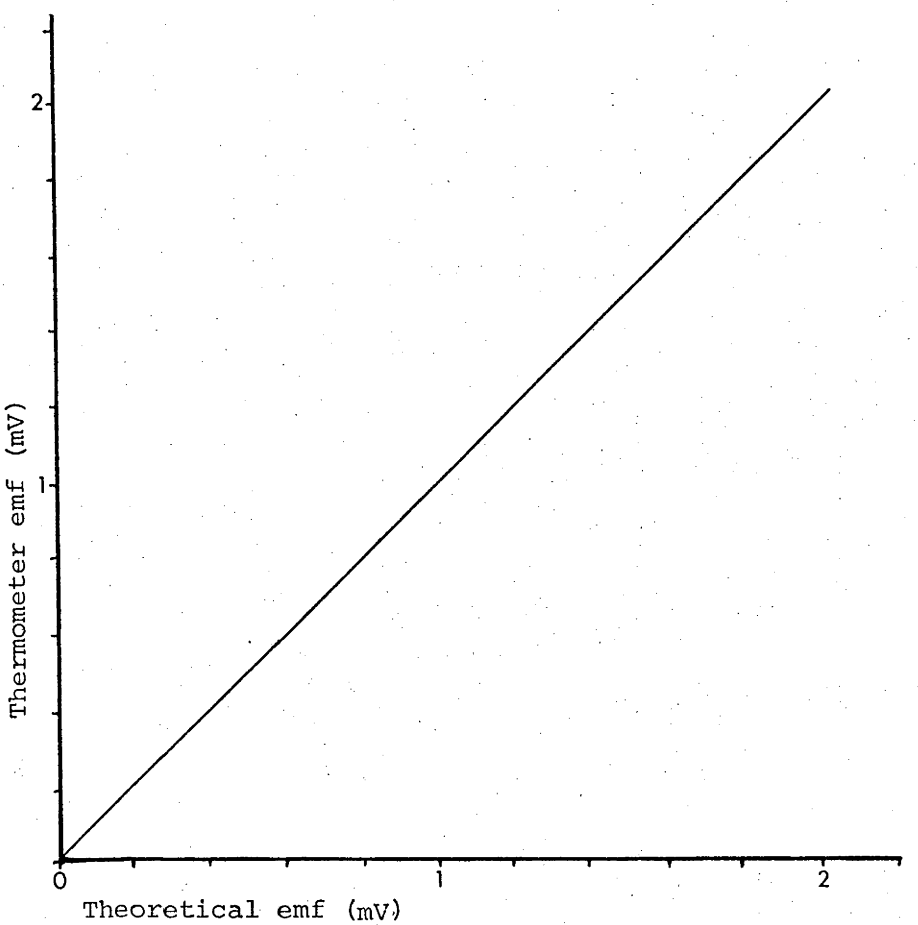

a) Accuracy of the thermometer

The calibration of the thermometer is described in Section 4.4. It was found to be accurate to .007°C.

b) 'Zero' on the thermometer

The 'zero' on the thermometer was set using an ice junction. The reading could drift up to .2°C between measurements and was therefore checked after each one.

c) Temperature - e.m.f. characteristics of thermocouples

Copper-constanstantin is one of the best combinations of materials for producing a reliable thermocouple. Uncalibrated wire is accurate to ± 1% (i.e. about .2°C at 20°C using an ice reference). (This information was gained from the Temperature Measurement Course at the National Measurement Laboratory, Sydney.)

d) Thermocouple junction errors

Since the contacts of the selector units are of stainless steel, an e.m.f. would be produced between the selector units and the thermometer if they were not at the same temperature. To minimise this problem, the thermometer was placed as near to the selector units as possible and aluminium foil was used to cover the windows of the measurement shed and thus stop the sun from shining on the junctions. By taking these precautions, the maximum observed temperature difference, on connecting the thermocouples directly to the thermometer was .2°C.

e) Static electricity

Particularly in dry weather, waving a hand over the thermometer would cause the needle to swing, owing to the poor shielding of the instrument from static electricity. To minimise this problem, aluminium foil was

placed around it and readings were always taken when standing away from the thermometer. An error of .2°C could be expected even then.

f) Parallax

Since measurements had to be taken whilst standing away from the thermometer, there was a possible parallax error of .1°C.

g) Wind

Wind would slightly strain the thermocouple lines between the silos and measurement shed and produce waving of the thermometer needle. Readings were not taken if the wind was too strong. An error of .1°C due to wind can be expected.

h) Radio-frequency interference

During the daytime it was usually impossible to take readings with the electronic thermometer. Eric Rumbo, an electronics expert from CSIRO studied the problem and suggested it may be caused by interference from the new TV tower nearby. However, on contacting them, it was found that they did not broadcast before 10 a.m. and problems with readings were experienced well before this. The exact cause of the problem was not found (perhaps it was electrical interference from the CSIRO site or radio waves), but it certainly was not noticeable before 1977. At many times it was impossible to 'zero' the thermometer.

By taking readings before 7 a.m. or after 10 p.m.,no problems from radio-frequency interference were observed.

Considering the problems of static electricity, wind and radio frequency interference, it is not surprizing that, although it was intended to take readings on Friday mornings, they were often not

obtainable until Saturday or Sunday. (In the graphs in Chapter 6 the exact day of the readings is plotted.)

By adding all of the above-mentioned errors, temperature readings can only be considered accurate to ± 1°C.

CHAPTER 5

PARAMETERS OF THE MODEL

PARAMETERS OF THE MODEL

A full list of parameters of the model was given in Table 3.1. It was indicated that several of these would be discussed in this chapter.

5.1 Moisture Content of the Wheat

The moisture content of the wheat, W_w, was determined at the start of the experiment, using part of the representative sample collected for malathion measurement. Two methods were employed.

In the more accurate oven method, 2 g wheat were weighed on a sensitive balance and placed on aluminium moisture dishes in a desiccator containing calcium oxide. The wheat was dried for 2 hr at 135°C and reweighed. The moisture content was calculated by dividing the weight lost in the oven by the original weight. The moisture content obtained was 9.9%.

A quicker, less precise method, using a Marconi meter, which works on the variation of electrical resistance with moisture content, gave a value of 10.1%.

5.2 Specific Heat of Wheat

The specific heat of wheat is affected to a large degree by moisture content, which is why the latter is a parameter of the model.[5]

Babbit and the Mechanical Engineering data sheet simply give one value (Table 5.1) but this is consistent with those of other workers for normal storage moisture contents.

It was decided to use the result of Disney which agrees well with that of Muir *et al.* but is given in terms of the wet weight of wheat, i.e.

$$c_b = 1.10 + 0.043\, W_w \qquad (5.1)$$

5.3 Conductivity of the Wheat

Table 5.2 gives several literature values for the conductivity of wheat[6] and Table 5.3 those obtained for the experimental wheat by Mr L.

TABLE 5.1 - Specific heat of wheat

Reference	Specific heat ($kJ.kg^{-1}\ °C^{-1}$)
Babbit (1945)	1.55
Pfalzner (1951)	$1.21 + .035\ W_w$
Disney (1954)	$1.10 + .043\ W_w$
Muir et al. (1972)	$1.10 + .041\ W_d$
Mech. Eng. (1975)	1.55

W_d = moisture content on a dry weight basis.

TABLE 5.2 - Literature values of the conductivity of wheat

Reference	Moisture content(%)	Average temp. (°C)	Thermal conductivity ($Wm^{-1}°C^{-1}$)
Kelly (1940)	-	-	.137
Oxley (1944)	11.7	31	.150
Babbit (1945)	8.4	37	.150
Moote (1952)	9.7	44	.146
Hooper et al. (1953)	-	-	.133
Mech. Eng. (1975)	-	-	.150

TABLE 5.3 - Conductivity of the experimental wheat as measured by L. O'Brien

Moisture content (%)	Average temp. (°C)	Thermal conductivity ($Wm^{-1}°C^{-1}$)
10.0	9.7	0.116
10.0	20.5	0.122
10.0	29.4	0.126

O'Brien of the CSIRO Division of Building Research in Melbourne.

O'Brien used a 30 cm x 30 cm guarded hot plate apparatus and the sample of wheat had a thickness of about 5 cm (Barned, 1970). His results are lower than all the literature values cited. There could be two main reasons for this:

(a) The small height of the sample - Since O'Brien's sample was only 5 cm thick, less heat would be transferred by convection than in all the other determinations quoted, where much larger samples were used.

(b) The drying of the sample prior to measurement - O'Brien dried the samples prior to measurement, since this is the normal practice in his determinations for building materials. Even though a 10% moisture content was attained after the three days of the experiment, the transfer of vapour would have been insignificant in the early stages. In Appendix A it is shown that the contribution of vapour diffusion to the apparent conductivity is very significant ($\simeq$ 30%).

In view of the above discussion it was decided not to adopt the measured value of conductivity for the model, but to use the highest value of 0.15 W m^{-1} $°C^{-1}$, as quoted by three sources.

5.4 Density of the Wheat

The density of wheat is a function of three main parameters:

(a) wheat type,

(b) moisture content,

(c) degree of packing.

Jones (1943) obtains values varying from 900 kg m^{-3} for tightly packed, hard, dry wheat to 680 kg m^{-3} for loosely packed, soft, wet wheat.

Measurements made on the experimental wheat give an average value of 823 kg m^{-3} and this value will be used for testing the model.

5.5 Radiative Properties of the Walls

Values must be given in the model for both the solar absorptance, α_w, and thermal emittance, ε_w, of the walls.

Table 5.4(a) gives literature values for galvanized iron. There is a wide range of values, depending on the exact composition of the material and its age. For this reason it was decided to have the thermal properties of the experimental silos determined. This was done by Mr E.A. Christie, of the CSIRO Division of Mechanical Engineering in Melbourne. The thermal emittance of envelon, with which the insides of the silos were sealed, was also determined. His results are shown in Table 5.5.

As can be seen from the tables, the experimental values agreed well with literature values for the two small bins, but the thermal emittance of the large bin was extremely high, rising between 1976 and 1977. It appears to be strongly oxidized, as can be seen by comparing with literature values for oxidized iron or steel given in Table 5.4(b).

Since the values given by Christie are consistent with the literature, they will be taken as representing the true thermal properties of the walls in the model.

5.6 Radiative Properties of the Grain and Ground

The values of ε_g, η and ε_t in Table 3.1 must be justified.

The thermal properties of the ground are obviously a function of the type of cover. Robinson (1966) gives various values of η. For green grass he suggests 0.26. This is used in testing the model, since the experimental bins are situated on grass. For a field of wheat Robinson gives η = 0.1 - 0.25 and for soil 0.1 - 0.3.

Kimball (1973) assumes $\varepsilon_g = 1$ in his simulation model for a greenhouse and Gates (1962) also assumes the earth's surface to radiate as a black body. A value of $\varepsilon_g = 1$ is therefore assumed in the model.

TABLE 5.4 - Literature values of radiative properties

	Solar absorptance	Thermal emittance
(a) Galvanized iron		
Dale and Giese (1953)	0.66-0.89	0.276-0.42
McAdams (1954)		0.228-0.276
Threlkeld (1962)	0.40-0.65	0.20-0.30
Petherbridge (1970)	0.65	
Kreith (1973)	0.66-0.89	0.23-0.28
(b) Oxidized iron or steel		
McAdams (1954)		0.64-0.94
Weast (1964)		0.7
Bolz and Tuve (1970)		0.6-0.85
Kreith (1973)		0.63-0.96
(c) White paint		
Dale and Giese (1953)	0.26	0.89
McAdams (1954)		0.906
Threlkeld (1964)		0.85-0.95
Weast (1964)	0.25	0.95
Bolz and Tuve (1970)	0.1-0.3	0.8-0.95
Christie (1971)	0.23	0.88
Kreith (1973)	0.18	0.95

TABLE 5.5 - Radiative properties of grain bins as measured by E. Christie in June 1977 (April 1976 values in brackets)

	Solar absorptance	Thermal emittance
Large bin	.794 (.752)	.904 (.750)
Small bin (unpainted)	.689 (.647)	.274 (.170)
Small bin (painted)	.232	.933
Envelon (white)		.93
Envelon (grey)		.83

As no literature value could be found for ε_t, it was hoped that Mr Christie, who measured the radiative properties for the silo walls, could measure the thermal emittance of wheat. However he felt this was not possible since the surface was so irregular, but he said it would be between 0.9 and 1. The value 0.95 was chosen.

5.7 Ventilation Coefficient

The ventilation coefficient for the head space, h_{ha}, is defined by Eq. (2.39). It is directly proportional to the volumetric rate of air exchange, v_h, which in turn is dependent on the size and location of holes in the bin walls and roof.

In order to estimate the hole size, the simple orifice equation of Hodgson (1917) can be used, as was done by Banks and Annis (1976). In this equation the volumetric flow rate, v, required to maintain a pressure difference between the inside and outside of the silo of Δp is given by:

$$v = C_o A_o \sqrt{\frac{2\Delta p}{\rho_a}} \qquad (5.2)$$

where C_o = Orifice coefficient

A_o = Hole area.

A 'pressure test' was performed on all three silos. A vacuum cleaner was used in its blowing mode to create a positive pressure inside the head space. The flow was altered using a stop-cock until the required pressure, as measured by a micromanometer, was obtained. The flow, measured on a flowmeter, was recorded. The apparatus is shown in Fig. 5.1 and the results plotted in Fig. 5.2.

From the slope of the graphs in Fig. 5.2, the effective hole sizes, $C_o A_o$, are found to be as follows:

Large bin - $C_o A_o = 1.3 \times 10^{-4}\ m^2$

Small painted bin - $C_o A_o = 4.8 \times 10^{-4}\ m^2$

Small unpainted bin - $C_o A_o = 7.5 \times 10^{-4}\ m^2$

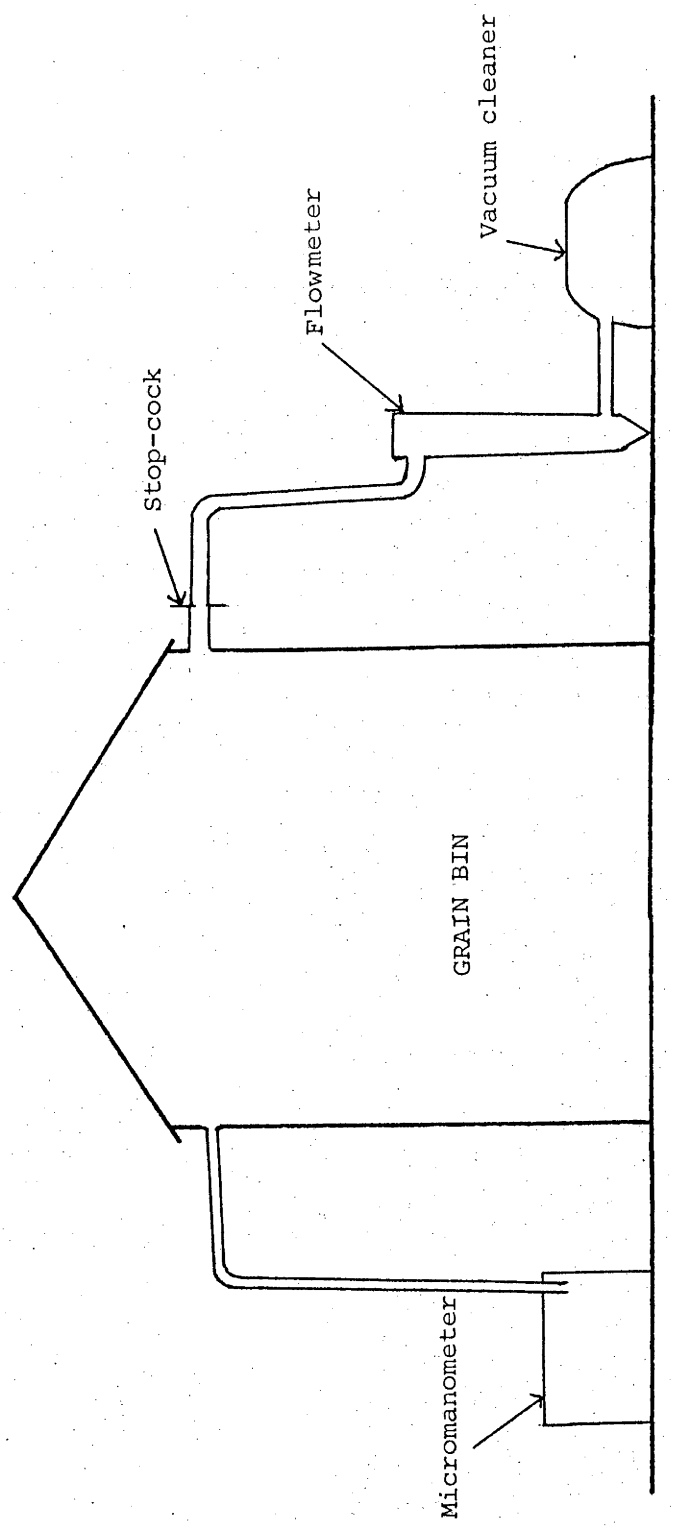

Figure 5.1 - Pressure test apparatus

Figure 5.2 - Pressure test results

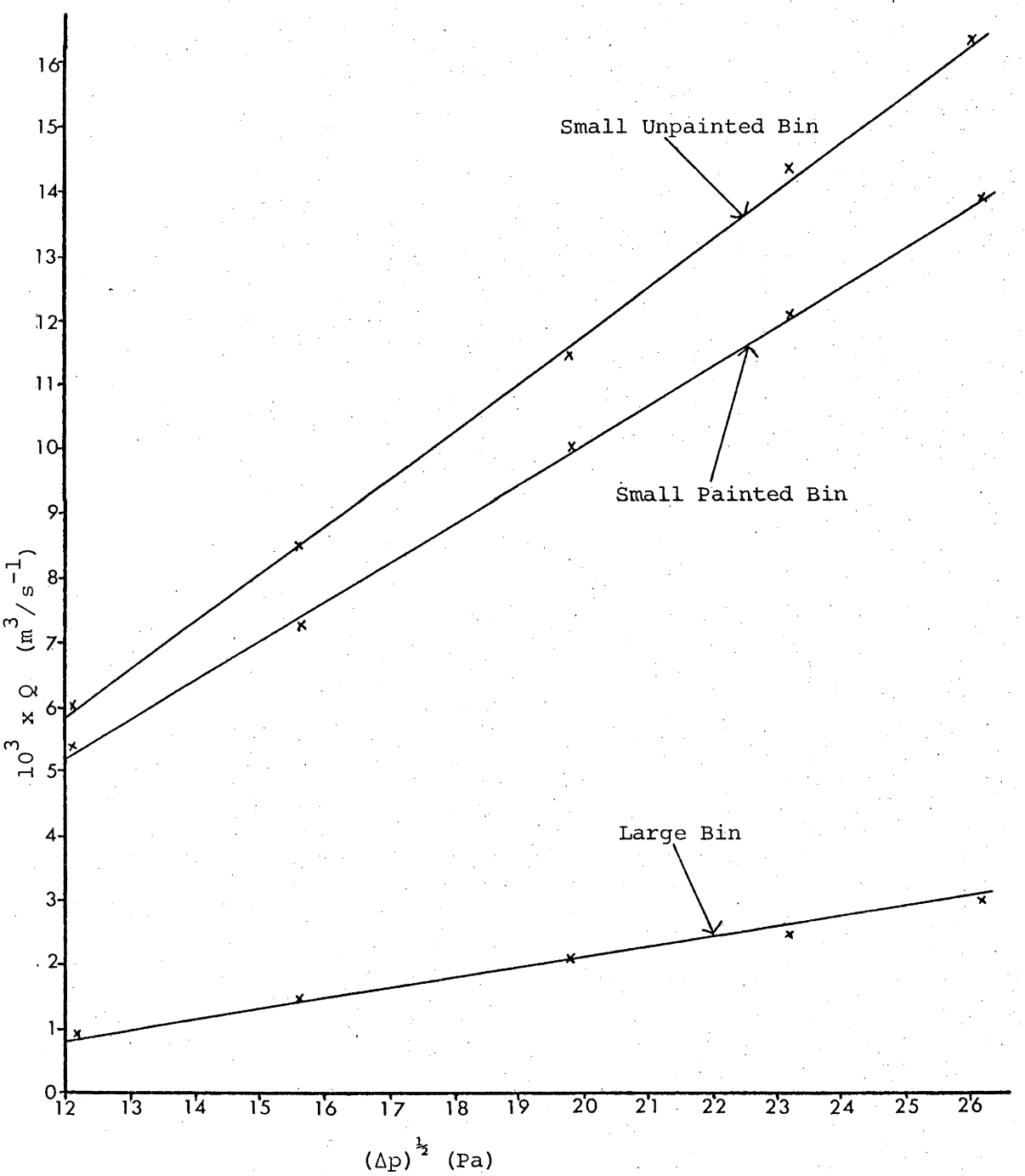

An estimate of v_h for each silo can be obtained using the results of Banks and Annis (1976), who calculated the contribution to v_h caused by all important effects - i.e. diffusion, temperature cycles, barometric fluctuations, the chimney effect and wind. One of the silos they considered had the dimensions of the small experimental silos. They found that for grain stores of this size, with holes approx. 10^{-4} - 10^{-5} m^2, the two predominant modes of air exchange were wind and the 'stack' effect.

5.7.1 Wind

The effect of wind can be estimated using the Bernouille equation. When wind flows through two holes the total pressure drop across them, Δp_u, is given by:

$$\Delta p_u = \frac{\rho_a}{2} \Delta C_p u^2 \qquad (5.3)$$

where ΔC_p = difference in pressure coefficients of the holes

u = wind velocity

Δp_u can be expressed in a form analogous to Eq. (5.2):

$$\Delta p_u = \frac{\rho_a}{2} \frac{v_u^2}{(C_o A_o)_{eq}^2} \qquad (5.4)$$

where v_u = volumetric rate of air exchange due to wind

$(C_o A_o)_{eq}$ = equivalent effective hole size.

The same effective hole size as was employed in Eq. (5.2) cannot be used for the case of wind as, in the pressure test experiments used to calculate $C_o A_o$, all the flow was out of the bin. For an air exchange caused by wind, air flows in one way and out the other.

$(C_o A_o)_{eq}$ is calculated as follows:

For two holes of effective sizes $C_1 A_1$ and $C_2 A_2$ with pressure drops across them of Δp_1 and Δp_2,

$$\Delta p_1 + \Delta p_2 = \frac{\rho_a}{2} v_u^2 \left(\frac{1}{(C_1 A_1)^2} + \frac{1}{(C_2 A_2)^2} \right) \qquad (5.5)$$

$$\Delta p_1 + \Delta p_2 = \Delta p_u \tag{5.6}$$

Combining these equations with Eq. (5.4)

$$(C_o A_o)^2_{eq} = \frac{(C_1 A_1)\ (C_2 A_2)}{(C_1 A_1)^2 + (C_2 A_2)^2} \tag{5.7}$$

Assuming the holes are of equal size:

$$C_1 A_1 = C_2 A_2 = \frac{C_o A_o}{2} \tag{5.8}$$

$$\therefore \quad (C_o A_o)_{eq} = \frac{C_o A_o}{2\sqrt{2}} \tag{5.9}$$

v_u can now be found from Eqs. (5.3), (5.4) and (5.9), i.e.:

$$v_u = \frac{C_o A_o}{2} \sqrt{\frac{\Delta C_p}{2}}\, u \tag{5.10}$$

In their wind tunnel experiments, Mulhearn *et al.* (1976) find values of pressure coefficients for model silos ranging from + 1.0 to - 1.8. To estimate the maximum air exchange, it will be assumed that the holes are oriented such as to give $\Delta C_p = 2.8$.

The average wind speed, u_r, at a reference height, Z_r, can be obtained from meteorological data. It seems logical to base u in the above equations on the wind speed, u_e, at the height of the eves, Z_e, since this is representative of the head space height and the join between the walls and roof is one of the most likely leakage sites. u_e can be calculated, assuming a logarithmic wing profile, from the relation:

$$u_e = \frac{\ln (Z_e/Z_o)}{\ln (Z_r/Z_o)}\ u_r \tag{5.11}$$

Using the average wind speed for Canberra ($u_r = 1.6 m s^{-1}$ at $Z_r = 2$ m) the maximum expected flow rates for the three silos are:

Large bin - $v_u = 1.3 \times 10^{-4}\ m^3 s^{-1}$

Small painted bin - $v_u = 4.7 \times 10^{-4}\ m^3 s^{-1}$

Small unpainted bin - $v_u = 7.4 \times 10^{-4}\ m^3 s^{-1}$

5.7.2 The Stack Effect

If two leaks in a structure are separated by a vertical distance, d, and the density of the air inside, ρ_h, is different from that outside, ρ_a, there will be pressure drop across both leaks, Δp_d, given by:

$$\Delta p_d = (\rho_a - \rho_h)\ gd \qquad (5.12)$$

where g = acceleration due to gravity.

The air exchange caused by this effect will be calculated for the three experimental bins, for a 10°C difference in inside and outside air temperatures, with holes at the top and bottom of the head space, i.e.:

ρ_h (30°C) = 1.185 kg m^{-3}

ρ_a (20°C) = 1.205 kg m^{-3}

Large bin d = 1.66 m

small bins d= 0.94 m

This gives:

Large bin - Δp_d = 0.325 Pa

Small bins - Δp_d = 0.184 Pa

From Eq. (5.4), the volumetric air exchange rate due to the stack effect, v_d, is:

$$v_d = \frac{C_o A_o}{2} \sqrt{\frac{\Delta C_p \Delta p_d}{2\rho_h}} \qquad (5.13)$$

For ΔC_p = 2.8, this gives:

large bin - $v_d = 0.4 \times 10^{-4}\ m^3 s^{-1}$

Small painted bin - $v_d = 1.1 \times 10^{-4}\ m^3 s^{-1}$

Small unpainted bin - $v_d = 1.7 \times 10^{-4}\ m^3 s^{-1}$

An estimate of the maximum value of v_h for the three silos can be found by adding v_u and v_d. (In practice these may oppose each other and

the combined effect may be less than either.)

By adding:

Large bin - $v_h = 1.7 \times 10^{-4} m^3 s^{-1}$

Small painted bin - $v_h = 5.8 \times 10^{-4} m^3 s^{-1}$

Small unpainted bin - $v_h = 9.1 \times 10^{-4} m^3 s^{-1}$

5.8 Convection Coefficient between Silo and Outside Air

In considering heat transfer from silo walls, Yacuick et al. (1975) used the expression presented by Kreith (1973) for long cylinders, i.e.:

$$Nu = GRe^J \tag{5.14}$$

with the Nusselt number, Nu, and Reynolds number, Re, being defined as:

$$Nu = \frac{h_{wa} \; 2 \; R_m}{k_a} \tag{5.15}$$

$$Re = \frac{u \; 2 \; R_m}{\upsilon} \tag{5.16}$$

where k_a = conductivity of air

υ = kinematic viscosity of air

They used the values of G and J recommended by Kreith for $40,000 < Re < 400,000$, i.e.:

$$G = 0.0239 \tag{5.17}$$

$$J = 0.805 \tag{5.18}$$

Yacuick et al. were only considering one dimensional heat flow. In the present study, particularly as the value of h_{wa} has a very large effect on the internal temperatures in a silo (Chapter 2), it seems appropriate to experimentally determine the Nu-Re relationship for a short cylinder with a cone on top.[7]

5.8.1 Theory

Kreith used the results of Hilpert (1933) in obtaining J = 0.805 in Eq. (5.18). Achenbach (1975) compared his results with Hilpert's and those

of Schmidt and Wenner (1941) and concluded that the value of J obtained by Hilpert was too high, probably because Hilpert was using too large a cylinder for the size of his tunnel.

Achenbach recommends the value of J to be 0.8 only for the region where there is a boundary layer around the cylinder (Fig. 5.3). He claims that the heat transfer from this region comprises 70-80% of the total for high Reynolds numbers. Launder (1976) quotes a series of data by various workers which suggests that for flow in the region of separation, $Nu \propto Re^{0.67}$.

Assuming the heat transfer from separated regions for a cylinder with cone above it to comprise 25% of the total, an appropriate expression for Nu would be:

$$Nu = G(0.75Re^{0.80} + 0.25Re^{0.67}) \qquad (5.19)$$

The value of G must be found by putting experimental values of Nu and Re in Eq. (5.19). Re must be calculated for a wind speed at some specified height. Since heat is transferred, in general, from the regions of the silo where wind speeds are highest, that is the upper parts of the walls and roof, the height of the eves, Z_e, will be used as the reference height. In the wind tunnel u is measured at a height of 33.3 cm (about three times the height of the silo) ~~This is because the logarithmic law profiles do not hold close to the rough surface.~~ to avoid any local disturbances caused by the model bin. Mulhearn (1978) shows that the logarithmic law of windspeed - height variation is applicable, so using the value he found for Z_o for the tunnel $(0.38 \times 10^{-3} m)$[8], Eq. (5.11) becomes:

~~The reference velocity should be measured 3-4 typical roughness heights above the surface, Z_o for the tunnel being 0.38×10^{-3} m (Finnigan 1977). The relationship between u_r and u_e is given in Eq. (5.11), which becomes:~~

$$u_e = 0.825\, u_r \qquad (5.20)$$

For finding Nu, similarity of heat transfer from the model silo and mass transfer of solid napthalene, coated onto the silo, is assumed. i.e. the Nusselt number is considered to equal the Sherwood number, defined by:

$$Sh = \frac{b\ 2\ R_m}{k_c} \qquad (5.21)$$

Figure 5.3 - Flow patterns around a cylinder for Re > 10^5

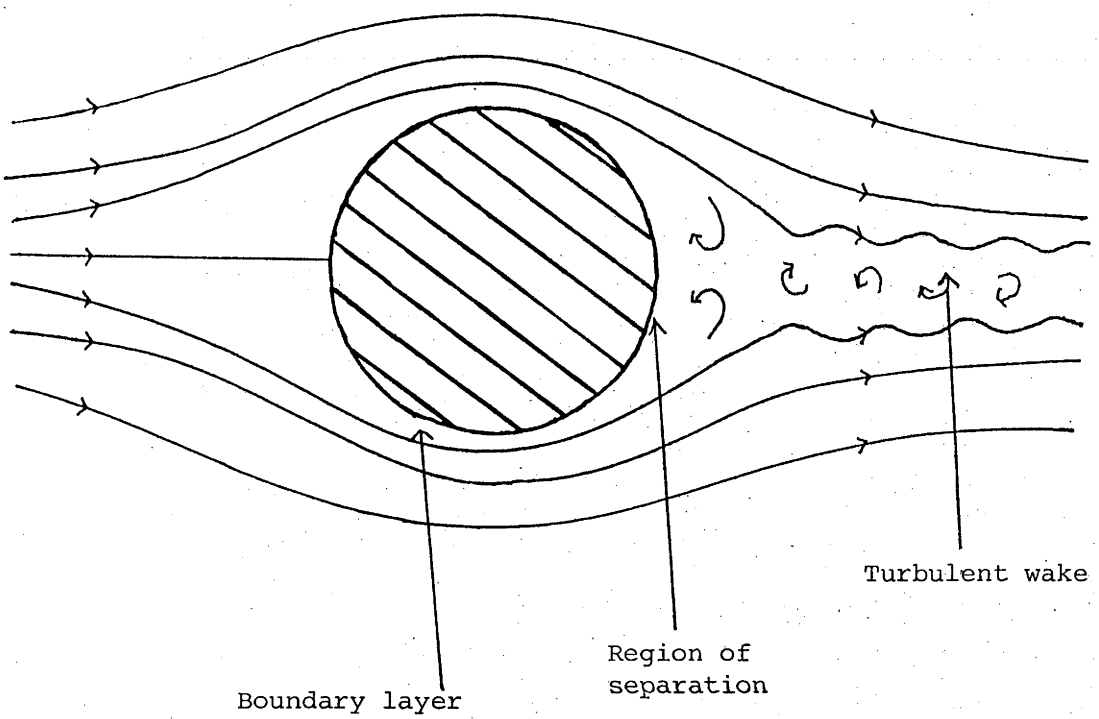

where k_c = molecular diffusivity of napthalene in air

b = mean coefficient of mass transfer.

For napthalene, Sogin et al. (1958) give:

$$k_c = \frac{\upsilon}{2.5} \tag{5.22}$$

$$\therefore \quad Sh = \frac{b\ .5\ R_m}{\upsilon} \tag{5.23}$$

Sogin presents two equations for finding b:

$$b = \frac{R_v\ T_w\ m_v}{p_v\ A_w} \tag{5.24}$$

$$p_v = 10^{(B_1 - B_2/T_w)} \tag{5.25}$$

where m_v = mass transfer rate

R_v = gas constant
T_w = wall temperature (°R)
p_v = vapour pressure of sublimating material

B_1, B_2 = constants.

For napthalene, in engineering units, Sogin gives:

$$R_v = 12.05 \tag{5.26}$$

$$B_1 = 11.884 \tag{5.27}$$

$$B_2 = 6713 \tag{5.28}$$

m_v must be determined experimentally.

5.8.2 Experimental procedure

A cylinder 4" high and 4" in diameter was cut from a perspex tube. A 30° roof was constructed out of cardboard and attached to the cylinder.[9] The complete model silo was sprayed with black water-based paint.

10 g organic napthalene was dissolved in 100 ml acetone and a pressure pack used to spray this solution evenly onto the model silo.[10]

The coated silo was weighed to the nearest mg and the napthalene lost outside the wind tunnel found by reweighing after one minute. The model was quickly placed in a cardboard box and taken to the wind tunnel, ensuring

that the total time to the tunnel was one minute. It was placed in the tunnel, behind a series of gravel chips on the tunnel floor (used to create a turbulent free stream). The model was left for four minutes and the air temperature just outside the tunnel was recorded. (This was assumed to represent the wall temperature, which would be difficult to measure without disturbing the flow.) The free stream wind velocity, as measured by a pitot tube at a height of 33.3 cm, was noted. The model was then quickly returned to its box and carried, in exactly one minute, back to the scales, where it was reweighed. It was again left for one minute on the scales and then the final weight was recorded.

5.8.3 Results

The results are shown in Table 5.6. The average weight losses and corresponding temperatures are shown in Table 5.7.

5.8.4 Calculations

The intermediate steps involved in the calculation of G are shown in Table 5.8.

The average value of G is 0.114. Using Eqs. (5.15) and (5.19) the heat transfer coefficient is found to be:

$$h_{wa} = \frac{0.057\ k_a}{R_m}(0.75Re^{0.80} + 0.25Re^{0.67}) \qquad (5.29)$$

5.8.5 Discussion and Conclusions

Sogin (1958) finds that the correlations of the sublimation of naphthalene from a circular plate and of heat transfer for the same configuration, measured by the evaporation of water (Powell 1940), coincided within the reproducibility of the experimentation ($\pm$ 7.5%).

The largest error in the present experiment is probably not caused by the analogy between heat and mass transfer mentioned above, but by assuming

TABLE 5.6 - Sublimation of napthalene

	t_a (°C)	u (m s^{-1})	Napthalene lost (g) a	b	c
Expt. 1	21	21.9	.007	.288	.005
	21	21.9	.002	.275	.003
	21	21.9	.004	.286	.006
Expt. 2	25	18.0	.007	.323	.003
	↓	18.0	.002	.348	.003
	26	18.0	.002	.360	.004

a = Weight lost in 1 minute in still air before carrying to tunnel

b = Total weight lost by carrying to tunnel, leaving 4 minutes and returning to scales (each journey taking 1 minute).

c = Weight lost in 1 minute in still air after returning from tunnel.

TABLE 5.7 - T_a and m_v for each experiment

	T_a (°R)	m_v (lb s^{-1})
Expt. 1	529.5	2.505×10^{-6}
Expt. 2	537.6	3.086×10^{-6}

TABLE 5.8 - Calculation of G

	p_v (lb ft^{-2})	A_{w_2} (ft^2)	b (ft s^{-1})	Sh	Re	G
Expt. 1	.1607	.460	.2162	1.12×10^3	1.23×10^5	0.118
Expt. 2	.2495	.460	.1742	0.90×10^3	1.01×10^5	0.111

the wall temperature of the silo equals that just outside the tunnel. If the wall temperature in Expt. 1 was in fact 5°C higher than that measured outside the tunnel, there would be a 35% decrease in the value of G.

Other errors include the assumption of uniform rate of loss of napthalene, inexact timing of the duration in the tunnel and inaccurate weighing.

Considering all the above sources of error the value of h_{wa} in Eq. (5.29) can only be considered accurate to $\pm$ 50%. However, Fig. 5.4 indicates that the experimental relationship obtained is a reasonable one since it gives values of Nu about 1.75 times those obtained by Achenbach (1977) for the non-separated region round a rough cylinder in a ~~laminar~~ with turbulence level 0.45% free stream. Since the free stream flow in the experiment was 15% turbulent, this would be expected to give a higher Nusselt number. (Kestin et al. (1971) noted up to 50% rise in Nusselt number of cylinders when they placed a turbulence promoter upstream).

Curve c in Fig. 5.4, used by Yacuick et al. (1975), clearly produces values of heat transfer coefficient which are too low, mainly because this relationship was developed for smooth cylinders in laminar flow.

Figure 5.4 - Nu-Re relationships.

(a) Current experiment - rough model silo in turbulent free stream

$$Nu = 0.114\ (0.75\ Re^{0.80} + 0.25\ Re^{0.67})$$

(b) Achenbach - rough cylinder in ~~laminar~~ free stream with turbulence level 0.45 %.

$$Nu = 0.0455\ Re^{0.81}$$

(c) Hilpert - smooth long cylinder in laminar free stream

$$Nu\ 0.0239\ Re^{0.805}$$

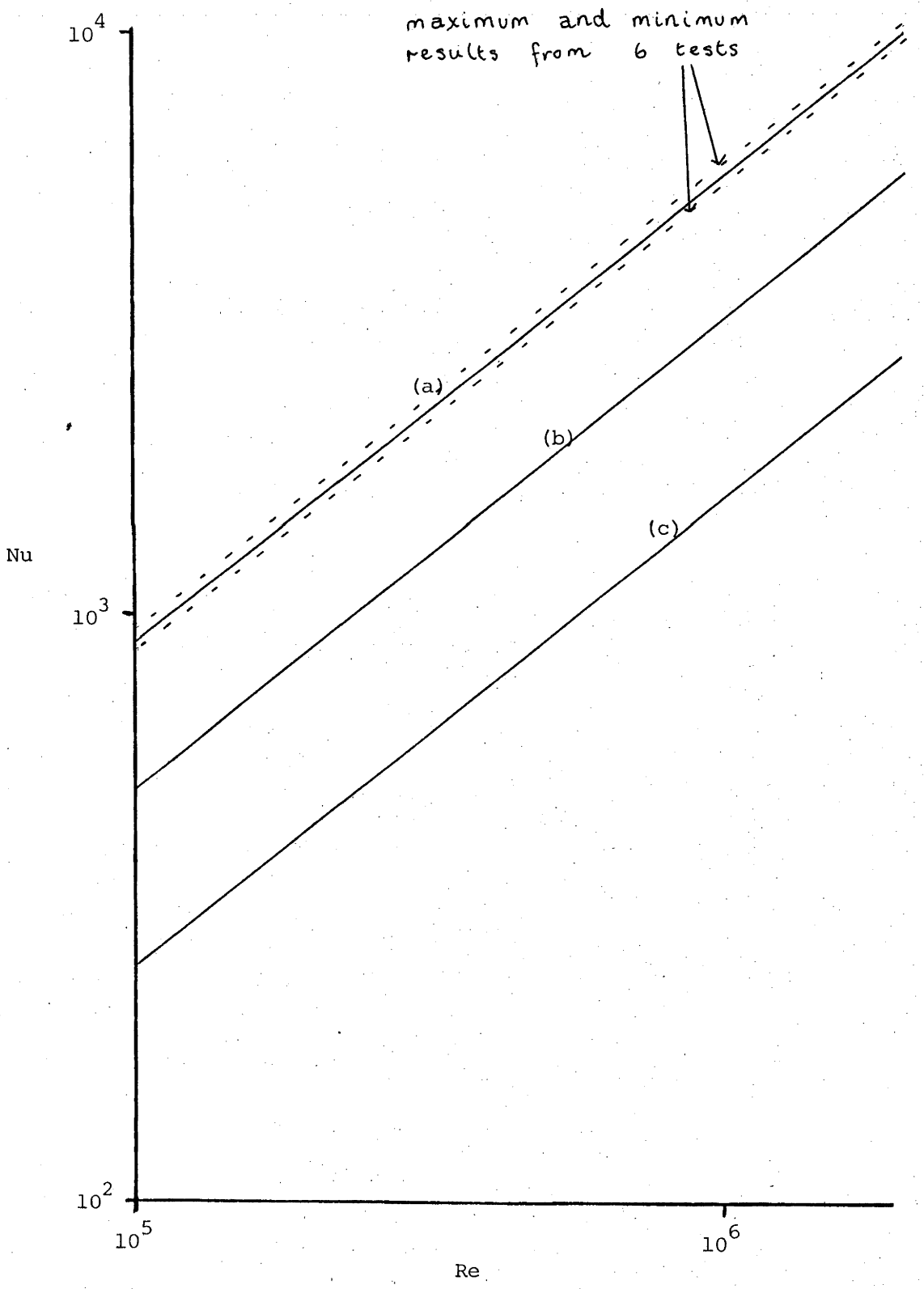

CHAPTER 6

RESULTS AND DISCUSSION

RESULTS AND DISCUSSION

Since the experimental silos are small, they are sensitive to day-to-day fluctuations in outside climatic conditions. Actual data on maximum and minimum temperatures, wind speed and hours of bright sunshine was therefore used to test the model. The data was collected each day by the meteorological bureau in Canberra, at a site only a few hundred metres from the grain bins. The data is shown in Fig. 6.1.

The temperatures recorded in the bins from October 14 1977 to January 6 1978 are compared graphically with those obtained by the computer program in the following sections. Several graphs are required in order to establish if the predicted temperature variations are occurring at all points of the silos. The positions of the thermocouples are shown in Figs. 4.4 and 4.5. Observed temperatures can only be considered accurate to $\pm 1°C$ (Section 4.5).

The actual temperatures on October 14 are used as the initial program temperatures, the linear interpolation technique, described in Section 3.3.9, being used to estimate initial temperatures at the program points.

6.1 Graphs for the Large Bin

Fig. 6.2 shows that there is good agreement between experimental and predicted temperatures for thermocouples near to the centre of the large bin. Clearly there is a large (approx. 4°C over 60 cm) variation of temperature with height, demonstrating that all previous models were inadequate, since they considered only radial heat flow.

Fig. 6.3 shows that there is up to a 10°C difference in temperature between the surface and bottom of the wheat in this bin. These temperatures are predicted fairly well by the model. A slight discrepancy for the lower thermocouple is not surprizing since the

Figure 6.1 Meteorological data used to test the model

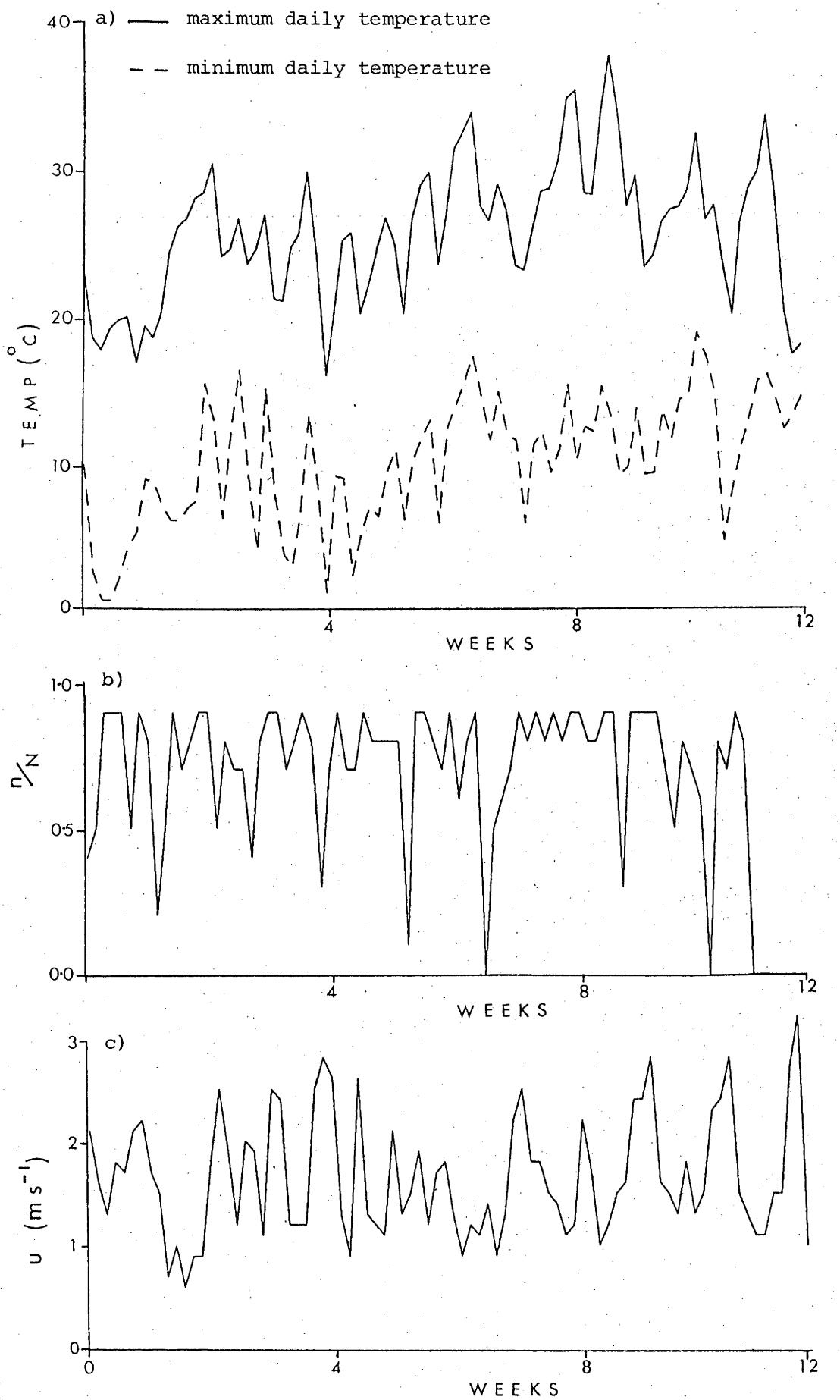

Figure 6.2 Temperature-time graphs for C2 and C3 in the large bin

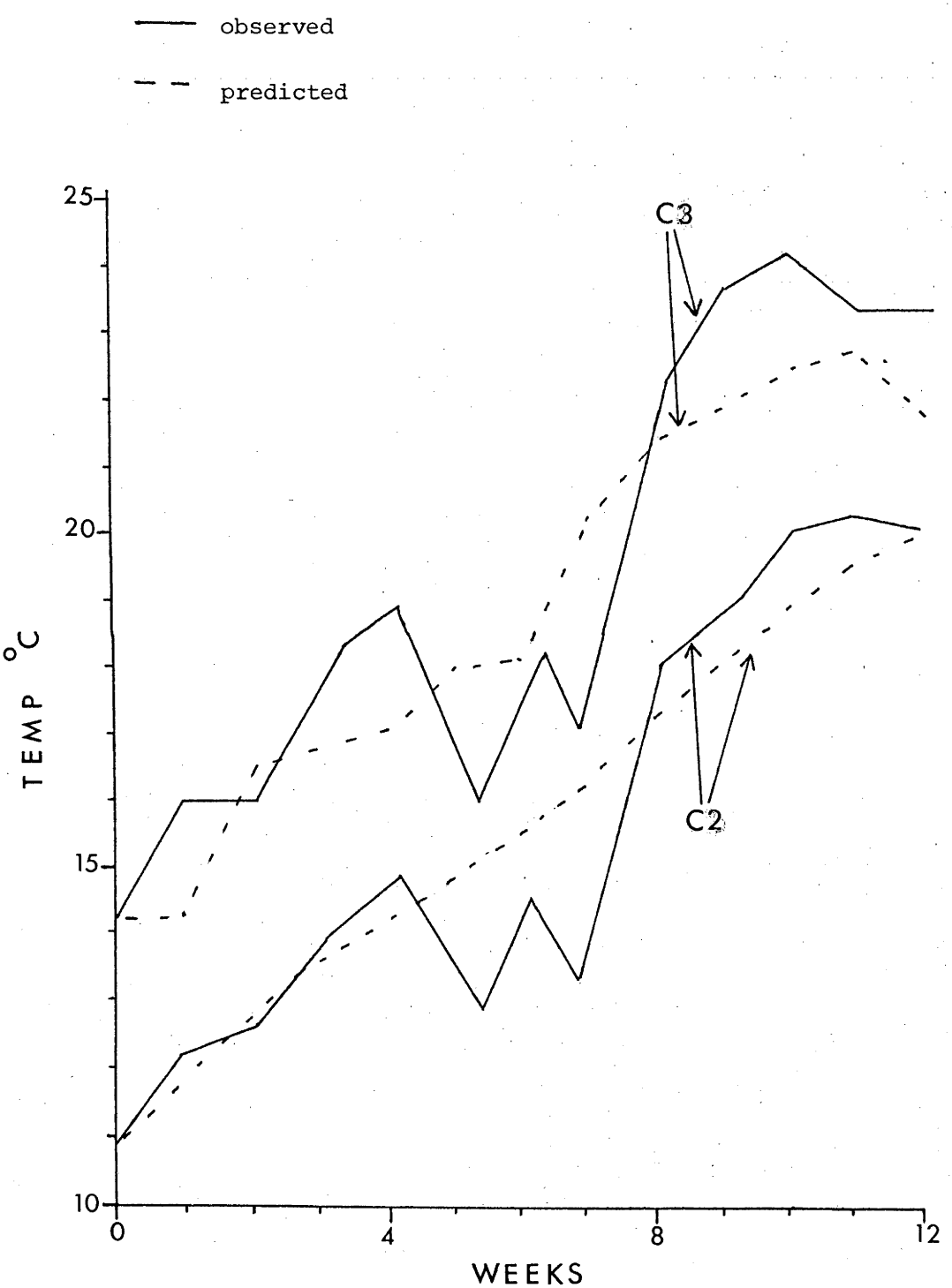

Figure 6.3 Temperature-time graphs for C1 and C4 in the large bin

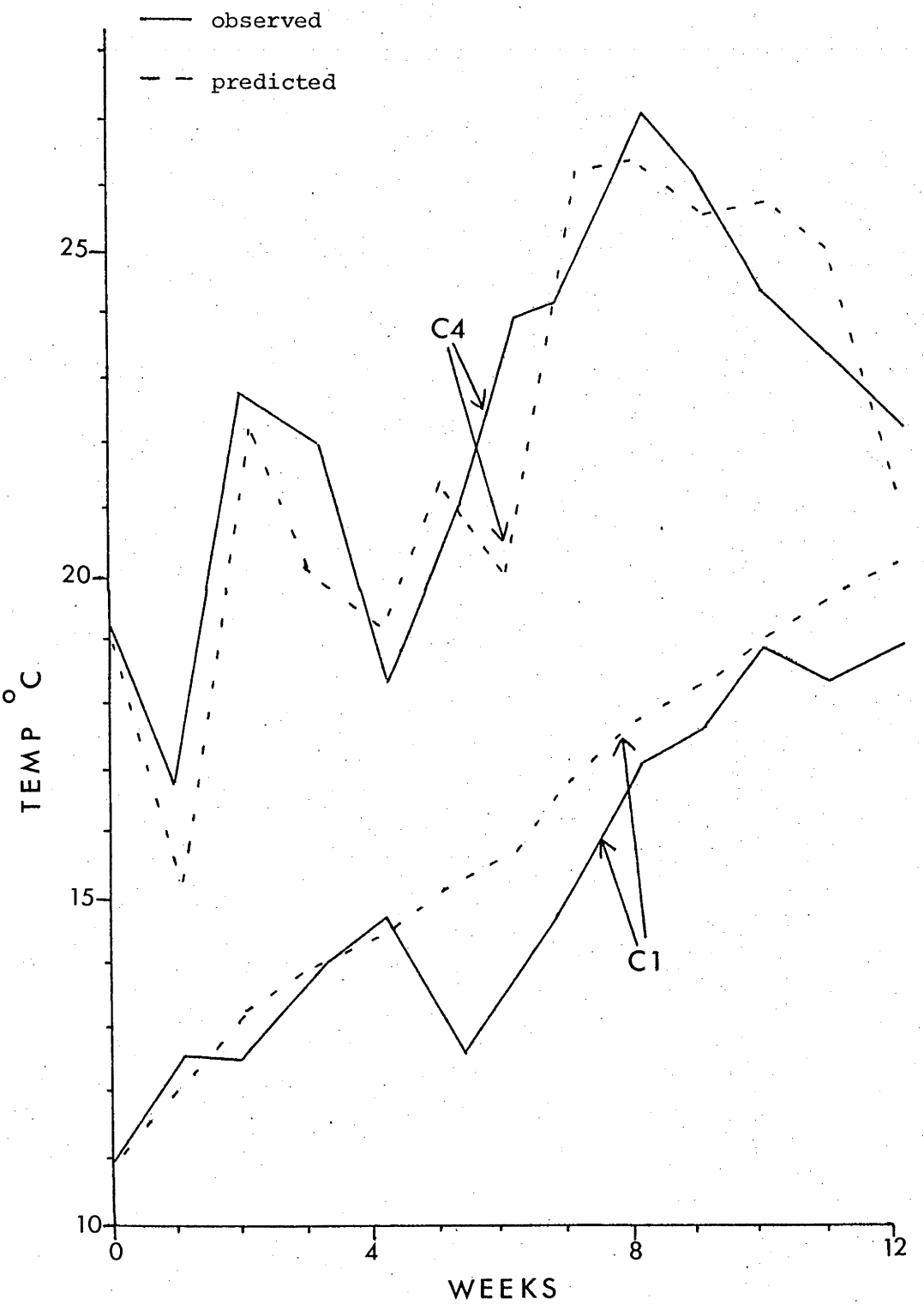

assumption was made that the temperature of the silo-ground boundary is equal to that of the ground around it.

Fig. 6.4 compares experimental temperatures for the east and west sides of the silo. The west side is always about 1°C lower. This is probably due to the shading of this side by the small silos in the late afternoon (Fig. 4.6)[11,12]. These experimental temperatures are also compared with theory. The agreement is extremely good, considering these thermocouples are near to the wall and surface of the wheat, where predicted temperatures are very dependent on the correct theory of heat transfer being used at the boundaries.

Figs. 6.5 and 6.6 show the temperature profiles across and down the large bin at the start of the experiment and after six and twelve weeks. The model accurately predicts the changing temperature patterns.

6.2 Graphs for the Small Bins

Figs. 6.7 a) and b) demonstrate that the thermal characteristics of the small bins were essentially the same before one was painted white. The maximum difference between the temperatures of thermocouples situated on the centre line, 92 cm above the sand base, is 1.9°C and neither is consistently warmer. Since results are compared over almost a year (from May 12 1975 to April 19 1976), this is very good agreement.

Figs. 6.8 to 6.10 are the temperature-time graphs for positions up the centre-line of the small bins from October 1977. By referring to Fig. 1.1 it can be seen that if insects were present during this period, there would be little population growth in the white bin whereas the temperature in the unpainted bin is ideal for rapid population increase. The dashed lines show the predicted values, using the foregoing theory. Good agreement is obtained for the uppermost thermocouple (Fig. 6.10), but the predicted temperatures at the other positions are too low.

Figure 6.4 Temperature-time graphs for E4 and W4 in the large bin

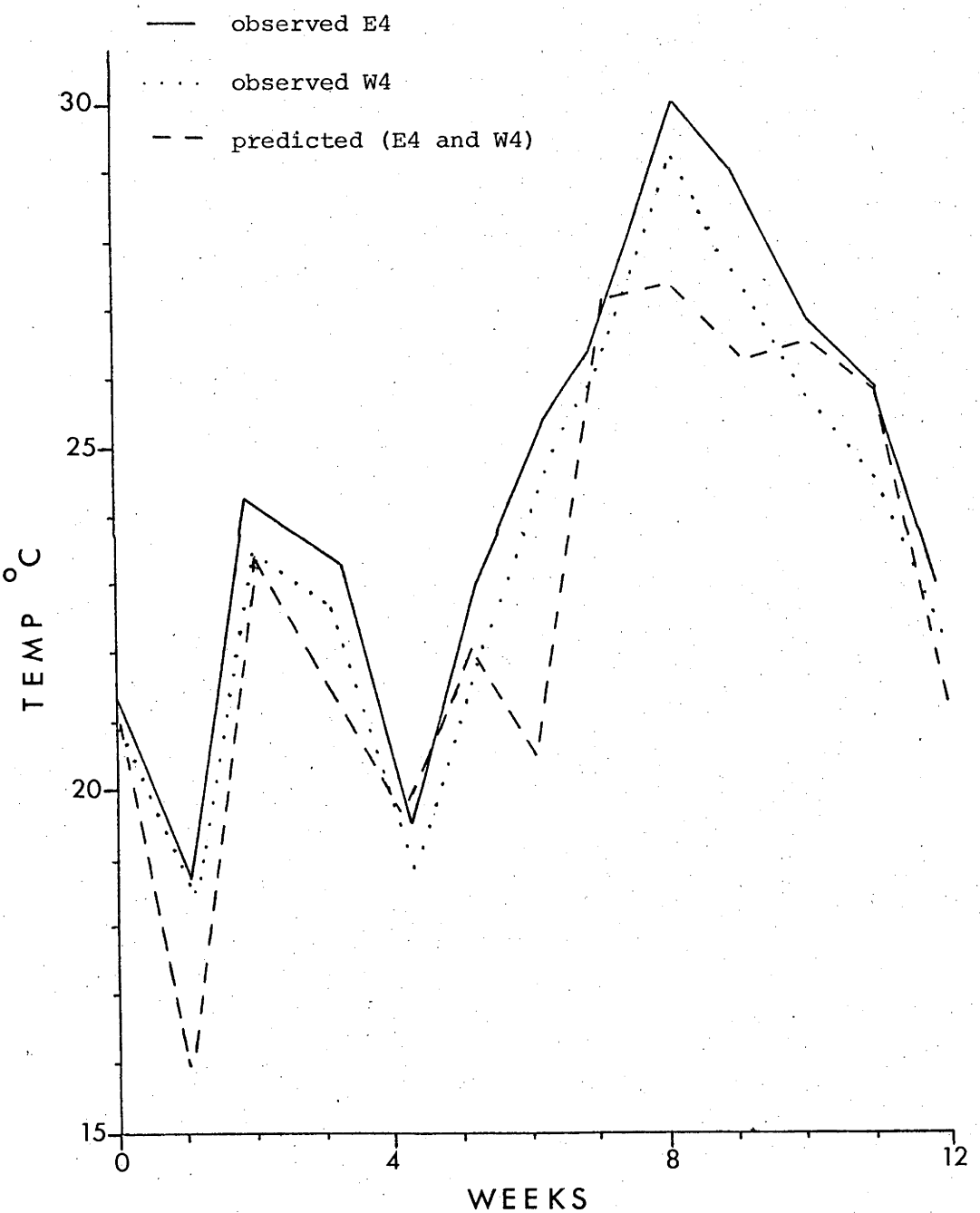

Temperature profiles for the large bin on October 14 and after 6 and 12 weeks

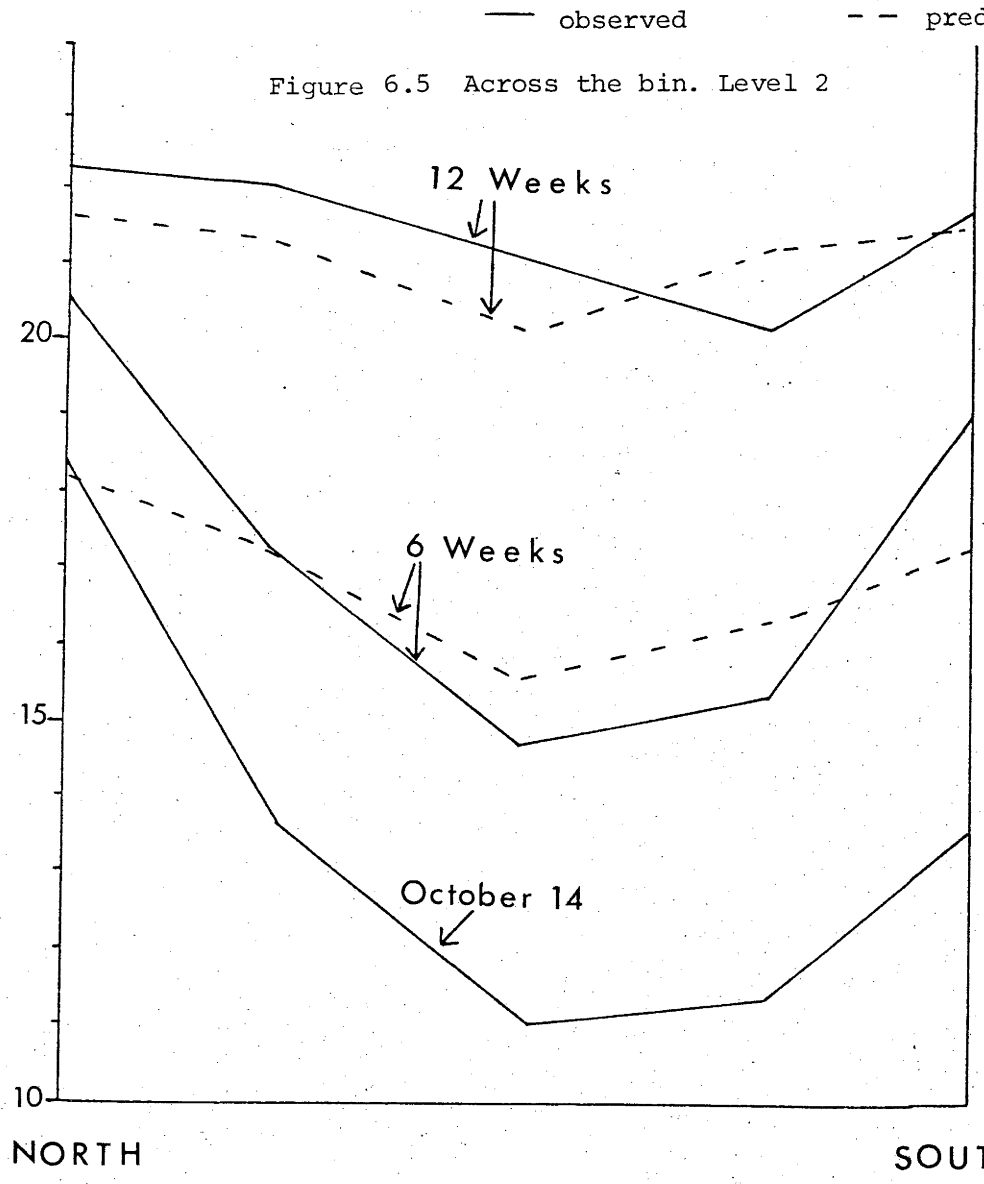

Figure 6.5 Across the bin. Level 2

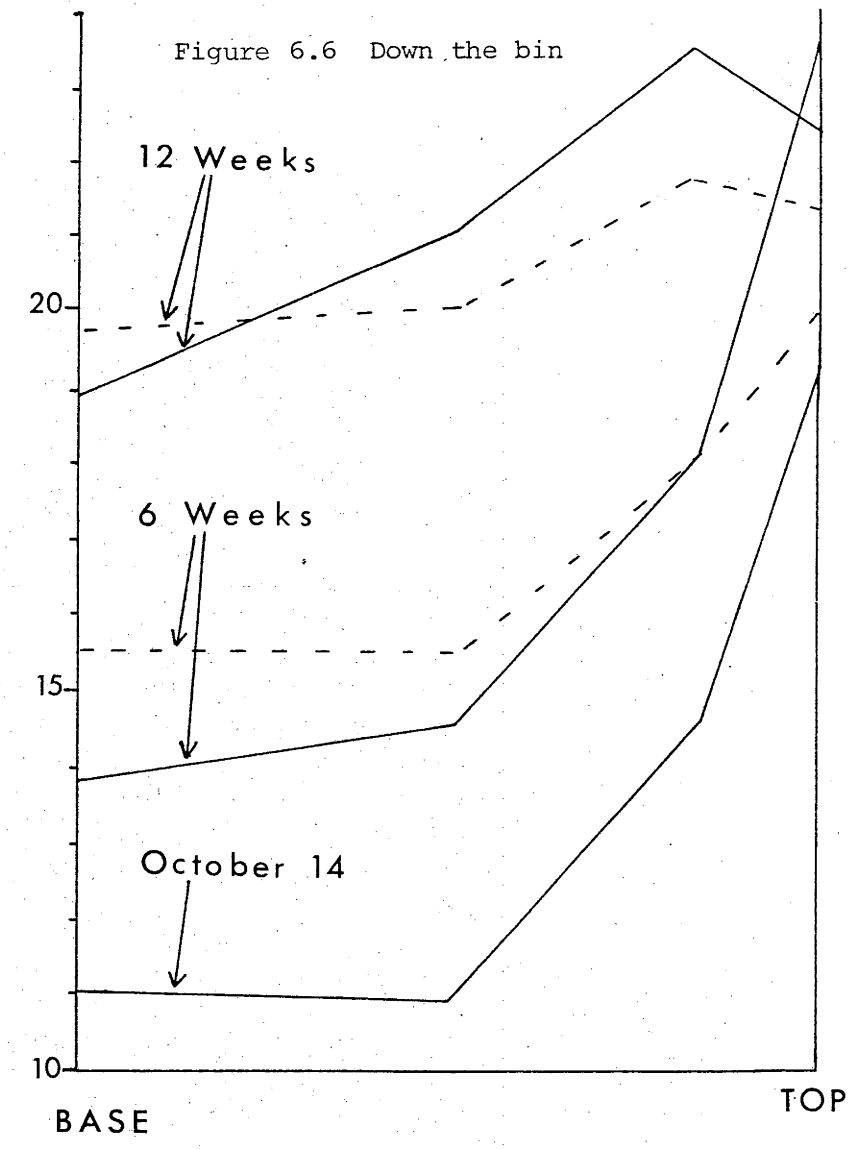

Figure 6.6 Down the bin

Figure 6.7 a) Temperature-time graphs of the small bins before one was painted

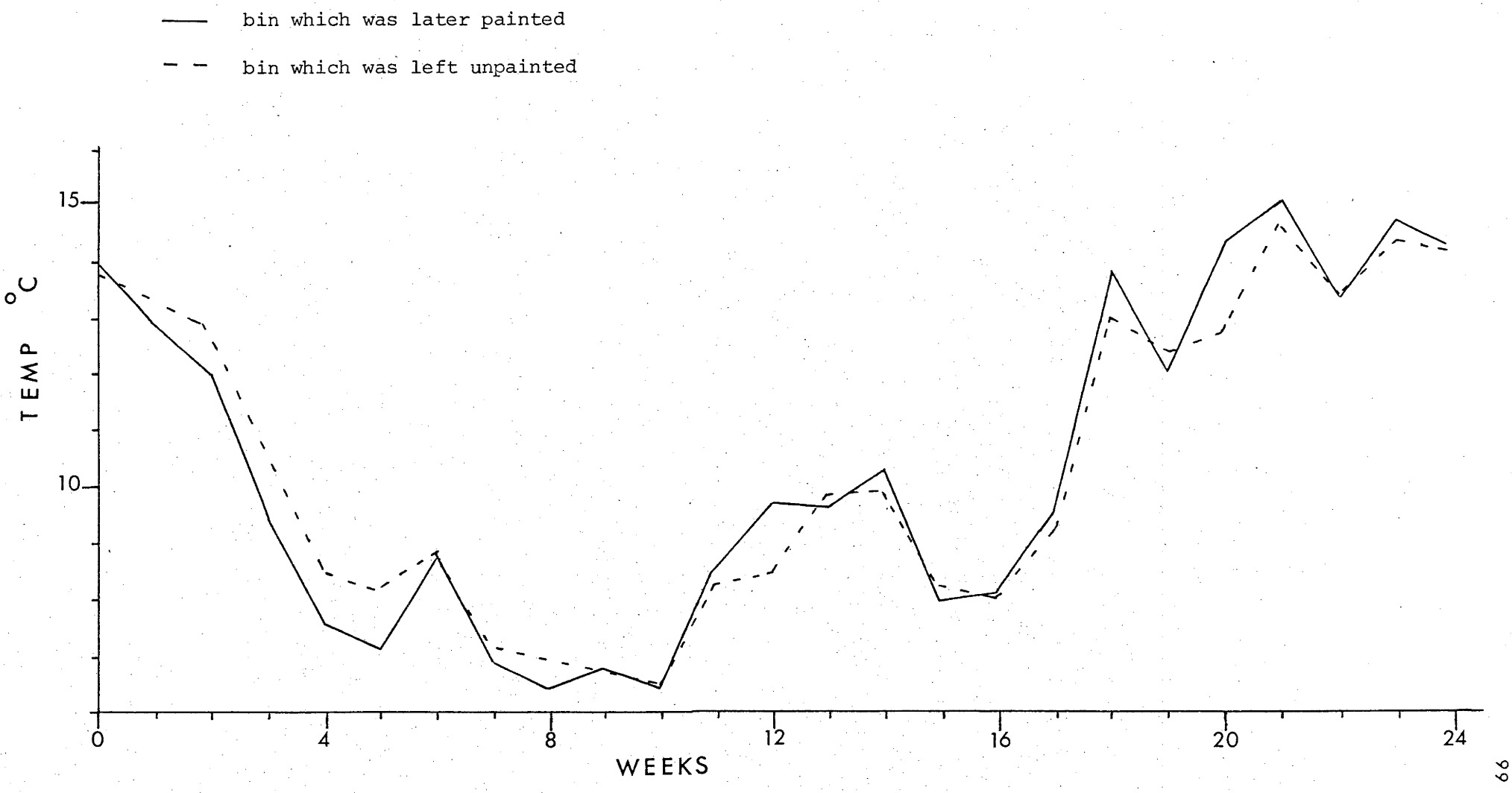

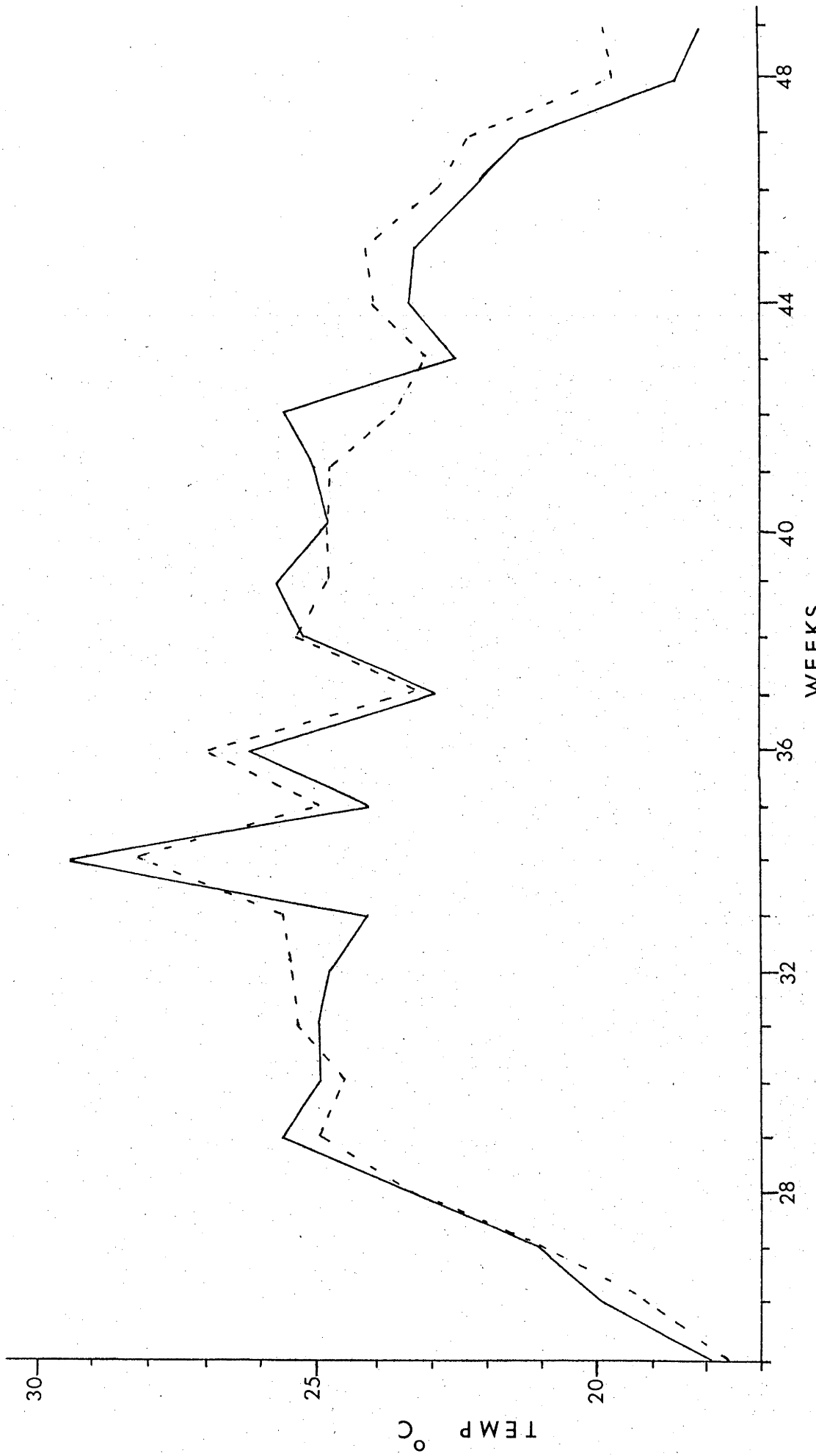

Figure 6.7 b) Continuation of Fig. 6.7 a)

Figure 6.8 Temperature-time graphs for C2 in the small bins

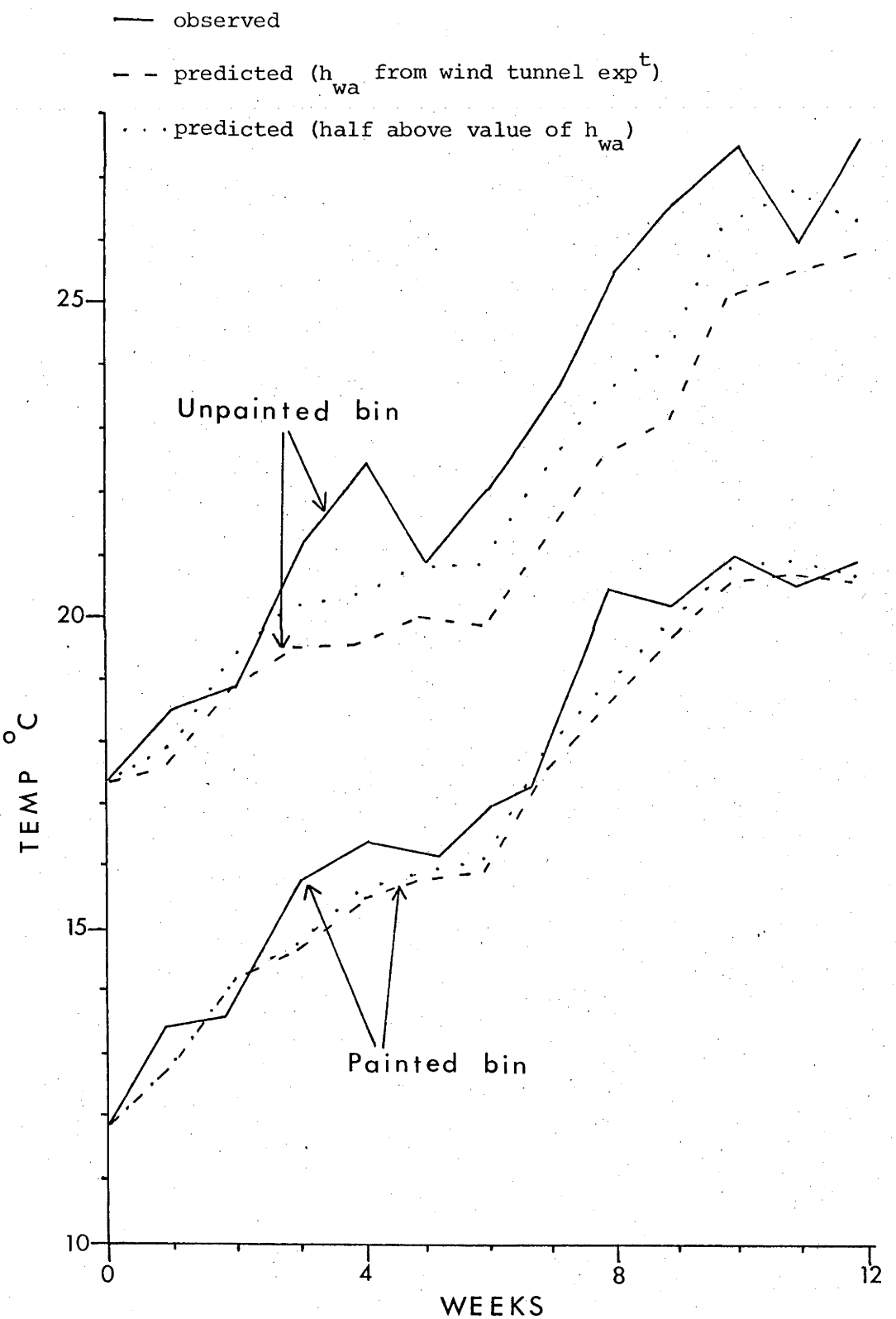

Figure 6.9 Temperature-time graphs for C1 in the small bins

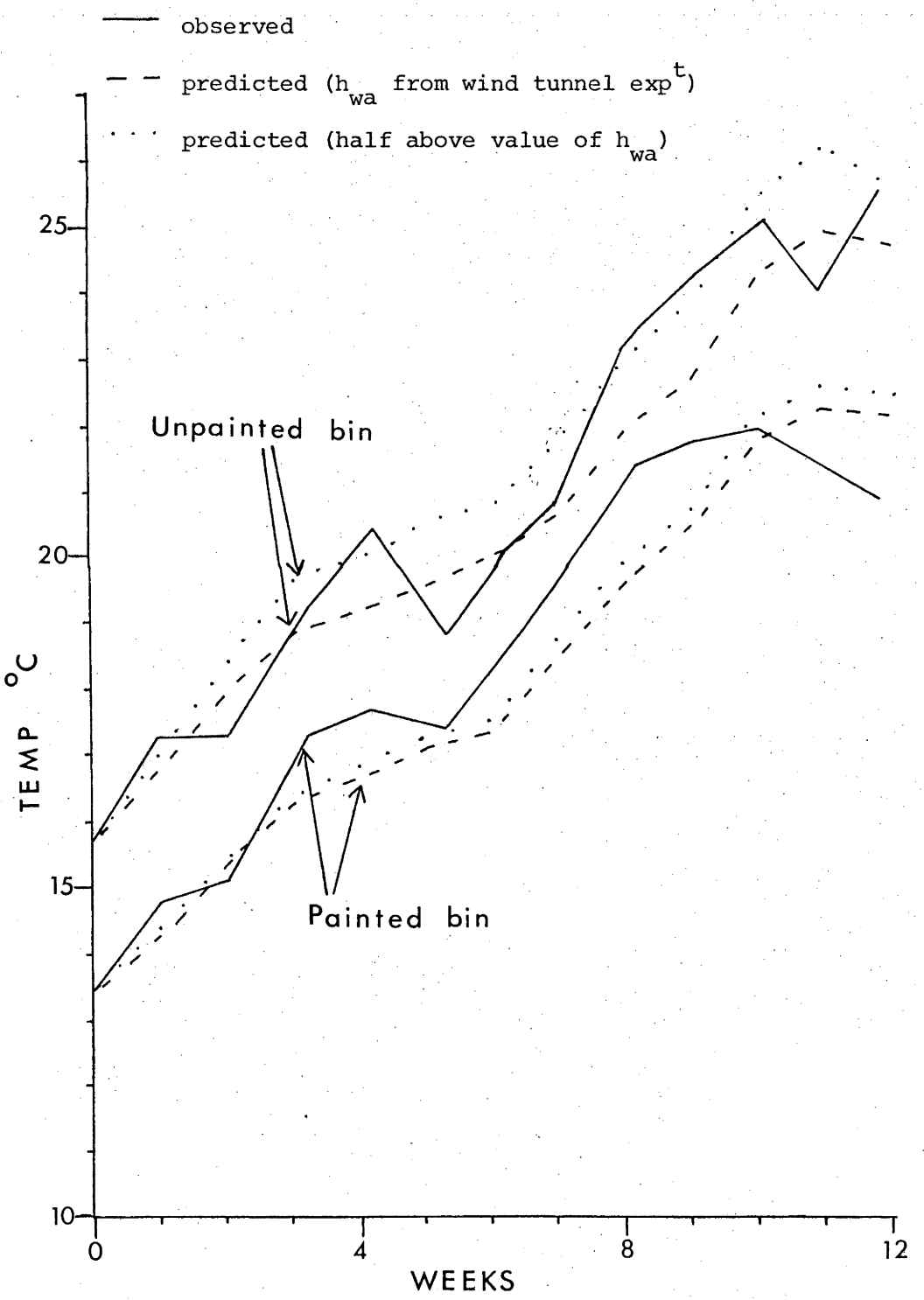

Figure 6.10 Temperature-time graphs for C3 in the small bins

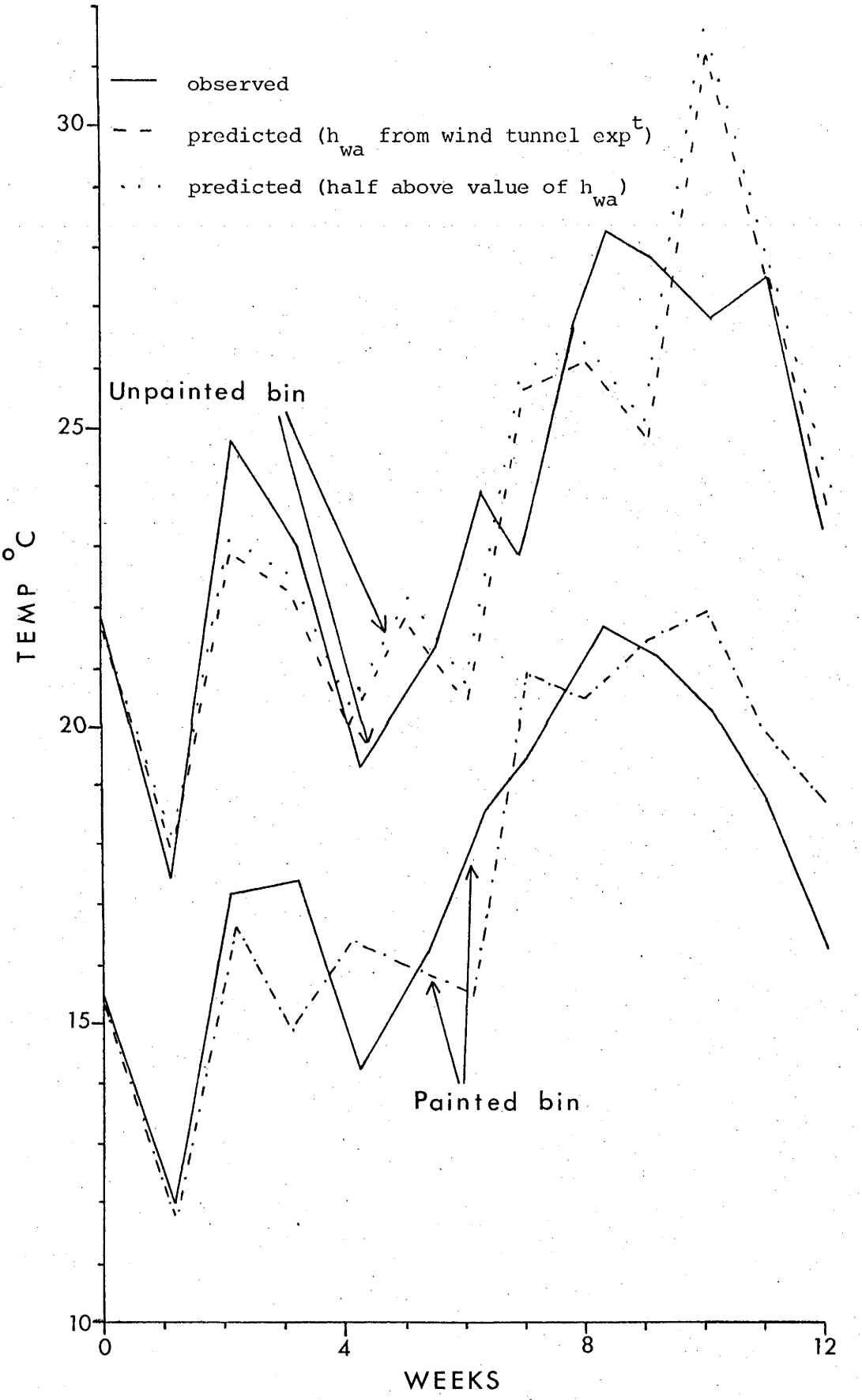

Now the most uncertain parameter of the model is the forced convective heat transfer coefficient for the walls and roof. In Section 5.8 the value calculated from the wind tunnel experiment was only claimed to be accurate to ± 50%. It can be seen from Fig. 4.1 that the large silo has prominent corrugations and would be expected to have a large value of h_{wa} since the wind flow is greatly disturbed and the surface area is greater than if it were flat. Eq. 5.29 appears to give a value of the right magnitude. The small silos, however, have much less defined corrugations, so would be expected to have a smaller value of h_{wa} (though a larger one has been used since h_{wa} is approx. $\alpha\ R_m^{-0.2}$). The value for the roof would probably be greater than that of the walls since the wind speed is greater at this height.

The effect of reducing h_{wa} for the walls by 50% and keeping the original value for the roof is shown by the dotted lines in Figs. 6.8 to 6.10. A better overall agreement is obtained. Before this value is accepted as a more accurate parameter of the model, however, it must be compared with other estimates for cylinders.

Fig. 5.4 shows the results of various workers. The new Nu-Re relation would give a graph between lines (a) and (b) - still giving Nusselt numbers greater than those obtained by Achenbach for a rough cylinder in ~~laminar~~ of turbulence level 0·45% flow, (and still nearly twice as those of Hilpert, as used by Yacuick et al. in their model). It appears therefore that the new value of h_{wa} is not necessarily too low and is probably a better one for the small silos than that of Eq. 5.29.

Fig. 6.11 shows the temperature-time graphs for the east and west sides of the small bins. Unlike the large silo, neither side of the small silos is consistently warmer. It can be seen from Fig. 4.6 that there is significant shading of the east side of the small bins in the

Figure 6.11 Temperature-time graphs for E3 and W3 in the small bins

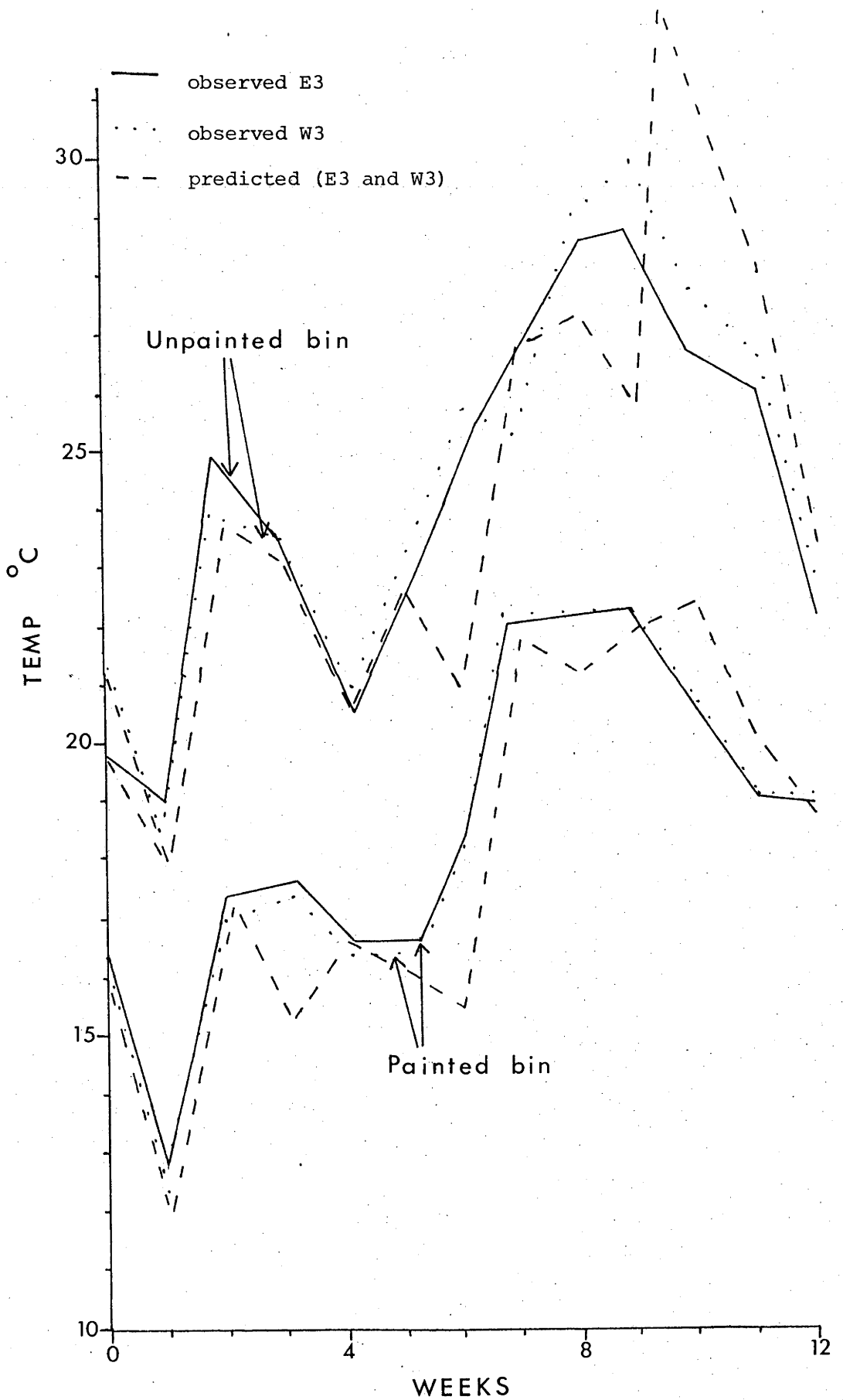

morning,but this is probably compensated for by the early setting of the sun over Black Mountain, just behind the silos. Using the lower value of h_{wa} for the walls, the experimental temperatures are compared with predicted. The agreement is generally good. Anomalies, such as the very high predicted temperature for the unpainted silo at ten weeks, can be expected since the thermocouples are near to both the wall and wheat surface, where temperatures fluctuate widely from week to week.

Figs. 6.12 to 6.15 show temperature profiles down and across the small bins, using the lower value of h_{wa}. The general trend of the predicted temperatures follows the pattern of those obtained experimentally.

Temperature profiles for the small unpainted bin after 6 and 12 weeks

observed — predicted

Figure 6.12 Across the bin. Level 2

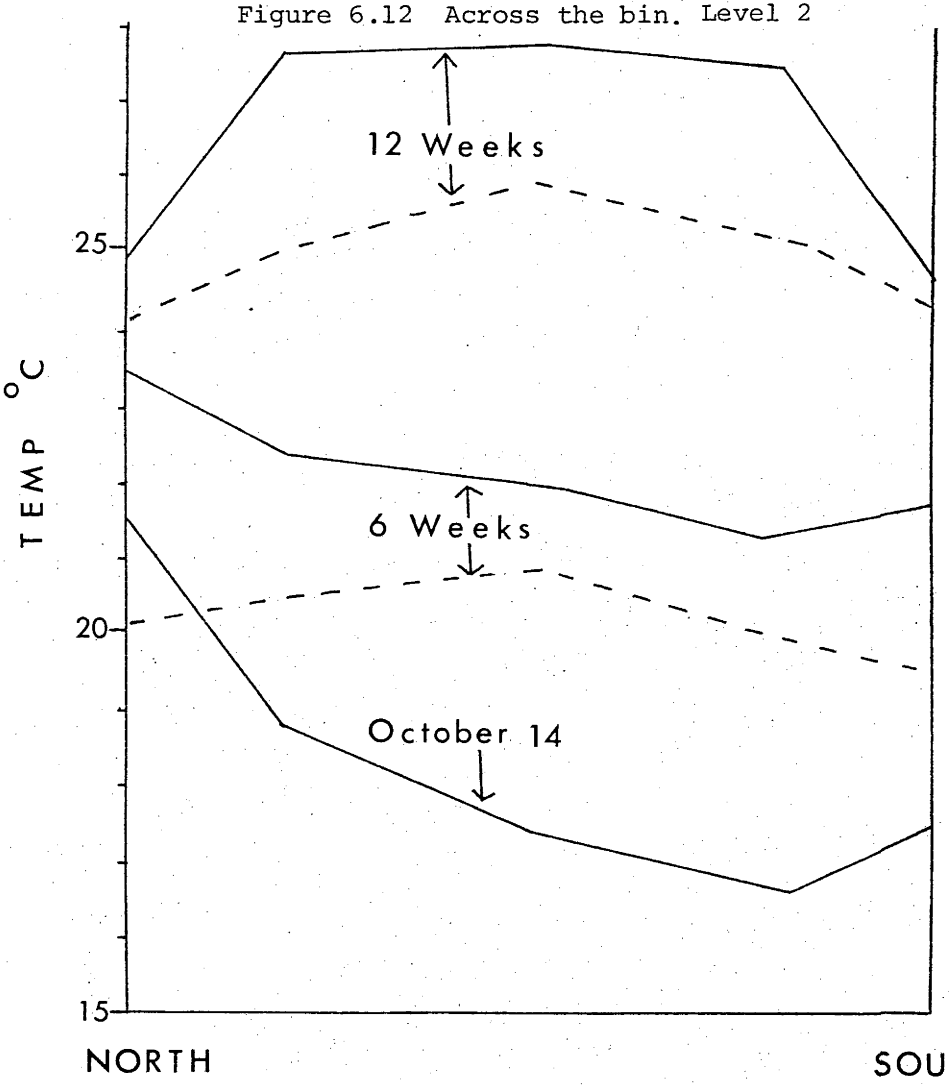

Figure 6.13 Down the bin

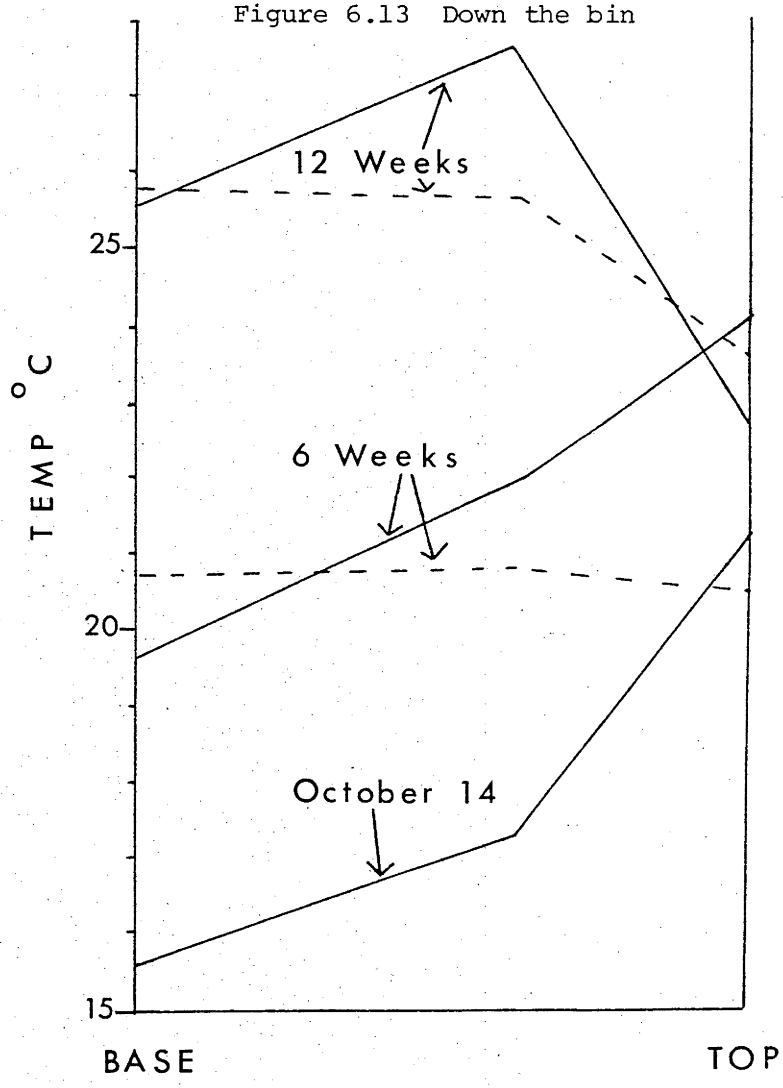

Temperature profiles for the small painted bin after 6 and 12 weeks

—— observed – – predicted

Figure 6.14 Across the bin. Level 2

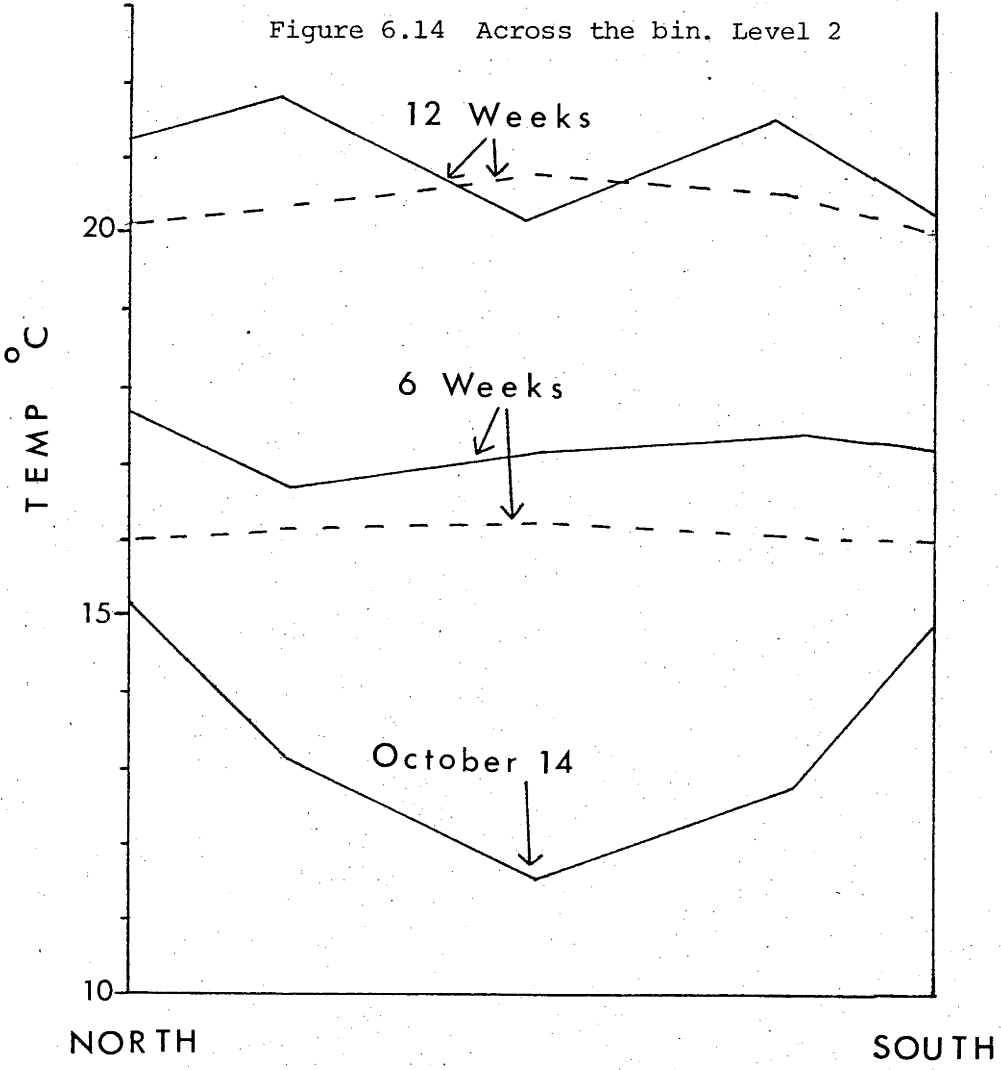

Figure 6.15 Down the bin

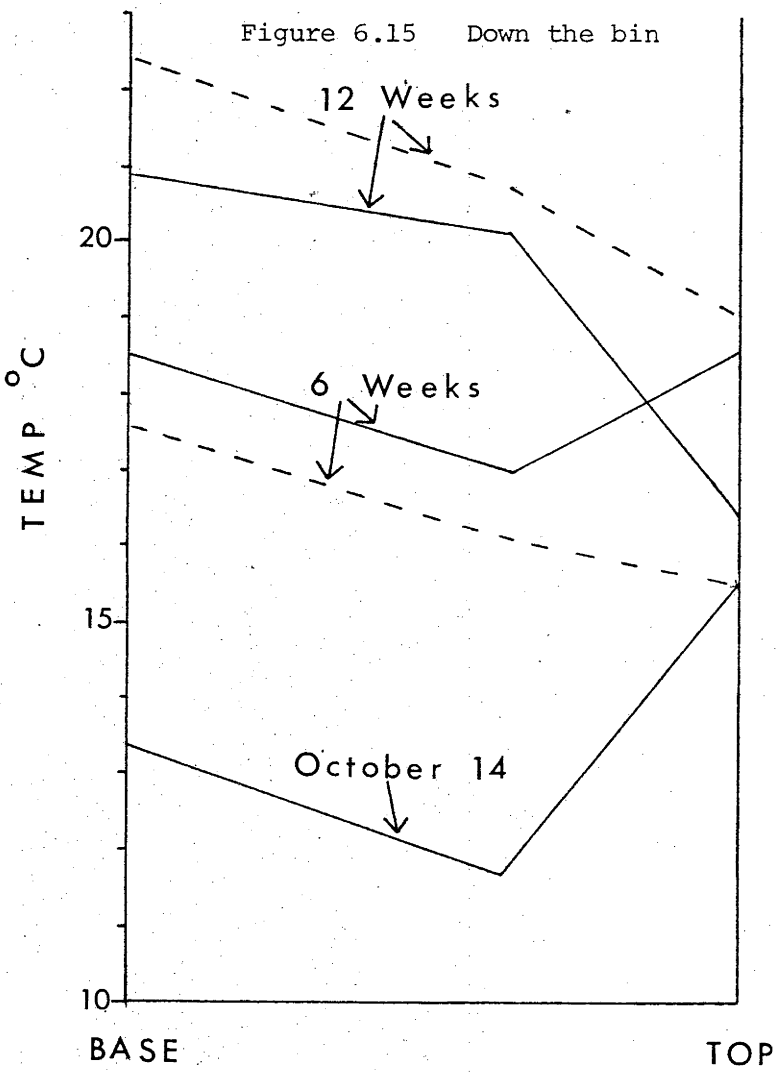

CHAPTER 7

CONCLUSIONS

CONCLUSIONS

The graphs in the last chapter indicate that the model satisfactorily predicts the general trend in temperature changes in metal grain bins, provided an appropriate air-wall heat transfer coefficient is used. However the predicted temperatures do not follow the exact fluctuations in ambient conditions. This is not surprizing because the bins are small and therefore temperatures change rapidly, though measurements were only taken once a week.

Other workers did not consider the spatial variation of temperatures in such detail (Section 1.7 and 1.8). Yacuick et al. (1975) only show results for the centre of bins and their predicted temperatures lagged behind experimental ones. Muir (1970) obtains results for 1.9 ft from the wall (a similar distance to the outermost lines in the small experimental bins) which are consistently too low. He attributes this to a neglect of solar radiation. Bakshi (1972) assumes that, by using the maximum instead of the average daily air temperatures, he is taking solar radiation into account. However his estimated temperatures are nevertheless too low.

It can be concluded that the current work, by treating the problem in three dimensions and comprehensively including solar radiation, is a step forward in the problem of temperature prediction in grain bins.

APPENDICES

APPENDIX A

THE EFFECT OF MOISTURE ON THE TRANSFER OF HEAT IN GRAIN

Both heat and moisture diffuse through grain under a temperature gradient. Assuming the only mechanism of moisture transfer is by diffusion through the air spaces, the vapour flux density, M_v, is given by:

$$M_v = \frac{-D\rho_a\omega}{p}\frac{de}{dx} \qquad (A.1)$$

where D = diffusion coefficient of vapour in air

ρ_a = density of air

ω = fraction of bulk occupied by air

p = atmospheric pressure

$\frac{de}{dx}$ = vapour pressure gradient

When vapour is transferred to a cooler region, it will condense and latent heat will be evolved. The heat flux density, Q_v, resulting from this process is:

$$Q_v = LM_v \qquad (A.2)$$

where L = latent heat of vapourization of water in wheat.

Gallaher (1951) gives L as about 1.1 times the latent heat of free water.

Now the sensible heat flux density, Q_t, is given by:

$$Q_t = -k_t\frac{dt}{dx} \qquad (A.3)$$

where k_t = true thermal conductivity of bulk

$\frac{dt}{dx}$ = temperature gradient

The total heat flux density, Q, is then:

$$Q = -k_t\frac{dt}{dx} - \frac{LD\rho_a\omega}{p}\frac{de}{dx} \qquad (A.4)$$

Letting the relative humidity of the air in the bulk be Y,

$$\frac{de}{dx} = \frac{Yde_s}{dx} = Y\frac{de_s}{dt}\frac{dt}{dx} \qquad (A.5)$$

where e_s = saturation vapour pressure.

Combining Eqs. (A.4) and (A.5):

$$Q = -\frac{dt}{dx}\left(k_t + \frac{LD\rho_a \omega}{p} Y \frac{de_s}{dt}\right) \qquad (A.6)$$

Defining the term in brackets in Eq. (A.6) as the apparent thermal conductivity, k_b:

$$k_t = k_b\left(1 - \frac{LD\rho_a \omega Y}{pk_b} \frac{de_s}{dt}\right) \qquad (A.7)$$

In measurements of thermal conductivity, it is always the value of k_b which is obtained since, as found by Anderson et al. (1943), the establishment of equilibrium (when no more moisture is transferred), "is a very long process and is unattainable for any practical length of time or mass of wheat."

A numerical example will be considered so that an approximate relationship between k_t and k_b can be found

For a temperature of 20°C:

$L = 2454 \times 10^3 \times 1.1 \text{ J kg}^{-1}$

$D = 2.6 \times 10^{-5} \text{ m}^2\text{s}^{-1}$

$\rho_a = 1.204 \text{ kg m}^{-3}$

$\omega = 0.4$

$Y = 0.5$

$p = 10^5 \text{ Pa}$

$\frac{de_s}{dt} = 29 \text{ Pa } °C^{-1}$

$k_b = 0.15 \text{ Wm}^{-1} °C^{-1}$

This gives $k_t = 0.7\ k_b$

The above analysis shows that moisture diffusion has a significant effect on the transfer of heat. Eq. (A.7), however, shows that the two processes can be linearly combined, so conduction equations developed for

heat transfer can be used, even when moisture transfer also takes place, provided the apparent thermal conductivity is employed.

APPENDIX B

FINITE DIFFERENCE SCHEMES

B.1 Explicit and Implicit Schemes

The implicit form of the finite difference heat transfer equation for calculation of bulk temperatures is given in Eq. (3.1).

The heat balance can also be expressed in terms of present temperatures, i.e.

$$C_i \frac{(t_i' - t_i)}{\tau} = \dot{\Sigma}_n \frac{k_{in} A_{in}}{x_{in}} (t_n - t_i) \qquad (B.1)$$

Solving for t_i gives:

$$t_i' = t_i(1 - \Sigma_n Fo_{in}) + t_n \Sigma_n Fo_{in} \qquad (B.2)$$

Now the coefficients of t_i in this equation must always be positive, or it is implied that the larger the value of t_i, the smaller will be the value of t_i'. This does not make sense thermodynamically, so the following stability condition must hold:

$$\Sigma_n Fo_{in} \leq 1 \qquad (B.3)$$

There is no such stability condition for the implicit case since the coefficient of t_i in Eq. (3.3) is always positive. However the method of solution is more complex since t_n' is unknown, so Eq. (3.3) must be solved at each time step.

B.2 Finite Difference Scheme Adopted

Yacuick et al. (1975) used an explicit method of finite difference solution. However their model was one dimensional, so there were only two Fourier moduli terms in Eq. (B.1), giving a stable solution for a fairly large spacing.

Although cylindrical coordinates will be used in the model, a rough estimate of the time step restriction can be found using the more simple rectangular system. For a cube of wheat of side d in the middle of a bulk,

$$\Sigma_n Fo_{in} = \frac{6\, k_b\, \tau}{c_b \rho_b d^2} \qquad (B.4)$$

Substituting Eq. (B.4) in Eq. (B.3),

$$\tau \leq \frac{c_b \rho_b d^2}{6\, k_b} \qquad (B.5)$$

Using the properties in Table 3.1, a value for τ of approximately one day is obtained.

A central cell in the bulk has the least stringent stability condition. For a cell in a concrete base, the time step would be shorter. The thermal diffusivity, δ, is the determining factor. It is defined as:

$$\delta = \frac{k}{c\rho} \qquad (B.6)$$

For wheat, $\delta \simeq 1.2 \times 10^{-7}\ m^2 s^{-1}$

For concrete, $\delta \simeq 8.6 \times 10^{-7}\ m^2 s^{-1}$

The allowed time step is inversely proportional to δ, so for a cube side 0.25 m in the centre of concrete, a time step of about 3 hr is needed to use the explicit method.

Since silos of about one metre radius are to be modelled, a cell dimension of 0.25 m is about the largest that can be used to give a reasonable number of points for a temperature profile. The finite difference approximation is also more accurate with small spatial divisions. However since the temperatures of the bulk only change slowly, it is not necessary to have a time step shorter than a week.

To save on computing time and avoid the problem of stability, the implicit scheme was adopted for the model.

APPENDIX C

CALCULATION OF FOURIER MODULI

The basic form of the Fourier modulus is given by Eq. (3.4). Each term of this equation will be considered in turn. In the following analysis j goes from 1 at the centre to $j_m + 1$ at the outside, m from 1 at the base to $m_m + 1$ at the top surface, l from 1 for north to l_m, going in an anti-clockwise direction.

C.1 x_{in}

x_{in} takes a different form in each direction, i.e.

Radial - in $\quad x_{i1} = r_j - r_{j-1} \qquad (j \neq 1)$ (C.1)

- out $\quad x_{i2} = r_{j+1} - r_j$ (C.2)

Vertical $\quad x_{i3} = x_{i4} = z$ (C.3)

Azimuthal $\quad x_{i5} = x_{i6} = R_j a$ (C.4)

a, the angle between each cell is calculated from:

$$a = \frac{2\pi}{l_m} \tag{C.5}$$

By dividing the silo on an equal volume basis, the radial distances shown in Fig. 3.1 are calculated to be as follows, for a silo of radius R_m with $j_m + 1$ radial divisions:

$$R_j = R_m^2(2j - 2)/(2j_m + 1) \qquad (j = 1 \rightarrow j_m + 1) \tag{C.6}$$

$$r_1 = 0 \tag{C.7}$$

$$r_j^2 = (R_{j+1}^2 + R_j^2)/2 \qquad (j = 2 \rightarrow j_m) \tag{C.8}$$

$$r_{j_m} = R_m \tag{C.9}$$

z, the vertical distance between cells, is calculated from:

$$z = \frac{H_f + H_b}{m_m} \tag{C.10}$$

where H_f = height of base

H_b = height of bulk

m_m = number of vertical divisions - 1

C.2 A_{in}

Since surface and wall temperatures are found before calculation of internal temperatures, the heat transfer areas of the upper ($m = m_m + 1$) and outer ($j = j_m + 1$) cells are not required. For the other cells:

Radial (inner)

$$A_{i1} = R_j az \qquad (m = 2 \rightarrow m_m) \qquad (C.11)$$

$$A_{i1} = R_j az/2 \qquad (m = 1) \qquad (C.12)$$

(outer)

$$A_{i2} = R_{j+1} az \qquad (m = 2 \rightarrow m_m) \qquad (C.13)$$

$$A_{i2} = R_{j+1} az/2 \qquad (m = 1) \qquad (C.14)$$

Vertical

$$A_{i3} = A_{i4} = (R^2_{j+1} - R^2_j)a/2 \qquad (C.15)$$

Azimuthal

$$A_{i5} = A_{i6} = (R_{j+1} - R_j)z \qquad (m = 2 \rightarrow m_m) \qquad (C.16)$$

$$A_{i5} = A_{i6} = (R_{j+1} - R_j)z/2 \qquad (m = 1) \qquad (C.17)$$

C.3 k_{in}

Before the conductivities, k_{in}, can be defined, the 'm value' of the 'transition cells' - those containing both grain and base material - must be defined. This value, m_t, is the integer value of s where s is given by:

$$s = \frac{(H_f - z/2) + 2}{z}^{13} \qquad (C.18)$$

The height of base material in the transition cell, x, is also required. It is given by:

$$x = H_f - (m_t - 1.5)z \qquad (C.19)$$

For a transition cell, whose index is t, the conductivity in the radial and azimuthal directions is:

$$k_{t1} = \frac{(z - x)k_b + xk_f}{z} \qquad (C.20)$$

where k_b = conductivity of bulk

k_f = conductivity of base

Using Fig. C.1, the conductivities in the vertical direction between a transition cell and its neighbours can be calculated.

For upward transfer when $x > z/2$,

$$k_{t3} = \frac{z}{\frac{3/2z-x}{k_b} + \frac{x-z/2}{k_f}} \qquad (C.21)$$

For downward transfer when $x < z/2$,

$$k_{t4} = \frac{z}{\frac{z/2-x}{k_b} + \frac{z/2+x}{k_f}} \qquad (C.22)$$

The conductivities in each direction for all cells can now be defined.

Radial and Azimuthal

$$k_{i1} = k_f \qquad (m < m_t) \qquad (C.23)$$

$$= k_{t1} \qquad (m = m_t) \qquad (C.24)$$

$$= k_b \qquad (m > m_t) \qquad (C.25)$$

Vertical (up)

$$k_{i3} = k_f \qquad (m<m_t-1 \text{ or } m=m_t-1,\ x\geq z/2) \qquad (C.26)$$

$$= k_{t4} \qquad (m=m_t-1,\ x<z/2) \qquad (C.27)$$

$$= k_{t3} \qquad (m=m_t,\ x>z/2) \qquad (C.28)$$

$$= k_b \qquad (m=m_t,\ x\leq z/2 \text{ or } m>m_t+1) \qquad (C.29)$$

Vertical (down)

$$k_{i4} = k_f \qquad (m<m_t \text{ or } m=m_t,\ x\geq z/2) \qquad (C.30)$$

$$= k_{t4} \qquad (m=m_t,\ x<z/2) \qquad (C.31)$$

$$= k_{t3} \qquad (m=m_t+1,\ x>z/2) \qquad (C.32)$$

$$= k_b \qquad (m=m_t+1,\ x\leq z/2 \text{ or } m>m_t+1) \qquad (C.33)$$

C.4 C_i

The volume, V_i, of a cell is calculated from:

$$V_i = A_{i3}z \qquad (m = 2 \rightarrow m_m) \qquad (C.34)$$

$$V_i = A_{i3}z/2 \qquad (m = 1) \qquad (C.35)$$

Figure C.1 - Distances required for calculation of vertical conductivities for a transition cell

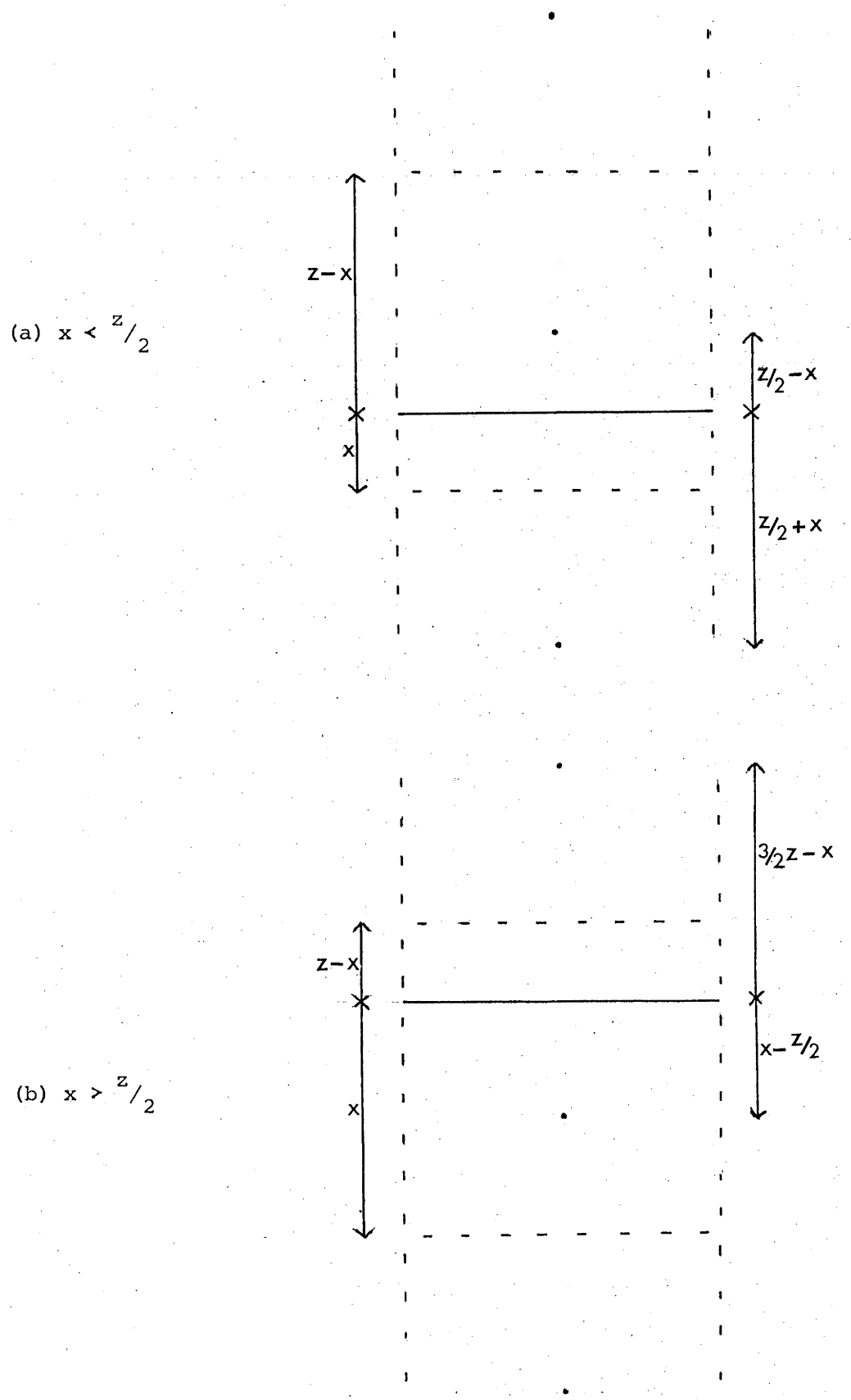

For transition cells, the specific heat, c_{bf}, and density, ρ_{bf}, are defined as follows:

$$c_{bf} = \frac{(z - x)\rho_b c_b + x\rho_f c_f}{(z - x)\rho_b + x\rho_f} \tag{C.36}$$

$$\rho_{bf} = \frac{(z - x)\rho_b + x\rho_f}{z} \tag{C.37}$$

where c_b = specific heat of bulk

c_f = specific heat of base

ρ_b = density of bulk

ρ_f = density of base

LIST OF SYMBOLS

LIST OF SYMBOLS

Where a subscripted variable is not explicitly defined, the subscripts are as follows:-

a - ambient air
b - grain bulk
f - silo base
g - ground
i - index of a cell
n - index of a neighbour to cell i
o - hole in structure
r - silo roof
t - grain surface
w - silo wall.

---

a - angle between adjacent cells. (rads)

a_A, a_d, a_w - coefficients for absorption of solar radiation by scattering, dust and water vapour respectively.

A - area. (m^2)

b - coefficient of mass transfer of napthalene. ($ft\ s^{-1}$)

B - turbidity of atmosphere.

B_1, B_2 - constants in equation for vapour pressure of napthalene (for P_v in $lb\ ft^{-2}$ and T_w in °R).

c - specific heat. ($J\ kg^{-1}\ °C^{-1}$)

C_c - factor in convection equation. $Wm^{-2}\ °C^{-4/3}$

C_s, C_s' - factor in sky temperature equation.

C_o, C_1, C_2 - orifice coefficients.

C_p - pressure coefficient.

d - distance. (m)

D - diffusivity of water vapour in air. ($m^2\ s^{-1}$)

D_γ - diffuse, clear sky solar irradiance on a horizontal surface on earth. (Wm^{-2})

D_c - diffuse solar irradiance passing through the clouds. (Wm^{-2})

D_{jm}, D_{jp} - radial distances between an experimental point and its neighbouring program points. D_{mm}, D_{mp} - vertical distance. (m)

e - vapour pressure of water, e_s - saturated vapour pressure. (Pa)

f_0, f_1, f_{01} etc. - coefficients in interpolation equation.

$f(^n/_N)$ - sunshine function.

f_{rt} - modulus accounting for emittances and relative geometrics of roof and grain surface.

F - view factor.

Fo - Fourier modulus.

g - acceleration due to gravity. (ms^{-2})

G - constant in Nu-Re relation.

G_γ - total clear sky solar irradiance on a horizontal surface on the earth. G_g, G_θ, G_r and G_w - total solar irradiance in partly cloudy weather on the ground, a surface of angle θ, the silo roof and walls respectively. (Wm^{-2})

h - heat transfer (film) coefficient; h_F - for free convection. ($Wm^{-2} \circ C^{-1}$)

H - height; H_a - of the earth's atmosphere, H_e - of wall above grain surface. (m)

i - index defining a cell.

I_γ - direct, clear sky solar irradiance perpendicular to the beam at the earth's surface; I_γ - direct clear sky solar irradiance per unit wavelength outside the earth's atmosphere; I_s - direct solar irradiance scattered by the atmosphere; $I_{m_r w}$ - direct irradiance with absorption by water, dust and gases, but with no scattering. (Wm^{-2})

j - index referring to radial position of a cell; j_m - maximum value of j.

k - thermal conductivity. ($Wm^{-1} \circ C^{-1}$)

k_c - molecular diffusivity of napthalene in air. (lb s^{-1})

K - day of the month .

k_γ - constant in equation for diffuse solar irradiance.

l - index referring to azimuthal position of a cell; l_m - maximum value of l.

L - latent heat of vaporization of water in wheat. ($J\ kg^{-1}\ °C^{-1}$)

m - index referring to vertical position of a cell; m_m - maximum value of m, m_t - index of cell containing base and bulk .

m_r - relative air mass at atmospheric pressure 10^5 Pa; m_r - at air pressure p.

m_v - mass transfer rate of napthalene. ($lb\ s^{-1}$)

M - month number.

M_v - water vapour flux density.($kg\ m^{-2}$)

n - index of neighbour .

$n/_N$ - relative number of hours of bright sunshine.

N_h - hour of the day .

N_M - number of days in month M .

Nu - Nusselt number .

p - atmospheric pressure .(Pa)

p_v - vapour pressure of napthalene .($lb\ ft^{-2}$)

P - polynomial for interpolation .

q - heat flux; q_F - free convection flux; q_k - conductive flux; q_s - solar radiation flux (W).

Q - heat flux density; Q_v - caused by water vapour; Q_t - sensible. (Wm^{-2})

r_j - radial distance of point from silo centre; r_m - maximum value of r_j. (m)

R_j - radial distance of inner edge of cell from centre; R_m - radius of silo. (m)

R_e - radius of the earth .(m)

Re - Reynolds number,

s - vertical index of transition cell.

Sh - Sherwood number.

t - temperature. t' - future temperature; t_{ar} - temperature range for day; t_M - mean monthly temperature; t_{max}, t_{min} - maximum and minimum monthly temperatures; t_{av} - average temperature of the day, t_O, t_I, t_U, t_D - temperatures at intersection of experimental and program grids. (°C)

T - absolute temperature. (°K)

u - wind speed; u_e - at height of eves; u_r - at reference height. (ms^{-1})

v_h - air flow rate into head space, v_d - due to stack effect; v_u - due to wind. ($m^3\ s^{-1}$)

V_i - volume of cell i. (m^3)

w - water content of the atmosphere. (cm)

W_w - moisture content of wheat - wet weight basis; w_d - dry weight basis. (%)

x - distance. (m)

y_0, y_1 etc. - function points to be interpolated at y.

Y - relative humidity.

z - vertical distance between cells. (m)

Z_o - surface roughness length. (m)

Z_r - height at which wind speed measured.; Z_e height of eves. (m)

α - absorptivity for solar radiation.

β - angle between normal to surface and sun. (°)

γ - angular weight of sun. (°)

δ - diffusivity. ($m^2\ s^{-1}$)

Δ_{m_r} - direct solar irradiance absorbed by ozone. (Wm^{-2})

ε - thermal emittance; ε_{ri} - of inside of roof.

η - albedo of ground .

θ - angle of surface.(°)

λ - wavelength.(μm)

ν - kinematic viscosity. ($m^2\ s^{-1}$)

ρ - density.(kg m^{-3})

$\frac{R_o}{R}$ - average/actual distance of the sun from the earth.

σ - Stefan-Boltzmann constant. ($Wm^{-2}\ °K^{-4}$)

τ - time.(s)

ϕ - latitude. (°)

χ - azimuth of sun. (°)

ψ - azimuth of surface. (°)

ω - fraction of bulk occupied by air.

REFERENCES

REFERENCES

Achenbach, E. (1975). "Total and local heat transfer from a smooth cylinder in cross-flow at high Reynolds number". *J. Heat Mass Transfer* 18, p. 1387.

Achenbach, E. (1977). "The effect of surface roughness on the heat transfer from a circular cylinder to the cross-flow of air", *Int. J. Heat Mass Transfer* 30, p.359.

Albrecht, F. (1951). "Intensität und Spektralverteilung der Globalstrahlung bei Klaren Himmel". *Arch. Meteorol. Geophys. Bioklimatol.* Ser. B 3, p.220.

Anderson, J.A., Babbit, J.D. and Meredith, W.O.S. (1943). "The effect of temperature on the moisture content of stored wheat". *Can. J. Res.* 21, C, p.297.

Angström, A. (1929). "On the atmospheric transmission of sun radiation and on dust in the air". *Geografiska Annaler* 11, p.156.

Babbit, J.D. (1945). "The thermal properties of wheat in bulk". *Can. J. Res.* 23, F, p.388.

Bakshi, A.S. and Bhatnagar, A.P. (1972). "Temperature study in grain storage bins". *J. agric. Engng.* 9, 2, p.30.

Banks, H.J., Bailey, S.W., O'Keefe, J.H. and McCabe, B. (1974). Unpublished reports. CSIRO Div. Ent., Canberra.

Banks, H.J. and Annis, P.C. (1976). "Factors influencing gas interchange between storage structures and the atmosphere". Unpublished report. CSIRO Div. Ent., Canberra.

Barned, J.R. (1970). "Thermal conductivity of building materials". *CSIRO Div. Building Res. Report* R2.

Belcher, R.S. and Minett, W. (1966). "Effect of grain moisture content and storage temperature on the breakdown of malathion on stored wheat". *Royal Aust. Chem. Inst. Cereal. Chem. Div. Conference*, Canberra.

Berck, B. (1975). "Determination of air movement in stored grain as a factor in dynamic dispersion and distribution patterns of gaseous pesticides". *Bull. environ. Contam. Toxicol.* 13, p.527.

Bolz, R.E. and Tuve, G.L. (1970). *Handbook of Tables for Applied Engineering Science*. (Chem. Rubber Co.; Cleveland, Ohio, U.S.A.)

Bosworth, R.C.L. (1952). *Heat Transfer Phenomena*. p.102 (Assoc. Gen. Pub. Pty. Ltd.; Sydney, Aust.)

Businger, J.A. (1963). "The glasshouse climate". *Physics of Plant Environment*. Ed. Van Wijk. p.276. (North Holland; Amsterdam.)

Chapman, A.J. (1960). *Heat Transfer*. p.156. (MacMillan; N.Y.)

Childs, D.P., Overby, J.E., Watkins, B.J. and Niffenegger, D. (1970) "Low temperature effect upon third and fourth instar cigarette beetle larvae". *J. econ. Ent.* 64, p.923.

Christie, E.A. (1971). "Integrated solar and thermal radiation properties of building materials". *Australian Refrigeration, Air conditioning and Heating*, 25, 10, p.28.

Converse, H.H., Graves, A.H. and Chung, D.S. (1973). "Transient heat transfer within wheat stored in a cylindrical bin". *ASAE Trans.* 16, 1, p.129.

Dale, A.C. and Giese, H. (1953). "Effect of roofing materials on temperatures in farm buildings under summer conditions". *Agric. Engng.* 34, p.167.

Deirmendjian, D. and Sekara, Z. (1956). "Atmospheric turbidity and the transmission of ultra-violet sunlight". *J. Opt. Soc. Am.* 46, 8, p. 565.

Desmarchelier, J., Bengstonm, M., Connell, M., Minett, W., Moore, B., Phillips, M., Snelson, J., Sticka, R. and Tucker, K. (1977). "A collaborative study of residues on wheat of chloropyrifosmethyl, fenitrothion, malathion, methacrifos and pirimos-methyl". *Pestic. Sci.* 8 (in press).

Disney, R.W. (1954). "The specific heat of some cereal grains". *Cereal Chem.* 31, 3, p.229.

Disney, R.W. (1969). "The formation of dew on a cooled surface in contact with wheat". *J. Stored Prod. Res.* 5, p.281.

Druce P.C. (1976). "Chairman's Review". *Bulk Wheat*, 10, p. 2.

Finnigan, J.J. (1977). Personal communication.

Gallaher, G.L. (1951). "A method of determining the latent heat of agricultural crops". *Agric. Engng.* 32, p.34.

Gates, D.M. (1962). *Energy Exchange in the Biosphere*. p. 64 (Harper and Row, N.Y.)

Gay, F.J. (1941). "A further study of the temperature changes during the 'turning' of bulk wheat". *J. Council Sci. and Ind. Res.* 14, 4, p.111.

Gebhart, B. (1961). *Heat transfer*. (McGraw Hill, N.Y., London.)

Goodspeed, M.J. (1970). "The computation of solar position in environmental models". *Aust. Computer Journal*. 2, 3, p.110.

Goodspeed, M.J. (1975). "Computer routines for solar position, daylength and related quantities". *CSIRO Div. Land Use Res. Tech. Memorandum* 75/11

Griffiths, H.J. (1964). "Bulk storage of grain: A summary of the effects governing control of deterioration". *CSIRO Div. Mech. Eng. Report.* E.D. 8, p.14.

Hardman, J.M. (1975). "The stored grain environment". *International Training Course in Preservation of Stored Cereals,* 1, p.35. (Aust. Dev. Assis. Agency.)

Hilpert, R. (1933) "Wärmeabgabe von geheizten Drähten und Rohren im Luftstrom". *Forsch. Geb. Ing Wes.* 4, p.215.

Holden, T.S. (1961). "Calculation of incident low temperature radiation upon building surfaces". *ASHRAE J.* 3, 4, p.51.

Hooper, F.C. and Chang, S.C. (1953). "Development of the thermal conductivity probe". *ASHVE Trans.* 59, p.463.

Howe, R.W. (1965). "A summary of the estimates of optimal and minimal conditions for population increase of some stored product pests". *J. Stored Prod. Res.* 1, p.177.

Idso, S.B. and Jackson, R.D. (1969). "Thermal radiation from the atmosphere". *J. Geophys. Res.* 74, 23, p.5397.

Jones J.D. (1943). "Intergranular spaces in some stored foods". *Food,* 12, 147, p.325.

Kelly, C.F. (1940). "Methods of ventilating wheat in farm storages". *USDA. Circ. 544.*

Kestin, J. and Wood, R.T. (1971). "The influence of turbulence on mass transfer from cylinders". *J. Heat Transfer.* 93, P321.

Kimball, B.A. (1973). "Simulation of the energy balance of a greenhouse". *Agric. Met.* 11, p.243.

Kreith, F. (1973). *Principles of Heat Transfer.* 3rd Ed. 656 pp. (Intext Educational publishers; N.Y. and London.)

Leeds Northrup (1975) *Leeds - Northrup Temperature - E.M.f Tables for thermocouples referenced to IPTS 68.*

Launder, B.E. (1976). *Topics in Applied Physics.* V 12, ch.6. Ed. P. Bradshaw (Springer-Verley; Berlin, N.Y.)

Lo, K.M., Chen, C.S., Clayton, J.T. and Adrian, D.D. (1975). "Simulation of temperature and moisture changes in wheat storage due to weather variability". *J. agric. Engng. Res.* 20, p.47.

McAdams, W.H. (1954). *Heat Transmission.* (McGraw Hill; N.Y., London.)

Mechanical Engineering *Data sheet* (1975). CSIRO Div. Mech. Engng., Highett, Vic.

Meiman, J.R. and Remmenga, E. (1971). "Snow distribution in relation to solar radiation on two Swiss pre-Alp watersheds". *Water Resources Res.* 7, 6, p. 1636.

Moote, I. (1953). "The effect of moisture on the thermal properties of wheat". *Can. J. Tech.* 31, p.57.

Muir, W.E. (1970). "Temperatures in grain bins". *Can. ag. Engng.* 12, 1, p.21.

Muir, W.E. and Viravanichai, S. (1972). "Specific heat of wheat". *J. agric. Engng. Res.* 17, p.338.

Mulhearn, P.J., Banks, H.J., Finnigan, J.J. and Annis, P.C. (1976). "Wind forces and their influence on gas loss from grain storage structures". *J. Stored Prod. Res.* 12, p.129.

Oxley, T.A. (1944). "The properties of grain in bulk. III. The thermal conductivity of wheat, maize and oats". *J. Soc. Chem. Ind.* 63, p.53.

Oxley, T.A. (1948). "The movement of heat and water in stored grain". *Trans. Am. Assoc. Cereal Chemists* 6, 2, p.84.

Petherbridge, P.(1970). *IHVE Guide* (Building Res. Est., Garston, Watford, England).

Pfalzner, P.M. (1951). "The specific heat of wheat", *Can. J. Tech.* 29, p.261.

Powell, R.W. (1940). "Further experiments on evaporation of water from saturated surfaces". *Trans. Inst. Chem. Engnrs.* 18, p.36.

Robinson, N. (1966). *Solar Radiation.* 347 pp. (Elsevier; Amsterdam, London, N.Y.)

Schmidt, E. and Werner, K. (1941). "Wärmeabgabe über den Umfangeines angelbrasenen geneizten Zylinders". *Forsche. Geb. Inghles,* 12, 2, p.65.

Sellers, W.D. (1965). *Physical Climatology.* p. 141 (Chicago Press; Chicago Univ.)

Sharp, A.K. (1974). "Transient dropwise condensation of water vapour from air onto cylindrical food cans". *Trans. Instn. Chem. Engnr.* 52, p.23.

Sinha, R.N. and Muir, W.E. (1973). *Grain Storage - Part of a System*, p.55. (Avi; Westport, Connecticut, U.S.A.)

Smart, W.M. (1960). *Celestial Mechanics*. (Longmans, London.)

Sogin, H.H. and Providence, R.I. (1958). "Sublimation from disks to air streams flowing normal to their surfaces". *ASME Trans.* 80, p.61.

Solomon, M.E. (1965). "Archaelogical records of storage pests from an Egyptian pyramid tomb". *J. Stored Prod. Res.* 1, p. 105.

Spencer, J.W. (1965). "Solar position and radiation tables for Canberra". *CSIRO Div. Building Res. Tech. paper* no. 16.

Sutherland, J.W. (1976). "Grain drying research at CSIRO", *Bulk Wheat* 10, p.27.

Sutherland, J.W., Pescod, D. and Griffiths, H.J. (1970). "Refrigeration of bulk stored wheat". *Refrig. Air Condit. Heat* 24, 8, p. 30.

Threlkeld, J.L. (1962). *Thermal Environmental Engineering* (Prentice-Hall Inc.; Englewood Cliffs, N.J., U.S.A.)

Ward, N. and Calverley, D.J.B. (1972). "A literature survey on the climatic relationships in stores". *Trop. Stored Prod. Inf.* 23, p.35.

Waterhouse, D.F. (1973). "Insects and wheat in Australia". *J. Aust. Inst. ag. Sci.* 39, p.215.

Weast, R.C. (1964). *Handbook of Chemistry and Physics*. 45th ed. (Chem. Rubber Co.; Cleveland, Ohio, U.S.A.)

Williams, P.W. (1973). *Numerical Computation*. p.122 (Nelson; London, Melbourne, Ontario).

Yacuick, G., Muir, W.E. and Sinha, R.N. (1975). "A simulation model of temperatures in stored grain", *J. agric. Engng. Res.* 20, p.245.

Hodgson, J.L. (1917). "The commercial metering of air, gas and steam". *Proc. Inst. Civil Engrs.* 204, p.108.

Mulhearn, P.J. (1978). "A wind-tunnel boundary layer study of the effects of a surface roughness change: Rough to smooth." *Boundary Layer Met.* (In press).

Strutt, J.W. (1881). *Scientific Papers* 1, No 9.

Winters, K (1978). Private communication.

NOTES

1. In Eq. (2.25), when $|\beta| \leq 90°$, $\cos\beta$ must be equated to zero. During daylight hours, therefore, all terms in this equation, except the two containing $\cos\beta$, are retained for a surface not receiving direct radiation.

2. The cylindrical wall was treated as four plane surfaces for the purpose of solar radiation calculations. By increasing the number of azimuthal divisions from four to eight, the temperature at any point in the bin was found to vary by a maximum of 0.1°C, indicating that four azimuthal divisions are sufficient.

3. Both the conical roof and the grain surface were considered to be isothermal. This is a reasonable approximation for the grain surface since chart recorder records taken over three days near the north and south walls of the large bin show a difference in daily average temperature of less than 0.2°C. It is not a good approximation for the roof, but roof temperatures are not explicitly required and calculations of free convection and thermal radiation in the head space are greatly simplified by using an average roof temperature. The roof was treated as four plane surfaces for the purpose of solar radiation calculations and the average value found.

4. Since only about five iterations were required to achieve convergence to 0.1°C, it was not considered necessary to use an extrapolation parameter.

5. Results of Disney (1954) suggest that there is no significant difference in the specific heats of various wheat types and even

between barley and rough rice. Degree of packing would have little effect on specific heat since the values for wheat and air are of the same order.

6. Oxley (1944) suggests that wheat type affects conductivity and that loose packing allows for freer movement of convection currents, increasing the apparent conductivity. However, these effects have not been quantitatively determined so are not included in Table 5.2.

7. The wind-tunnel experiment was designed for a free-standing bin because the computer model had been developed for this case (e.g. in regard to solar and thermal radiation), even though in the actual situation there would be considerable aerodynamic interaction between the bins.

8. For the correct simulation of wind profiles, Z_o/R_m should be of similar magnitude for the model and real bins. Since Z_o for short grass is $\simeq 1$ cm (p.45), the ratio is $\simeq .005$ for the small field bins and $\simeq .0023$ for the large bin. Z_o/R_m is $\simeq .0038$ for the model, which is of the correct order for simulating both bins.

9. The heat transfer coefficients of the roof and the bin walls will be different and a model bin has now been made with a removable cone, so that the two parts can be studied separately. However, time did not permit this experiment to be performed for the thesis. The method of determination used, however, was felt to be a first step in acquiring a more accurate convective heat transfer coefficient for a grain bin than had been used by other workers.

10. When sprayed with napthalene, the surface of the model bin becomes irregular since the napthalene forms globules up to about 5mm high. Since the bin is about 10 cm in diameter, the ratio of the height of the irregularities to the bin diameter is $\simeq .005$, similar to the value for the small experimental bins.

11. In summer in Canberra there tends to be more direct sunshine in the mornings (Winters, 1978) and this could also be the cause of the observed temperature differences between east and west. The variation in grain temperatures with the time of the sunshine is illustrated in the table below, which shows the computed results for the large bin after twelve weeks.

n/N	morning	afternoon	Grain Temperature °C		
			C2	E4	W4
	0.5	0.5	22.6	24.1	24.1
	1.0	0.0	21.5	23.0	22.2
	0.0	1.0	22.1	23.0	23.9

Hourly values of sunshine could be included to give a more accurate model.

12. Wind tends to be strongest in the afternoon in Canberra's summers (Winters, 1978). This would also cause a difference in temperature between east and west, as shown by the table below.

$u(ms^{-1})$	morning	afternoon	Grain Temperature °C		
			C2	E4	W4
	1.6	1.6	22.2	22.6	22.6
	3.2	0.0	24.7	26.4	27.0
	0.0	3.2	23.8	25.3	24.7

If there is a great difference between windspeeds at different times of the day, this should certainly be included in the model since it has a large effect on grain temperature.

13. These errors were not carried through into the computer program.